

Microplastics in the surface water and sediments of western Lake Superior as determined
via microscopy, Pyr-GC/MS, and FTIR.

A thesis SUBMITTED TO THE FACULTY OF THE UNIVERSITY OF MINNESOTA
BY

Erik Scott Hendrickson

IN PARTIAL FULFILLMENT OF THE REQUIREMENTS FOR THE DEGREE OF
MASTER OF SCIENCE

Dr. Elizabeth Minor

September, 2017

Copyright of Erik Scott Hendrickson, September 2017.

Acknowledgments:

We would like to thank Sarah Grosshuesch, Julia Halbur, Noah Holden, and Roselynd Lin for analytical assistance, committee members Dr. Elizabeth Minor, Dr. Kathryn Schreiner, Dr. Melissa Maurer-Jones, and Dr. John Evans, the captain and crew of the R/V Blue Heron and the captain of the R/V Kingfisher for sampling assistance, and the University of Minnesota Office of the Vice President for Research, Grant-in-Aid of Research, Artistry & Scholarship Program and the University of Minnesota Duluth EVCAA Research and Scholarship Grants Program for funding.

Abstract:

While the presence of plastic pollution is well known in the world's oceans and is beginning to be documented in the world's freshwater systems, there is not yet an in-depth understanding of the distributions, chemical compositions, fates and ecological impacts of plastic particles in most aquatic systems. Microplastic particles are of particular concern due to their direct biological effects (such as false satiation), their roles as sorbents of other chemical compounds, and as vectors for invasive species. In this study, we evaluate the magnitude, distribution, and common polymers of microplastic pollution in surface waters and sediments in western Lake Superior, the deepest and most pristine of the Laurentian Great Lakes. Microscopy, Pyrolysis-Gas Chromatography/Mass spectrometry (Pyr-GC/MS), and Fourier Transform Infrared spectroscopy (FTIR) were used to quantify and identify microplastic particles. Despite the low human population density in Lake Superior's watershed, microplastic particles (particularly fibers, fragments, and films) were identified in western-lake surface waters at levels significantly greater than those previously reported in Lake Superior's eastern basin (p -value < 0.05). Microplastic concentrations in western-lake surface waters were found to range from 0 to 110,000 particles \cdot km $^{-2}$ ($n=15$, mean: 39,000 particles \cdot km $^{-2}$, standard deviation: 28,000 particles \cdot km $^{-2}$, and 95% confidence interval: $\pm 14,000$ particles \cdot km $^{-2}$). Fibers were the most frequently observed morphology in lake surface waters and sediments. The most common polymer in surface waters and sediments was PVC; for surface waters, PP and PE were the next most frequently observed, and PET was the only other polymer observed in sediments. Our ability to evaluate microplastic abundances in Lake Superior's waters and sediments was in part determined by the need to correct for ambient contamination from atmospheric deposition of microplastics during sampling and sample processing. The effects of this contamination, coupled with the small sample area of sediment obtainable by multi-corer, made determining microplastic concentrations in surface sediments problematic. Results presented here provide quantitative and qualitative data on microplastic pollution in western Lake Superior using improved analytical methodology, including polymer characterization by two different techniques. This study also provides insights into possible sources of microplastic pollution in Lake Superior, and ways to improve future microplastics studies in aquatic systems.

Table of Contents

List of Tables.....	VI
List of Figures.....	VII
List of Acronyms.....	VIII
Introduction.....	1
Methods.....	7
Results and Discussion.....	19
Conclusions.....	33
Bibliography.....	36
Appendix.....	61

List of Tables:

Table I.....	41
Table II.....	42
Table III.....	43
Table IV.....	44
Table V.....	45
Table VI.....	46
Table VII.....	47
Table VIII.....	48

List of Figures:

Figure I.....	49
Figure II.....	50
Figure III.....	51
Figure IV.....	52
Figure V.....	53
Figure VI.....	54
Figure VII.....	55
Figure VIII.....	56
Figure IX.....	57
Figure X.....	58
Figure XI.....	59
Figure XII.....	60

List of Acroynyms:

AAB-Adopt-A-Beach
ASTM- American Society for Testing Materials
ATR-FTIR- Attenuated Total Reflectance-Fourier Transform Infrared Spectroscopy
CPE- Chlorinated Polyethylene
DDP-Didecyl Phthalate
DDT- Dichlorodiphenyltrichloroethane
FPA-Focal Plane Array
GCSC- Great Canadian Shore Clean-up
LCS-Laboratory Control Sample
MDPE- Medium-Density Polyethylene
MSD-Mass Selective Detector
NIST- National Institute of Standards and Technology
NOAA- National Oceanographic Atmospheric Administration
PAH- Polyaromatic Hydrocarbon
PCB- Polychlorinated Biphenyl
PDMS-Polydimethylsiloxane
PE-Polyethylene
PET-Polyethylene Terephthalate
PP-Polypropylene
PS-Polystyrene
PVC-Polyvinylchloride
Pyr-GC/MS- Pyrolysis-Gas Chromatography/Mass Spectrometry
SPI- Society of the Plastics Industry
SEM-Scanning Electron Microscopy
UV-Ultraviolet
VOC- Volatile Organic Compound
WWTP- Waste Water Treatment Plant

Introduction:

Since the advent of mass-produced plastic in the middle of the 20th century, plastic pollution has become a significant environmental concern.¹ Plastic pollution has been declared to be a worldwide issue that threatens biodiversity in environmental systems.² Marine plastic pollution is particularly worrisome, as marine system debris typically consists of 60-80% plastic and significant plastic abundances in surface waters (e.g., 100,000 items per m³) have been observed.^{2,3} Many inputs of plastic pollution to aquatic systems exist, including wastewater treatment plants, shoreline debris, river outflows, landfills, industrial pollution, illegal dumping into aquatic systems, and atmospheric inputs.⁴⁻⁶ While the Clean Water Act prohibits the release of recognized pollutants from point sources without a permit, microplastic pollution is commonly discharged without a permit and with no legal consequences.⁷ Most plastic particles in oceanic gyres are less than 10 mm in length, which encompasses part of the mesoplastic size range as well as microplastic size range, as established in Crawford, et al., 2016.⁸ Microplastic particles have been inconsistently defined, particularly when establishing an upper-size limit;¹ however, the definition established for the present work, which is influenced by the National Oceanographic and Atmospheric Administration (NOAA), is a particle of plastic with no dimension longer than 5.0 mm.^{9,10} The microplastic size range typically extends from 5.0 mm to 1 μm ,^{6,8} however, effective lower-limits are usually dictated by sampling methodology;^{11,12} for the current study, 333 μm for surface waters and 250 μm for sediments were the lower size limits (see Methods section). Microplastic particles have several recognized morphologies, including beads (pellets),

foams, films, fragments, fibers (lines), and other shapes resulting from the degradation of larger plastics.^{2,4,8,13}

Negative or potentially negative effects of microplastic pollution include: physical damage to organisms upon ingestion, false satiation, toxicological effects from adsorbed substances and speculated toxicity from polymers and additives, and serving as vectors for invasive species.^{2,14} Much of the focus on potential toxicological damage from microplastic pollution regards hydrophobic substances adsorbing to microplastic particles, including PCBs (polychlorinated biphenyls), DDT (dichlorodiphenyltrichloroethane) related compounds, and PAHs (polyaromatic hydrocarbons),¹⁴ although the uptake of these adsorbed substances from hydrophobic microplastic surfaces into organism biomass is not well known.¹⁵ Recent research has revealed the presence of inorganic contaminants in microplastic paint pigments as well, including copper (Cu), lead (Pb), and cadmium (Cd)¹⁶, and the uptake of these pigment-related contaminants into aquatic organisms is unknown.

Microplastic particles may be mistaken for food by fish species, as shapes and colors of microplastic can mimic food sources in the environment.³ Ingestion of microplastic particles has been well-documented in marine settings, and negative effects observed in experimental conditions include: reduced feeding rates, reduced energy production, inability to remove pathogenic bacteria, and reproductive inhibition.¹⁷ Although research on toxicity related to microplastic consumption in humans is limited, there is evidence of plastic particle assimilation in intestinal tissue of mammals.¹⁸ Due to the acidic conditions and enzymes within the stomach, it is speculated that adsorbed

substances on microplastic particles are removed during digestion and adsorbed later in the less acidic bowels.¹⁸

In aquatic systems, low density plastic polymers, such as polyethylene (PE) and polypropylene (PP), may initially float at the surface, but can eventually sink into sediments over time via accumulating biofilm and mineral deposits.^{4,19} In sediments, microplastics may further persist due to their inherent resistance to biodegradation and lack of ultraviolet light exposure, which can lead to degradation of plastic polymer structures through direct or indirect photoreactions.^{13,19,20} Due to the potential for microplastic particles to sink, either innately or as part of aggregate particles, sediments are a suspected significant sink for plastics in aquatic environments.^{14,19,21} Conversely, when microplastics are not buried in sediments, but are exposed to sunlight, ultraviolet light (UV-B) has the ability to degrade microplastic particles^{3,9}, thus, exposed plastic pollution in areas like shorelines has a greater potential to degrade.^{3,4,22} While biodegradation of standard, non-oxidized plastic polymers is limited to a few, specific microbial species (such as *Rhodoccus ruber*, *Brevibaccillus borstelensis*, and *Penicillium simplicissimum* in degrading PE), polymer oxidation can enhance biodegradation by other species.²²

Much of the research regarding microplastic pollution has focused on marine systems and much less so on freshwater systems.^{2,14} Recently, there has been an increasing interest in studying microplastics in freshwater systems, including investigations of Lakes Bolsena and Chiusi of Italy, Lake Hovsgol of Mongolia, Lake Geneva and Lake Constance (and others) of Switzerland, Lake Victoria of the Great African Rift Lakes (investigating Nile Perch), Lake Winnipeg of Canada, and the

Laurentian Great Lakes.²³⁻³⁰ Previous studies in the Laurentian Great Lakes have observed microplastic pollution in both surface waters and shorelines.^{26,27} According to a review paper by Driedger, et al., 2015, the ultimate fate and geographic distribution of plastic pollution in the Great Lakes is not well understood,⁴ in part because little quantitative microplastic data exists for plastic pollution in the water columns and underlying sediments of the Laurentian Great Lakes.⁴

Despite Lake Superior's status as the largest lake on earth by area, there is a lack of data, quantitatively and qualitatively, regarding microplastic pollution in Lake Superior. To the author's knowledge, only two published works present quantitative data on microplastic pollution in surface waters related to Lake Superior and no studies present quantitative data for microplastic pollution in Lake Superior sediments. Of the studies that regard Lake Superior, one study of 21 sites across Lakes Superior, Huron and Erie includes 5 stations from the relatively unpopulated eastern basin of Superior, and the other contains data on two tributaries flowing into Lake Superior as part of an overview of selected tributaries across the entire Laurentian Great Lake system^{26,31}

Previous studies of microplastic pollution on the Laurentian Great Lakes have shown that microplastic pollution has a propensity to be elevated in near-shore areas, especially near areas of high human population density and industrial activity, where extensive clean-up projects have not been performed.^{4,26,32} Previous studies of microplastic pollution in the Laurentian Great Lakes found that average open-water plastic density resembled severely polluted ocean gyres^{4,26} and plastic was often found to be greater than 80% of anthropogenic shoreline debris items.⁴ Shoreline clean-ups and

surveys of the Great Lakes revealed that cigarette butts (cellulose acetate), food wrappers, and containers were the most common items of plastic pollution.⁴

Quantification of microplastic particles often relies on visual sorting from a processed sample and recording the number of particles observed.⁸ For reporting microplastic quantities in the environment, typical units used regard a count of plastic items per unit area or volume, i.e. “items per km²” or “items per m³”, although, some previous studies have used mass per mass units as well.^{13,33–35} Pyrolysis-Gas Chromatography/Mass Spectrometry (Pyr-GC/MS), Fourier Transform Infrared Spectroscopy (FTIR), Focal-Plane Array (FPA) FTIR, Raman spectroscopy, and Scanning Electron Microscopes (SEM) are qualitative techniques used for identifying and characterizing microplastic polymers.^{8,13,36,37} These techniques are typically used after isolating microplastic particles via a density separation procedure; density separations are conducted by subjecting environmental samples to concentrated or saturated salt solutions, followed by filtration or other separation techniques, and then optical identification/selection of microplastic particles.^{13,14,36,38}

The polymers most commonly observed in plastic pollution of Great Lakes surface waters and shorelines are low density polymers PP, PE, and expanded polystyrene (PS); see Table I.⁴ While the prevalence of these polymers in plastic debris, as well as the primary control of particle transportation and fate, has largely been attributed to polymer density, evidence of more dense polymers in surface waters and less dense polymers in sediments has suggested that other factors are significant as well.^{4,8,39} Other factors thought to control microplastic particle fate include: surface currents, long-term circulation patterns, adhesion to marine snow, ingestion and defecation, biofouling,

mineral deposition, air pockets within particles, and polymer additives.^{4,8,11,19,39} To the authors' knowledge, only the two published works alluded to previously and data available from volunteer groups, Adopt-A-Beach (AAB) and Great Canadian Shore Cleanup (GCSC), present quantitative plastic pollution data related to Lake Superior; the data provided from these sources regard surface waters²⁶, tributaries³¹, and shoreline plastic pollution.^{4,26,31}

The goals established for the present study were to quantify and evaluate the distribution of microplastic pollution in surface waters and sediments of western Lake Superior, to identify polymers present in microplastic debris, and to improve upon existing quantitative methods. As previous works have called for, accurate quantification, identification, and thorough investigatory work will be needed to evaluate the magnitude of microplastic pollution in the Laurentian Great Lake systems, especially in near-shore and urban areas.^{2,4,26,32} Little quantitative data exists for the extent and severity of microplastic pollution in Lake Superior; for the most populated and most densely populated urban area of Lake Superior: Duluth, Minnesota and Superior, Wisconsin (as of the 2016 censuses for the United States and Canada)^{40,41}, a high stress region,^{42,43} published data is essentially non-existent.

Furthermore, previously established methods have been criticized for having a lack of "clean techniques".¹⁵ While a number of investigations of aquatic microplastic pollution have taken place, various publications provide detailed critiques of these commonly used and published methods, including: sorting/identification errors, difficulty distinguishing among natural materials and microplastics, bias associated with not selecting small and uncolored particles, and poorly isolating denser plastics unless

heavier and expensive salts like NaI, ZnCl₂, and polytungstates are used in density separations^{8,32,37,38,44}. Here, we attempt to address some of the analytical issues present in quantifying microplastic pollution, as elaborated in previous publications, by including “clean” analytical techniques in our methods: washing sampling gear methodically between samples, collecting sampling control samples and sample processing control samples for assessing ambient contamination as well as lab control samples (LCS) using analytical plastic standards to assess efficiency.^{12,15}

Methods:

Methodology Motivation and Influence:

Methods for water and sediment sampling, sample processing, and analysis were influenced by previous works, in particular, NOAA’s publication regarding standardized microplastic sampling and sample processing written by Masura, et al., 2015.^{10,26,36,38,45} Microplastic polymers focused on were: polyethylene (PE), polypropylene (PP), polyvinylchloride (PVC), polystyrene (PS), and polyethylene terephthalate (PET). These polymers were chosen because they are the most commonly produced and encountered in the environment.^{1,32} These polymers correspond with designator codes 1-6 created by the Society of The Plastics Industry (SPI) and currently used by the American Society for Testing and Materials (ASTM).⁸ While these polymers were the primary references for analysis, other polymers isolated, analyzed, and identified were reported as well. Plastic standards medium-density polyethylene (MDPE, catalog #: EV306010), PS (catalog #: ST316051), PVC (catalog #: CV316010), and PET (catalog #: ES306030), all in powder form (250-350 μm) were from Goodfellow, Inc., amorphous PP standard was from

Sigma-Aldrich (product #: 428175), and sphere/bead PE and PP standards were from Cospheric (product #'s: WPMS-110 600-700 μ m and PPS-0.9 2.45 \pm 0.05mm-100, respectively).

Morphological Categories:

Microplastic particles were defined as belonging to one of 6 morphological categories, similar to those defined in Crawford and Quinn, 2016.⁸ Note that while the effective upper-limit based upon sieving is that at least 2 dimensions were less than 4.0 mm, any non-fibrous particles with a dimension of 4.0 to 5.0 mm that passed through the 4.0 mm sieve were isolated during microscopy, were recorded, and used for quantifying microplastic abundance, frequency of morphological categories, and were subject to qualitative analysis. See Table III and Figure II for each morphological category, respective definition, and examples.

Study Area and Sample Sites:

Twelve sample sites were chosen in western Lake Superior. These sites represent key environments speculated to differ in their microplastic distributions based upon proximity to believed sources (local wastewater treatment plant, urban shorelines, river outflows). Sites were categorized into generalized, regional environments, including: shoreline, estuary/harbor, and offshore/open water (see Figure I and Table II). Dates of sample cruises were: August, 15th, 2016 (cruise #1), August 17th, 2016 (cruise #2), September 8th (cruise #3), September 28-30th, 2016 (cruise #4), March 19th, 2017 (cruise #5), May 9th, 2017 (cruise #6), and July 5th, 2017 (cruise #7).

Water Sampling:

An NQS-45-60 manta tow net (Ocean Instruments, San Diego, CA, USA) was used for surface water sampling. The net was 3 m in length with a frame opening 14 cm deep by 85 cm wide. The mesh size of the net was 333 μm . At each sample site, a target tow length of 500 to 2000 m was established with length based upon the amount of floating debris. Tows were taken at a speed of 2.0 knots. Accurate determination of distance towed was measured using a flowmeter and was compared to tow length estimation by measuring the duration of a tow at a constant velocity. To avoid contaminating samples, the manta net and collection vessel were rinsed methodically. Before each tow, the net was rinsed in surface water without the collection vessel in place, and was then thoroughly rinsed from the outside using an on-vessel hose using lake water to prevent sample contamination prior to taking a tow. The collection vessel was tripled-rinsed using Millipore water before attaching to the net and beginning a tow.

After a tow was completed, the net was rinsed thoroughly from the outside using water sprayed from the on-vessel hose to isolate materials into the collection vessel. Contents captured in the collection vessel were quantitatively transferred to 4.0 mm and 250 μm metal sieves in series. Contents isolated on each sieve were transferred via forceps and/or Millipore water or <0.7 μm filtered Lake Superior water into combusted glass containers with Teflon caps. Contents captured on the 4.0 mm sieve that could not be washed through were archived; contents captured on the 250 μm sieve were later subjected to sample processing and analysis. Samples were stored in cool, dark storage vessels until they could be further processed in a laboratory.^{10,26}

Due to the potential presence of microplastics in dust around sampling areas⁵, two clean, empty/dry Petri-dish bottoms, 5.5 cm in diameter, were placed on the boat while collecting samples. After sampling, the Petri-dishes were rinsed 3 times with Millipore water and rinses were collected to establish if ambient plastic contamination had occurred, similar in purpose to the wet filter papers used in Woodall, et al., 2014²¹; Petri-dish ambient control samples were later filtered and microscopically examined. To further prevent sample contamination, cotton or wool based clothes were worn as much as possible during water sampling, sediment sampling, sample processing, and microscopy.

Sediment Sampling:

Sediment samples were collected using an Oceanic Instruments multi-corer unit with the R/V Blue Heron used as sampling platform. Individual core tubes are 10 cm in diameter. From each site (Duluth Outskirts, Western Mooring, and Nemadji River), a 4-core extraction was attempted. If successful, the flocculent, the unconsolidated layer at the top of the core, and the 0-2 cm layer from 3 cores were extruded, combined, and wet sieved using a series of 4.0 mm and 250 μm metal sieves, creating composited, representative samples of the flocculent and 0-2 cm layers. The 4th core was archived. Collected materials on the 250 μm sieve were thoroughly rinsed with Millipore water or <0.7 μm filtered Lake Superior water and then were quantitatively transferred to glass containers with Teflon caps and stored in a dark place until samples could be further processed. When fewer than 4 cores were obtained, 1 core was always archived and the remaining cores were used for creating composited samples as described above.¹⁰ Again,

empty, dry Petri-dish bottoms were placed around work areas and used to assess ambient microplastic contamination.

Surface Water Tow and Sediment Sample Processing:

Collected materials from sieving were treated to an oxidation step to degrade labile organic matter and a density separation step to isolate lighter plastic particles from denser, inorganic materials. Some denser plastic polymers may have been included with the inorganic fraction. Both of these steps were performed to aid in microscopic examinations for isolating microplastic particles.

For the oxidation procedure, sieved samples were quantitatively transferred to a pre-weighed beaker and dried at 90°C. After drying, samples were weighed and then subjected to 30% hydrogen peroxide (H₂O₂) treatment catalyzed by Fe²⁺ at ~75°C. The oxidation treatment consisted of adding 20 ml of 30% H₂O₂ (Fisher, Pittsburgh, PA, USA) and 20 ml of 0.05 M ferrous sulfate heptahydrate (FeSO₄•7H₂O) to sample beakers covered with a watch glass. Once the reaction was visually effervescing, beakers were removed from heat to let the reaction subside. Samples were then again heated for 30 minutes at 75°C to ensure the reaction had been completed. Temperature was monitored by a thermometer present in the sample solution. If organic matter persisted, where components visually identified as organic matter were present after adding 30% H₂O₂, another 20 ml aliquot of 30% H₂O₂ with subsequent heating (30 minutes, 75°C) was repeated as necessary (typically between 3-5 aliquots).¹⁰

After oxidation treatment had taken place, enough sodium chloride (NaCl) was added to create an approximately 5 M NaCl solution. Contents of the beaker were

transferred to long stem funnels, where solids denser than the solution (~1.15 g/ml) settled overnight with aluminum foil covering the top of the funnel. Tubing which had been clamped at the bottom of the funnel overnight was opened to allow settled solids to drain out. These settled solids were archived for later analysis.¹⁰ The remaining supernatant solution was filtered through 180 µm Nylon filters (Millipore, reference number: NY8H04700, lot numbers: R6BA87287 and R7AA53191). After filtration, sample filters were left to dry, covered with Petri-dish glass covers in a sealed container with a silica desiccant packet before microscopy; if a more immediate microscopic examination was desired for a given sample, the sample was dried at 90°C in an oven until moisture content was not visually obvious.

Density separation was conducted using a concentrated NaCl solution.⁸ Although the use of NaCl solutions has been found to be inefficient for separating more dense plastic polymers from environmental matrices^{8,32,38}, NaCl is commonly used in density separations for microplastic particles and has advantages over other salts because it is inexpensive and has less potential for negative environmental impacts.^{8,37,38} Hence, the efficacy of using a NaCl solution was evaluated here by analyzing both the supernatant and archived pellets of surface water samples. The pellet of one flocculent sediment layer, site G, was also analyzed, and as it was the only flocculent sample obtained that did not contain overwhelming quantities of inorganic materials. The pellets of the 0-2 cm layers of sediment samples were not analyzed due the prevalence of minerals, which made sorting via microscopy difficult.

During sample processing and microscopic examinations (see below), a Petri-dish bottom filled with Millipore water was used to assess potential ambient microplastic

contamination in laboratories. Petri-dishes were open whenever respective samples were being processed in the lab. Once samples were no longer exposed, Petri-dish water was collected and quantitatively transferred to a collection vial. Once the supernatant and pellet layers had microscopic examinations completed, the collected water of the lab ambient control samples were filtered using 180µm nylon filters and analyzed via microscopy to assess ambient microplastic contamination. Petri-dishes were exposed while beakers were covered with watch glasses during the oxidation treatment, thus, in-lab sample processing ambient controls represent a worst-case scenario for the extent of microplastic contamination in samples. Hence, in establishing a generalized minimum detection limit, averages from method blanks described later were favored relative to sample processing control samples, as sample processing control samples were suspected to be biased high.

Microscopic Examination:

Sample filters were analyzed on an Olympus SZH10 microscope for counting and isolating microplastic particles. As previous microscopic examinations have been subject to inconsistent particle counts among individual analysts, 2 analysts conducted microscopic examinations simultaneously.⁴⁶ A camera provided a live-feed of the sample to a monitor for both analysts to view during the examination. A custom, gridded, plastic overlay was taped to the bottom of the Petri-dishes containing the sample filter to help guide analysts through samples efficiently. After examining an individual filter once, the analysts conducted a review scan of the entire filter and under the filter to ensure no particles had been missed. Size, color, and morphology of particles were recorded on a

spreadsheet before transferring the particles to a pre-weighed vial, where total microplastic mass could be determined prior to qualitative analysis of individual particles. Between collecting individual particles, forceps were cleaned with methanol. Size measurements were made via a micrometer calibrated ocular scale at 40x magnification. Initially, a “break test” was used for the determination of particle composition as plastic or otherwise, as described in Masura, et al., 2015; however, this led to the misidentification of particles, notably, cotton fibers, as plastic particles.¹⁰

A “hot needle” or “melt test” was later adopted for distinguishing amongst plastic and non-plastic particles.^{45,47} Melt tests were carried out by heating a common sewing needle with a lighter until approximately 2 mm of the needle tip glowed and was then brought near the particle in question. A plastic positive particle under a melt test liquefied or beaded from melting.⁴⁷ The melt test was conducted on analytical plastic standards, polyester fibers, cotton and wool fibers, paint chips from research vessels, and Teflon® from a GC vial cap septa. All analytical standards and polyester fibers melted in the melt test, cotton and wool fibers burned, and paint chips and Teflon® exhibited no noticeable response.

Qualitative Analysis by Pyr-GC/MS to Evaluate Microplastic Composition:

Isolated particles from microscopic examinations were analyzed via Pyr-GC/MS for polymer characterization using a pyrolysis and thermal desorption unit (TDU) manufactured by Gerstel GmbH & Co. KG, Germany and an Agilent 7890B Gas Chromatograph with an Agilent 5977A mass-selective detector (MSD).

Approximately 10% of particles collected or a minimum of 5 particles were chosen for analysis from selected sites, with a focus on choosing different morphologies and characteristics, if possible. To establish its mass, each particle was manually inserted into a tared quartz tube, previously cleaned by soaking in NOCHROMIX overnight, rinsed at least 3 times with Millipore water, and combusted for 4 hours at 550°C and weighed directly on a Mettler Toledo XP2U microbalance. Particles less than 20 µg were analyzed using splitless introduction into the gas chromatograph; particles greater than 20 µg were introduced using a 1:100 split.

When an analysis was initiated, the TDU was pneumatically unlocked to allow the sample to be placed within the TDU/pyrolyzer unit. After the TDU was again locked, a hold-time of 1.5 minutes was used to allow atmospheric gases to elute from the TDU. After the 1.5 minute hold-time elapsed, the TDU ramped from an initial temperature of 50°C to 300°C at a rate of 720°C per minute; the final temperature of 300°C was held for 1 minute. After the TDU reached 300°C, approximately 30 seconds into the run, the pyrolyzer unit began pulsed pyrolysis at 550°C and ended at 500°C; pyrolysis occurred for approximately 20 seconds. The cooled-injection system liner (CIS), which served as a heated intermediate between the pyrolyzer/TDU and the GC inlet, was set at 300°C for an initial temperature and increased at a rate of 12°C per minute until an end temperature of 320°C was reached; end temperature was held for 1 minute.

The GC oven was equipped with a 30 meter Agilent HP-5MS column. The GC temperature program started at a temperature of 50°C for 2 minutes, and then ramped up to 320°C at a rate of 10°C per minute for 27 minutes, and finally, the oven was held at 320°C for 3 minutes; thus an injection's total run time was 32 minutes. After each run

was completed, the GC underwent an equilibration time of 3 minutes at 50°C before another run could be initiated. The transfer line between the GC and MSD was set at 280°C.

The MSD used electron impact (EI⁺, 70 eV) as an ionization source. The MS source and MS quadrupole had set points at 230°C and 150°C, respectively. The MSD scanned for ions from m/z 10-550. Total ion chromatograms/pyrograms of analyzed particles were assessed using the National Institute of Standards and Technology (NIST) mass spectral library (version 2.0, 12/4/12, available through the mass spectrometer's software package), analysis of analytical plastics standards mentioned previously as well as household products made of known polymers, and comparison with published data.^{36,48-50} When pyrograms could not be confidently distinguished as a given polymer due to the low number of pyrolytic products (< 3 or 4 pyrolytic products) and low pyrolytic product abundances, pyrograms were evaluated on Mass Hunter qualitative analysis software. Mass Hunter qualitative analysis software was used to integrate total ion chromatogram peak areas of pyrolytic products and calculate a signal-to-noise (S/N) ratio. A 3:1 S/N ratio was used to establish the presence of pyrolytic products, similar to previous studies that have used mass spectrometry and have referenced detection limits or substance presence based on signal-to-noise ratios of 3:1.⁵¹⁻⁵³ See Figure III.

Qualitative Analysis by ATR-FTIR:

Data from FTIR analysis was obtained to complement Pyr-GC/MS data and further confirm Pyr-GC/MS identifications. A Thermo Nicolet 380 Fourier Transform Infrared Spectrometer using an ATR cell with a germanium (Ge) crystal from SensIR

was used for obtaining infrared spectra of isolated microplastic particles. A total of 200 scans were taken and averaged for each spectrum, with a wavenumber resolution of 1 cm^{-1} . All spectra were smoothed by using 11 Savitsky-Golay convolution points⁵⁴ using Origin 8.1 and a break was placed in the wavenumber axis of the spectra, as high noise was in spectra between $\sim 1,900$ and $2,500\text{ cm}^{-1}$, regardless of how well the crystal was covered by a particle. Particles were chosen if they were deemed easily visible, with low risk of difficulty in recovering from the ATR-FTIR unit for subsequent analysis by Pyro-GC/MS. If necessary, particles with the potential to damage the Ge crystal were ground by an agate pestle and mortar (i.e, irregularly shaped particles like fragments); the pestle and mortar was cleaned with methanol prior to grinding particles. The Ge crystal was cleaned with methanol prior to taking a blank spectrum and sample spectrum. In interpreting FTIR spectra, Abdulla, et al, 2010, Crawford and Quinn, 2016, and comparison to plastic standards were used for interpreting microplastic particle composition and functional group bands.^{8,54}

Controls of Laboratory Methods

Replicate trials of the sample processing protocol were performed using purchased standards from Goodfellow, Inc. and Sigma Aldrich to assess mass loss and efficiency in isolating microplastic particles using the sample processing protocol described above. Replicate method blank trials were also performed with 100 ml of Millipore water to further assess contamination during sample processing. For both method blanks and standard analyses, the sample processing protocol was followed as listed above, with the following changes: 3 additions of 10 ml aliquots, rather than 20 ml

aliquots of 30% H₂O₂ were used to accommodate the smaller sample size of test samples and the smaller beakers thus used to minimize weighing errors. For trials concerning the use of standards, initial masses of microplastic particles in these methods tests ranged from 10-21 mg.

Statistical Analysis:

Microplastic concentrations observed in specific regions (shoreline, offshore, estuarine; see Figure I) of western Lake Superior were compared to concentrations observed in other regions of the lake as well as the data reported in Eriksen, et al., 2013a for eastern Lake Superior.²⁶ Variances were evaluated via F-tests among the reported concentrations, analysis of variance (ANOVA) was used to evaluate mean concentrations among study area regions, and a two-tailed T-test was used to compare mean concentrations between Eriksen, et al., 2013a and the current study. Microsoft Excel 2007's Data Analysis Toolpak was used to conduct statistical analyses. An alpha of 0.05 was used to denote significance for both ANOVA and T-test analyses.

Investigation of Winter Matrices:

As ice coverage on Lake Superior can be intermittent, leading to challenges in winter sampling, a brief investigation was conducted to assess microplastic presence in ice, snow, and sub-ice water matrices in Barr's Lake, Minnesota (a small lake approximately 10 miles from Lake Superior's north shore) on March, 19th, 2017. Collected samples of ice and snow were melted in clean buckets and were covered with aluminum foil to avoid ambient contamination. Sample volumes obtained were 3.9 L of

snow, 11 L of ice, and 100 L of sub-ice water. All 3 samples were filtered through 180 μm nylon filters and were subsequently analyzed by the same microscopic examination protocol mentioned previously.

Results and Discussion:

A total of 621 microplastic particles were isolated from surface water and sediment samples. Surface water samples (isolated from $1.56 \times 10^{-2} \text{ km}^2$ of surface water) accounted for 584 microplastic particles, while sediments (isolated from $5.50 \times 10^{-2} \text{ m}^2$ of sediments) accounted for 37. Of the 37 microplastic particles isolated from 6 sediment samples (3 sites); 30 were from the flocculent layers and 7 were from the more-consolidated 0-2 cm layers. The most frequent particles observed in surface waters were fibers (229), followed by fragments (200), and then films (121). Beads/spheres (10), foams (3), and others (21) were observed in lesser quantities (see Figure 3). Fibers were also the most common particles in sediments (22 in total, 18 from the flocculent layers and 4 from the 0-2 cm layers). Fragments, films, and others were observed in lesser quantities (total from both layers: 10, 2, and 3, respectively; see Figures IV, V, and VI as well as Tables IV, V, and VI).

While it is difficult to discern the sources of microplastic particles, the quantities of fibrous particles isolated, particularly at the Western Mooring (site G), which is far offshore, suggests that atmospheric inputs and greywater/wastewater effluents may be significant sources of microplastic particles in Lake Superior.^{5,55} The increased frequency of extreme precipitation events associated with climate change may assist mobilization of microplastic particles to aquatic systems, in particular, airborne fibers, to

“pristine” systems such as Lake Superior.^{5,55,56} Regarding the other 2 dominant morphologies, films and fragments, mobilization from urban areas in the western arm of Lake Superior via surface currents was thought to be the most likely process for their presence in offshore sites like the western mooring. In circumstances where secondary microplastic particles like films or fragments were prevalent, shoreline runoff and litter were the most suspected sources.^{5,13} In regard to surface water samples, where films or fragments were common (using the investigation of Port Wing (site H) on 8/17/16 as an example) it is suspected that small tributaries, similar to the tributary within the town of Port Wing, mobilized plastic and microplastic debris from human-occupied areas to pelagic surface waters of Lake Superior. The low prevalence of beads/spheres in Western Lake Superior in this study may be due to recent legislation banning microplastic beads in products passed in Minnesota.⁵⁷ Overall, fibers, typically low mass particles, were the most prevalent in western Lake Superior; processes attributed to mobilization of fibers were wind, atmospheric deposition, and greywater/wastewater effluents.⁵⁵ See Figure IV and Table IV.

Total surface water microplastic masses in our samples ranged from <0.1 mg to 4.7 mg ± 0.2 mg (uncertainty) and sediment-sample microplastic masses ranged from <0.1 mg to 0.4 mg ± 0.2 mg. Between both surface water and sediment matrices, 15.9 mg ± 0.5 mg (uncertainty, propagated from all masses measured) was collected, where 15.2 mg ± 0.5 mg was collected from surface waters and 0.7 mg ± 0.2 mg from flocculent sediments (none of the 0-2 consolidated sediment samples contained measurable masses of microplastic particles). Where mass was measurable and normalized to area

encompassed, microplastic mass/area ranged from 91 to 3,538 mg•km⁻² (\bar{x} = 1,200 mg•km⁻²) for surface waters. The largest mass/area ratio for surface waters was observed at the mouth of the Nemadji River (site K) with 3,538 mg•km⁻²; the smallest measurable mass/area was observed at site D. Larger masses/area of microplastics present at the mouth of the Nemadji River (site K) and outside of Port Wing (site H, 8/17/16) were likely transported via turbulent river or tributary currents, providing enough force to keep heavier particles suspended in surface waters. Conversely, other more open water sites, site L on 9/30/17 and site G on 9/30/16, had relatively larger mass/areas of 1,200 and 1,500 mg•km⁻², respectively; despite the fact that these sites are more likely depositional areas, relatively larger microplastic masses were retained in their surface waters. See Table V.

To correct for ambient contamination of microplastic particles during sampling and sample processing, the number of particles isolated from individual ambient control samples during sampling and the average number of particles from replicate method blank trials were used. Due to suspected bias high in ambient controls during sample processing, method blank averages were chosen; method blank averages better represent potential exposure to atmospheric inputs during sample processing, as method blanks were exposed to the atmosphere for more similar durations of time. A total of 5 particles were collected from replicate method blank trials; 3 particles were fibers and 2 were films (2 fibers, 2 films from method blank 1, and 1 fiber from method blank 2). A minimum detection limit (MDL) was established based upon the sum of the average quantity of particles isolated from sampling ambient control samples (2.6) and method blanks (2.5);

by summing these averages, an MDL of 5 particles was established. Hence, any samples with fewer than 5 particles after applying corrections were deemed under detection limits. For surface waters, 1 sample (Duluth Outskirts, Site E, 9/28/16), had a concentration that was under detection limits after correcting. All but 1 sediment fraction (flocculent sediment, site G, 9/30/16), were under detection limits via corrections. See Table V.

Uncorrected areal particle abundances of surface waters ranged from 11,000-120,000 particles•km⁻² (n= 15, mean: 43,000 particles•km⁻², standard deviation: 28,000 particles•km⁻², and 95% confidence interval: ±15,000 particles•km⁻²), while corrected concentrations ranged from 0-110,000 particles•km⁻² (n= 15, mean: 39,000 particles•km⁻², standard deviation: 28,000 particles•km⁻², and 95% confidence interval: ±14,000 particles•km⁻²). After corrections, estuary/harbor concentrations ranged from 21,000-110,000 particles•km⁻² (n=4), open water concentrations ranged from 25,000-54,000 particles•km⁻² (n=3), and shoreline concentrations ranged from 0-78,000 particles•km⁻² (n=8). For corrected regional concentrations, on average, the estuary and harbor region had the greatest abundance of microplastic particles (\bar{x} = 54,000 particles•km⁻², s=39,000 particles•km⁻²), followed by open water sites (\bar{x} = 38,000 particles•km⁻², s=15,000 particles•km⁻²), and then shoreline sites (\bar{x} = 28,000 particles•km⁻², s=22,000 particles•km⁻²). The greatest abundance of microplastic particles (110,000 particles•km⁻² after corrections) was observed at site B (8/15/16) near the local wastewater treatment plant. The minimum microplastic abundance observed was at site E (9/28/16) with no detectable particles (after corrections). See Figures VII and VIII as well as Table V.

Variances in corrected surface water concentrations among the harbor/estuary, shoreline, and open-water regions (n= 4, 8, and 3, respectively) of the current study were not statistically significantly different (p-value > 0.05). Statistical evaluation of corrected areal microplastic concentrations between the current study (n=15) and eastern Lake Superior concentrations reported in Eriksen, et al., 2013a (n=5) did reveal significantly greater variance (p-value= 1.6×10^{-3}) and a significantly greater mean areal microplastic concentration (p-value = 6.5×10^{-4}) in the current study. Land use has been attributed as the primary reason for significantly greater concentrations in western Lake Superior; the Twin Ports region of western Lake Superior is the heaviest stress area of Lake Superior and is more urban than sites investigated by Eriksen, et al., 2013.^{26,42,43}

To assess the magnitude of microplastic pollution in western Lake Superior, concentrations were compared to other investigations of the Laurentian Great Lakes, other inland lake systems, and marine systems (Fig.IX). Western Lake Superior microplastic abundances were greater than average values in Lakes Huron²⁶ and Michigan²⁹ but considerably lower than average values in heavily urban Lake Erie.²⁶ Western Lake Superior microplastic abundances tended to be lower on average compared to other inland lake systems, including Lake Winnipeg, Canada, Swiss Lakes investigated by Faure, et al., 2015 (, and central Italian lakes Lake Bolsena and Lake Chiusi.^{23,24,30} Lake Hovsgol, a remote mountain lake in Mongolia, had slightly lower microplastic values ($20,264 \text{ particles} \cdot \text{km}^{-2}$)²⁸ than seen in this study. While western Lake Superior's concentrations were comparable/slightly larger than marine study averages of Law, et al., 2010 (north Atlantic Ocean, $20,300 \text{ particles} \cdot \text{km}^{-2}$) and Eriksen, et al., 2013b (southern Pacific Ocean, $26,898 \text{ particles} \cdot \text{km}^{-2}$), the ranges of microplastic abundances in the ocean

studies were much larger^{39,58} Northern Pacific Ocean microplastic concentrations reported by Moore, et al., 2001 (average: 334,271 particles•km⁻², range: 31,982-969,777 particles•km⁻²)⁵⁹ were much higher than Lake Superior values. In general, western Lake Superior microplastic abundances were greater than lake systems regarded as pristine or relatively pristine, but overall are relatively low (Figure IX).

As a result of the low number of particles that were isolated from sediment samples relative to ambient controls and method blanks, only one microplastic abundance observed in sediment samples could be reported with confidence. Before corrections, flocculent sediment concentrations ranged from 40-1,300 particles•m⁻² (n= 3, \bar{x} = 800 particles•m⁻², standard deviation: 700 particles•m⁻², and 95% confidence interval: \pm 700 particles•m⁻²) and the concentrations in the 0-2 cm fractions of sediment ranged from 0-510 particles•m⁻² (n= 3, \bar{x} = 230 particles•m⁻², standard deviation: 250 particles•m⁻², and 95% confidence interval: \pm 290 particles•m⁻²). After corrections, only the flocculent sediment of the western mooring had a concentration that was above the MDL (1,000 particles•m⁻²). The challenge for sediment sampling is that to obtain an undisturbed sediment-water interface, multi-coring is usually used and thus was chosen for this study. The multi-corer tubes encompassed small areas of sediment ($7.85 \times 10^{-3} \text{ m}^2 - 2.36 \times 10^{-2} \text{ m}^2$), hence why low numbers of particles were isolated from sediment samples. Results reported here highlight the necessity for sediment sampling techniques to encompass large areas and/or masses of sediment (traditional samplers such as Ponar grabs) or to take an adequate number of replicate samples (if a multi-corer is desired to obtain the

sediment-water interface and resolved layers of sediments) to more confidently report abundances of microplastics in sediment. See Table VI.

Petri-dish ambient control samples monitoring microplastic contamination during sampling and in-lab sample processing collected a total of 39 and 100 particles, respectively. For sampling ambient control samples, the number of particles collected ranged from 0-12 (\bar{x} = 2.6 particles) while individual surface water sample lab processing ambient control sample ranged from 0-20 (\bar{x} = 6.7 particles). In ambient control samples for the sediment lab processing steps, a total of 18 particles were found (9 particles total from processing the flocculent layers and 9 particles total from processing the 0-2 cm layers; \bar{x} = 3 particles for both layers; see Appendix Tables I-IV.

Method testing samples using standard polymers yielded replicate average mass recoveries that ranged from 8%-93%. Polyethylene and PS yielded high mass recoveries (93% and 94%, respectively), while PET and PP yielded moderate mass recoveries (66% and 67%, respectively). Polyvinyl chloride mass recovery was low (8%), which was attributed to high polymer density ($1.38\text{-}1.41\text{ g}\cdot\text{cm}^{-3}$)⁴, as particles were observed in the archived pellets from density separation. Similarly, particles from PET method-testing samples (density of $1.38\text{-}1.41\text{ g}\cdot\text{cm}^{-3}$)⁴ were also observed in the pellet. While PP has a lighter density ($0.85\text{-}0.92\text{ g}\cdot\text{cm}^{-3}$) and was expected to have a greater mass recovery from density separation, Sigma-Aldrich PP standard used was manually ground from larger fragments and were inconsistent in size, unlike the Goodfellow powder standards; hence, some mass loss was attributed to unaccountable, small particles lost through filtration. Mean count recoveries were greater than 70% for polymers PE (93.0%), PET

(80.8%), PS (78.5%), and PP (76.6%); Again, PVC exhibited a low-recovery (11.6%). Method testing reinforced previous critiques of using NaCl as a reagent for density separation of denser plastics. However, these results only regard microplastics in a fragment or powdered form; microplastic polymers of other morphologies, such as films and fibers, of more dense polymers like PVC and PET, were recovered from supernatants of density separation solutions. Furthermore, polymer density is not the sole control of particle recoverability by density separation. Particles with certain morphologies, such as films or fibers, may float via surface tension in surface waters and density separation solutions. See Table VII.

Method efficiency was also evaluated by calculating percent of total microplastic particles isolated from the supernatants of density separation solutions relative to the total number of microplastics obtained from both the supernatant and pellet layers. Efficiency determined in this manner ranged from 44%-94% of the total particles collected from samples, with an average of $77\% \pm 15\%$ (standard deviation). Efficiencies for surface water samples from dock harbor (site C) and center bay (site L, 9/30/16) were not calculated due to the misidentification of cotton fibers as plastic, therefore, actual numbers of microplastic particles isolated from supernatant could not be determined confidently. As reflected by method efficiency recoveries, using NaCl is moderately effective for separating microplastic particles from environmental matrices, but losses due to this density separation approach should be estimated and it is best that pellet layers are also analyzed. See Table VIII.

Analysis of isolated particles by Pyr-GC/MS revealed the presence of 7 different polymers and a plasticizer resin (see Appendix, Figures I-XXIX as well as Tables V-XII,

for further information). Pyrolytic products characteristic of PE were: terminal dienes, terminal alkenes, and alkanes of carbon chains from ~8-30 carbons in length.^{36,48} Characteristic pyrolytic products of PP included 2,4-dimethylheptene, followed by successive “groups” of 2 or 3 peaks; in general, these groups roughly formed a pattern, where the first peak alternated in having either 1 carbon longer in chain length or methylation of the second to last carbon. Peaks after the first in given “groups” were different stereoisomers and tacticities of the first peak.^{48,53} Pyrograms of PP identified particles displayed varying resolution between pyrolytic products, which was attributed to the different tacticities of PP; groups as described above were less distinguishable in atactic PP identified pyrograms relative to syndiotactic and isotactic PP identified pyrograms (see pyrograms in appendix).⁴⁸ Polymers PS, PVC, and PET shared many pyrolytic products, primarily volatile organic compounds (VOCs) and PAHs, including: benzene, toluene, xylenes, indene, styrene, naphthalene and biphenyl.^{36,48} While these 3 polymers had unique pyrolytic products, usually in small abundances, these polymers were primarily distinguished by the dominant pyrolytic product formed in splitless mode (PS-styrene, PVC-naphthalene, and PET-biphenyl; Benzene was the dominant pyrolytic product of PVC in split mode). While polymers of PVC and PET themselves do not contain sulfur, the presence of sulfur dioxide, benzothiophene, and dibenzothiophene was frequently observed in pyrograms; a study conducted by Toraman, et al., 2014 analyzed the oil generated by pyrolysis of plastic waste and revealed the presence of the same or similar compounds.⁶⁰ Polymers polydimethylsiloxane (PDMS), chlorinated polyethylene (CPE), and plasticizer resin were infrequently encountered. The silicate based polymer, PDMS was identified by several cyclosilicate compounds.^{48,49} Although a CPE standard

was not analyzed by Pyr-GC/MS, characteristic pyrolytic products listed before for PVC as well as triplet-peaks containing hydrocarbons reminiscent of PE were observed, similar to Tsuge, et al., 2012's CPE reference.⁴⁸ A plasticizer resin was identified as didecyl phthalate from phthalate pyrolytic products, including phthalic anhydride and diethyl phthalate, as well as a broad peak matching the NIST library's didecyl phthalate reference spectrum.⁴⁸

A total of 73 particles were analyzed by Pyr-GC/MS, where 68 were from surface water samples and 5 were from flocculent sediment. The most common polymer observed in surface waters was PVC (11 particles), followed by PP (9), PE (8), and PET (7). Other observed polymers include CPE (4), PS (2), PDMS (1), and didecyl phthalate plasticizer resin (1). Of the 5 particles analyzed from flocculent sediments, PVC was also the most common polymer observed (2), followed by PET (1), and the other 2 particles analyzed had no discernible response (2). Cotton was commonly analyzed among the particles isolated from the supernatants of surface water samples from dock harbor (site C, 8/15/16) and center bay (site L, 9/30/16), as cotton was frequently misidentified as plastic prior to the introduction of the melt test. Cotton was analyzed in one instance after the introduction of the melt test; this particle was suspected to have entered the sample's GC vial ambiently, rather than through misidentification during microscopy. A total of 14 particles displayed little or no signal and 3 particles could not be confidently assigned single polymer identification (see Figure X).

A paint chip from the R/V Blue Heron was analyzed by Pyr-GC/MS to assess polymer composition and to determine if such paint chips may have been part of the samples collected using that research vessel. The resulting pyrogram was reminiscent of

PVC, particularly in that the same VOC and PAH pyrolytic products were formed and naphthalene was the dominant pyrolytic product formed in split mode. It is unlikely that Blue Heron paint chips were isolated from samples during microscopy, as the paint chips did not melt via a hot-needle test and were visually obvious. Regardless, this raises the issue of potential quantitative bias high of microplastic abundances and incorrect polymer identification via the introduction of paint-related particles during sampling. While Pyr-GC/MS is heralded for its in-depth characterization of polymeric materials,^{8,61} here, the potential for incorrect identification microplastic polymers has been demonstrated by analyzing plastic-related particles. Future studies must fully investigate sampling regimes and sample processing protocols for potential sources of microplastic-like or related contaminants with similar chemical structures and assess these potential source materials to avoid incorrect identification of microplastic particles.

Qualitative analysis by ATR-FTIR largely confirmed identifications made from Pyr-GC/MS data. Characteristic band regions included aromatic C-H stretching between 3,000-3,100 cm^{-1} , aliphatic C-H stretching between 2,800-3,000 cm^{-1} , carbonyl C=O stretching around 1,720 cm^{-1} , CH_2 rocking between 1,325-1,475 cm^{-1} , and various fingerprint bands under 1,325 cm^{-1} .^{8,54} Due to the similar FTIR bands in PVC and PP spectra, results from pyrograms were used by default to assign a polymer composition in these cases; past investigations using FTIR have expressed the difficulty in discerning PVC from other polymers, especially when additives are prevalent.⁶² While a PDMS standard was not analyzed, the single particle identified as PDMS had aliphatic bands (2,962 and 2,903 cm^{-1})⁸ and a large peak at 1,008 cm^{-1} attributed to silica based functional groups within its polymeric structure.⁶³ In some instances, non-PET identified

microplastic particles had bands between 1700-1750 cm^{-1} , indicative of polymer oxidation.²⁷ See Appendix Figures XXX-XXXV and Tables XIII-XVIII.

In total, 19 particles analyzed by Pyr-GC/MS were also analyzed by ATR-FTIR. All particles analyzed by ATR-FTIR are from surface waters, as particles isolated from sediment were too small to analyze and recover for Pyr-GC/MS analysis. By ATR-FTIR, the most frequently observed polymer was PE (8, although 3 of these particles had pyrograms that suggest the particle was not entirely comprised of PE), followed by PET (4, with 1 pyrogram that suggested the particle was not solely PET), PVC (3), PP (2), and then PS (1) and PDMS (1).

In 3 instances, the pyrograms of particles were reminiscent of PVC or CPE, while the corresponding IR spectrum resembled PE; the speculated cause for this inconsistency between qualitative analysis techniques has been attributed to heterogeneous chlorine content common in the chlorination of PE and PVC.⁶⁴ Similarly, a particle was identified by ATR-FTIR as PET, while the pyrogram had pyrolytic products attributed to cotton and PET. While the particles were identified based on their pyrograms, as the primary qualitative analysis technique (due to smaller particle mass required for analysis by Pyr-GC/MS), the inconsistency in polymer identification by different analytical techniques suggests that particles found in the environment may contain copolymers, making the determination of polymer composition more difficult.⁸ Given the broad number of possibilities of plastic polymers, co-polymers, and additives^{8,36}, in addition to natural processes that can alter particle composition (photo-oxidation and biodegradation)⁸, accurate identification of microplastics continues to pose a challenge in assessing microplastic pollution. Thus for environmental work, the methods should be optimized

for distinguishing polymers with greater certainty. For Pyr-GC/MS, pyrograms should yield several pyrolytic products unique to single polymer in appreciable abundances; relying on the greatest abundance of a single pyrolytic product will not provide sufficient identification. Likewise, IR methods should be optimized to best distinguish between various polymers and the presence of co-polymers and additives.

In relating morphological categories to polymers identified, most fibrous particles analyzed (9) had low/no discernible signals, attributed to the tendency of fibrous particles to be low in mass. When fibers did yield significant enough numbers and abundances of pyrolytic products that could be used for identification, fibrous particles were primarily identified as PET (7), with lesser instances of PP (2), PVC (1), and uncertain interpretations (1). Fragments were primarily PVC (6), PP (5), or had low/no signals (5); in lower quantities, fragments were identified as PE (1), didecyl phthalate resin (1), or had uncertain interpretations (1). Film particles were found to represent a range of different polymers, including PVC (6), PP (2), PE (6), CPE (4), and PDMS (1). Of the 3 bead particles analyzed, 2 were interpreted as PE and PS, while 1 had an uncertain interpretation, but appeared to be PE related. The only foam analyzed was found to be PS. See Figure XI.

Fibrous particles were thought to have originated mainly from synthetic textile materials due to their frequent identification as PET.⁴ The frequency of chlorinated polymers PVC and CPE in a variety of morphological categories reflected the utility of chlorinated polymers given their impact strength⁶⁴; polyvinylchloride in particular is often used as a structural component, making it versatile for a variety of construction applications.^{4,5} The common use of PE for food packaging and bags was the suspected

cause for the prevalence of films existing as PE.⁵ While PP was primarily found to exist primarily as fragments, due to the diversity in the use of PP (food packaging, car parts, etc.),^{4,5,25} it was difficult to discern original sources or applications of the particles analyzed. The only foam particle analyzed was likely a secondary microplastic particle of polystyrene foam, a form of expanded PS typically used as packaging.^{4,5}

The winter analysis of microplastics in a small lake near Lake Superior provides further insight into the relationship between particle morphology and source. In this sampling, a total of 37 particles were isolated from the snow sample, 34 from the ice sample, and 0 from the sub-ice water sample; thus, concentrations were calculated as 9.5 particles/L, 3.1 particles/L, and 0 particles/L, respectively. Fibers were the most common particles isolated from snow (30) and ice (29) samples, followed by fragments (6 and 5, respectively), and 1 film in snow. For the snow sample, a number of fibers (15) were thought to have been contamination from a sampler's gloves based upon visually similar color and morphology to fibers pulled from these gloves; correcting for these speculated fiber contaminants, a corrected concentration of 5.6 particles/L was calculated. Given the prevalence of fibers in these sample matrices, atmospheric deposition was thought to be the most likely sources of microplastic particles to Barr's Lake.⁵ As a result of no particles isolated from sub-ice water, microplastic particles present in Barr's Lake were thought to have been concentrated and incorporated into ice upon formation, similar to microplastic pollution observed in arctic sea ice.⁶⁵ Winter-related matrices should be further investigated to assess the fate and sinks of microplastic particles in the environment during winter seasons. See Figure XII.

Conclusions

An average corrected microplastic abundance of 39,000 particles•km⁻² was observed for western Lake Superior. Significantly greater microplastic abundances (p-value = 6.5x10⁻⁴) observed in this study relative to Lake Superior's eastern basin²⁶ are likely due to local land use differences. Where eastern basin concentrations were reported²⁶, near-by land use is heavily forested⁶⁶, in contrast to the Duluth, MN/Superior, WI area, the most populated part of the Lake Superior watershed, and deemed a heavy stress area in Lake Superior.^{26,40-43} Methodology differences may have also resulted in significantly greater concentrations observed in western Lake Superior, including: tow length/duration, sample processing, microplastic particle identification techniques, and microscopic counting regime.²⁶ Based upon the high frequency of fibers in surface water samples, especially at offshore sites, it has been speculated that atmospheric inputs join effluent and riverine inflows, and runoff from surrounding land, as a significant source of microplastic particles into Lake Superior^{5,23}, and, in fact, may dominate the inputs at open-lake locations

While some improvements in quantifying microplastic pollution have been introduced here, particularly for using visual microscopy, further research and efforts to standardize and improve methodology are necessary. Future studies need to further optimize methods for assessing microplastic particle contamination of samples during collection and processing. The magnitude of potential contamination of microplastic particles relative to the low numbers of microplastics collected in sediment samples was very large in this investigation. Future sediment sampling methodologies should obtain substantial quantities of sediment representing larger areas and masses of sediment to

avoid concentrations that are biased due to the small sediment surface area currently accessible via multi-corer. Analogous to the famous investigation into the age of the Earth by Patterson, et al., 1955, “super-clean” laboratories could be used to better control for the ambient contamination of microplastic particles.⁶⁷

Future investigations should also focus on how physical limnological and oceanographic processes affect microplastic particle fate. By further understanding how microplastic particles are transported and more effectively locating sinks of microplastic pollution, improved sampling regimes and quantitative assessments of microplastic pollution can be obtained. Despite the common perception that polymers more dense than water should sink quickly after entering aquatic systems, PVC and PET were both observed in surface water samples, including those from off-shore sites like the Western Mooring (site G) and were isolated from the supernatants of density separation solutions (~1.15 g/ml).¹⁰ These observations reinforce the argument that polymer density alone is not the most significant control on microplastic particle fate.^{19,39} Instead, it is likely that microplastic incorporation into copolymeric materials and into aggregates of varying, overall densities may play a major role in microplastic distributions within the aquatic environment.

The distribution and fate of microplastic particles in Lake Superior may be subject to certain physical processes more commonly observed in marine environments rather than the typical, smaller inland lakes. In Lake Superior, shoreline sites had the lowest concentrations on average, while offshore open-water sites had higher concentrations, similar to microplastic distributions in the western Atlantic ocean as reported by Law, et al., 2010.³⁹ The western mooring’s surface water microplastic abundance (site G,

9/30/17), was the 3rd most concentrated of all sites (54,000 particles•km⁻² after corrections). Elevated offshore concentrations suggest that microplastic pollution may have been mobilized by surface currents and concentrated in current convergence zones. Similarly to Law, et al., 2010, microplastic pollution observed at the western mooring may be trapped by gyre-like surface currents, with microplastic levels reflecting surface current patterns inherent within Lake Superior.³⁹ An additional factor, as yet not quantified, is the amount of atmospheric deposition of microplastics at various sites in the lake; the prevalence of fibers at site G indicates that atmospheric deposition was important..

Studies with similar goals to those in Kim, et al., 2015 (i.e., assessing mass loads of plastic into aquatic environments and discerning the locations of plastic pollution sinks) should be performed in the Laurentian Great Lakes.⁶⁸ While concentrations reported here and in similar works provide insight to the relative magnitude of microplastic pollution in specific sites of aquatic systems, these concentrations represent only snapshots of microplastic abundance. The large variances in concentration seen at sites visited more than once suggest that both long-term, passive monitoring of microplastic pollution and more detailed time-scale-specific investigations (such as diurnal and seasonal sampling) may provide more insight to the extent and duration of microplastic pollution for specific areas of aquatic systems.⁶⁸

Bibliography:

- (1) Mattsson, K.; Hansson, L.-A.; Cedervall, T. Nano-plastics in the aquatic environment. *Environ. Sci. Process. Impacts* **2015**, *17* (10), 1712–1721.
- (2) Eerkes-Medrano, D.; Thompson, R. C.; Aldridge, D. C. Microplastics in freshwater systems: A review of the emerging threats, identification of knowledge gaps and prioritisation of research needs. *Water Res.* **2015**, *75*, 63–82.
- (3) Foekema, E. M.; De Gruijter, C.; Mergia, M. T.; van Franeker, J. A.; Murk, A. J.; Koelmans, A. A. Plastic in North Sea Fish. *Environ. Sci. Technol.* **2013**, *47* (15), 8818–8824.
- (4) Driedger, A. G. J.; Dürr, H. H.; Mitchell, K.; Van Cappellen, P. Plastic debris in the Laurentian Great Lakes: A review. *J. Great Lakes Res.* **2015**, *41* (1), 9–19.
- (5) Magnusson, K.; Eliasson, K.; Fråne, A.; Haikonen, K.; Hultén, J.; Olshammar, M.; Stadmark, J.; Voisin, A. Swedish sources and pathways for microplastics to the marine environment. A review of existing data. **2016**, No. C 183, 1–87.
- (6) Nerland, I. L.; Halsband, C.; Allan, I.; Thomas, K. V. *Microplastics in marine environments: Occurrence, distribution and effects*; 2014.
- (7) Doughty, R.; Eriksen, M. Plastic Pollution: The Case for a Ban on Microplastics in Personal Care Products. *Tulane Environ. Law J.* **2014**, *27* (277), 1–22.
- (8) Crawford, C.; Quinn, B. *Microplastic Pollutants*; Elsevier Inc., 2016.
- (9) Arthur, C.; Baker, J.; Bamford, H. Proceedings of the International Research Workshop on the Occurrence, Effects, and Fate of Microplastic Marine Debris. *Group* **2009**, No. January, 530.
- (10) Masura, J.; Baker, J.; Foster, G.; Arthur, C. Laboratory methods for the analysis of microplastics in the marine environment: recommendations for quantifying synthetic particles in waters and sediments. *NOAA Tech. Memo. NOS-OR&R-48* **2015**, No. July, 1–29.
- (11) Enders, K.; Lenz, R.; Stedmon, C. A.; Nielsen, T. G. Abundance, size and polymer composition of marine microplastics 10–1000 µm in the Atlantic Ocean and their modelled vertical distribution. *Mar. Pollut. Bull.* **2015**, *100* (1), 70–81.
- (12) Hanvey, J. S.; Lewis, P. J.; Lavers, J. L.; Crosbie, N. D.; Pozo, K.; Clarke, B. O. A review of analytical techniques for quantifying microplastics in sediments. *Anal. Methods* **2017**, *9* (9), 1369–1383.
- (13) Hidalgo-Ruz, V.; Gutow, L.; Thompson, R. C.; Thiel, M. Microplastics in the marine environment: A review of the methods used for identification and quantification. ... *Sci. Technol.* **2012**, *46*, 3060–3075.
- (14) Wagner, M.; Scherer, C.; Alvarez-Muñoz, D.; Brennholt, N.; Bourrain, X.; Buchinger, S.; Fries, E.; Grosbois, C.; Klasmeier, J.; Marti, T.; et al. Microplastics in freshwater ecosystems: what we know and what we need to know. *Environ. Sci. Eur.* **2014**, *26* (1), 12.
- (15) Twiss, M. R. Standardized methods are required to assess and manage microplastic contamination of the Great Lakes system. *J. Great Lakes Res.* **2016**, *42* (5), 921–925.
- (16) Imhof, H. K.; Laforsch, C.; Wiesheu, A. C.; Schmid, J.; Anger, P. M.; Niessner, R.; Ivleva, N. P. Pigments and plastic in limnetic ecosystems: A qualitative and

- quantitative study on microparticles of different size classes. *Water Res.* **2016**, *98*, 64–74.
- (17) Taylor, M. L.; Gwinnett, C.; Robinson, L. F.; Woodall, L. C. Plastic microfibre ingestion by deep-sea organisms. *Sci. Rep.* **2016**, *6* (1), 33997.
- (18) Vandermeersch, G.; Van Cauwenberghe, L.; Janssen, C. R.; Marques, A.; Granby, K.; Fait, G.; Kotterman, M. J. J.; Diog??ne, J.; Bekaert, K.; Robbens, J.; et al. A critical view on microplastic quantification in aquatic organisms. *Environ. Res.* **2015**, *143*, 46–55.
- (19) Corcoran, P. L. Benthic plastic debris in marine and fresh water environments. *Environ. Sci. Process. Impacts* **2015**, *17* (8), 1363–1369.
- (20) Thompson, R. C.; Olsen, Y.; Mitchell, R. P.; Davis, A.; Steven, J.; John, A. W. G.; McGonigle, D.; Russell, A. E.; Science, S.; Series, N.; et al. Lost at Sea: Where Is All the Plastic? Author(s): Richard C. Thompson, Ylva Olsen, Richard P. Mitchell, Anthony Davis, Steven J. Rowland, Anthony W. G. John, Daniel McGonigle and Andrea E. Russell Source: *Science* (80-.). **2004**, *304* (5672), 838.
- (21) Woodall, L. C.; Sanchez-vidal, A.; Paterson, G. L. J.; Coppock, R.; Sleight, V.; Calafat, A.; Rogers, A. D.; Narayanaswamy, B. E.; Thompson, R. C. The deep sea is a major sink for microplastic debris Subject category : Subject Areas : Author for correspondence : **2014**.
- (22) Sivan, A. New perspectives in plastic biodegradation. *Curr. Opin. Biotechnol.* **2011**, *22* (3), 422–426.
- (23) Fischer, E. K.; Paglialonga, L.; Czech, E.; Tamminga, M. Microplastic pollution in lakes and lake shoreline sediments - A case study on Lake Bolsena and Lake Chiusi (central Italy). *Environ. Pollut.* **2016**, *213*, 648–657.
- (24) Faure, F.; Demars, C.; Wieser, O.; Kunz, M.; De Alencastro, L. F. Plastic pollution in Swiss surface waters: Nature and concentrations, interaction with pollutants. *Environ. Chem.* **2015**, *12* (5), 582–591.
- (25) Biginagwa, F. J.; Mayoma, B. S.; Shashoua, Y.; Syberg, K.; Khan, F. R. First evidence of microplastics in the African Great Lakes: Recovery from Lake Victoria Nile perch and Nile tilapia. *J. Great Lakes Res.* **2016**, *42* (1), 146–149.
- (26) Eriksen, M.; Mason, S.; Wilson, S.; Box, C.; Zellers, A.; Edwards, W.; Farley, H.; Amato, S. Microplastic pollution in the surface waters of the Laurentian Great Lakes. *Mar. Pollut. Bull.* *77* (1–2), 177–182.
- (27) Zbyszewski, M.; Corcoran, P. L.; Hockin, A. Comparison of the distribution and degradation of plastic debris along shorelines of the Great Lakes, North America. *J. Great Lakes Res.* **2014**, *40* (2), 288–299.
- (28) Free, C. M.; Jensen, O. P.; Mason, S. A.; Eriksen, M.; Williamson, N. J.; Boldgiv, B. High-levels of microplastic pollution in a large, remote, mountain lake. *Mar. Pollut. Bull.* **2014**, *85* (1), 156–163.
- (29) Mason, S. A.; Kammin, L.; Eriksen, M.; Aleid, G.; Wilson, S.; Box, C.; Williamson, N.; Riley, A. Pelagic plastic pollution within the surface waters of Lake Michigan, USA. *J. Great Lakes Res.* **2016**, *42* (4), 753–759.
- (30) Anderson, P. J.; Warrack, S.; Langen, V.; Challis, J. K.; Hanson, M. L.; Rennie, M. D. Microplastic contamination in Lake Winnipeg, Canada. *Environ. Pollut.* **2017**, *225*, 223–231.

- (31) Baldwin, A. K.; Corsi, S. R.; Mason, S. A. Plastic Debris in 29 Great Lakes Tributaries: Relations to Watershed Attributes and Hydrology. *Environ. Sci. Technol.* **2016**, *50* (19), 10377–10385.
- (32) Rocha-Santos, T.; Duarte, A. C. A critical overview of the analytical approaches to the occurrence, the fate and the behavior of microplastics in the environment. *TrAC - Trends Anal. Chem.* **2015**, *65*, 47–53.
- (33) Claessens, M.; Meester, S. De; Landuyt, L. Van; Clerck, K. De; Janssen, C. R. Occurrence and distribution of microplastics in marine sediments along the Belgian coast. *Mar. Pollut. Bull.* **2011**, *62* (10), 2199–2204.
- (34) Ivar do Sul, J. A.; Spengler, Â.; Costa, M. F. Here, there and everywhere. Small plastic fragments and pellets on beaches of Fernando de Noronha (Equatorial Western Atlantic). *Mar. Pollut. Bull.* **2009**, *58* (8), 1236–1238.
- (35) Reddy, M. S.; Shaik Basha; Adimurthy, S.; Ramachandraiah, G. Description of the small plastics fragments in marine sediments along the Alang-Sosiya ship-breaking yard, India. *Estuar. Coast. Shelf Sci.* **2006**, *68* (3–4), 656–660.
- (36) Fries, E.; Dekiff, J. H.; Willmeyer, J.; Nuelle, M.-T.; Ebert, M.; Remy, D. Identification of polymer types and additives in marine microplastic particles using pyrolysis-GC/MS and scanning electron microscopy. *Environ. Sci. Process. Impacts* **2013**, *15* (10), 1949.
- (37) Tagg, A. S.; Sapp, M.; Harrison, J. P.; Ojeda, J. J. Identification and Quantification of Microplastics in Wastewater Using Focal Plane Array-Based Reflectance Micro-FT-IR Imaging. *Anal. Chem.* **2015**, *87* (12), 6032–6040.
- (38) Nuelle, M.-T.; Dekiff, J. H.; Remy, D.; Fries, E. A new analytical approach for monitoring microplastics in marine sediments. *Environ. Pollut.* **2014**, *184*, 161–169.
- (39) Law, K. L.; Moret-Ferguson, S.; Maximenko, N. A.; Proskurovski, G.; Peacock, E. E.; Hafner, J.; Reddy, C. M. Plastic Accumulation in the North. *Science* (80-.). **2010**, *329* (September), 1185–1189.
- (40) United States Census Bureau www.census.gov/newsroom/releases/.
- (41) Statistics Canada <http://www12.statcan.gc.ca/census-recensement/2016/dp-pd/prof/index.cfm?Lang=E>.
- (42) Sterner, R. W.; Ostrom, P.; Ostrom, N. E.; Klump, J. V.; Steinman, A. D.; Dreelin, E. A.; Zanden, M. J. Vander; Fisk, A. T. Grand challenges for research in the Laurentian Great Lakes. **2017**, No. Eccc 2016.
- (43) Allan, A. J. D.; McIntyre, P. B.; Smith, S. D. P.; Halpern, B. S.; Boyer, G. L. Title : Joint analysis of stressors and ecosystems services to enhance restoration effectiveness. **2012**, No. April.
- (44) Shaw, D. G.; Day, R. H. Colour- and form-dependent loss of plastic micro-debris from the North Pacific Ocean. *Mar. Pollut. Bull.* **1994**, *28* (1), 39–43.
- (45) De Witte, B.; Devriese, L.; Bekaert, K.; Hoffman, S.; Vandermeersch, G.; Cooreman, K.; Robbens, J. Quality assessment of the blue mussel (*Mytilus edulis*): Comparison between commercial and wild types. *Mar. Pollut. Bull.* **2014**, *85* (1), 146–155.
- (46) Dekiff, J. H.; Remy, D.; Klasmeier, J.; Fries, E. Occurrence and spatial distribution of microplastics in sediments from Norderney. *Environ. Pollut.* **2014**, *186*, 248–

256.

- (47) Marine & Environmental Research Institute. Guide to Microplastic Identification. 2015, pp 1–15.
- (48) Tsuge, S.; Ohtani, H.; Watanabe, C. Pyrolysis GCMS data book of synthetic polymers. Elsevier: Amsterdam 2012, p 390.
- (49) Kusch, P. Pyrolysis-Gas Chromatography / Mass Spectrometry of Polymeric Materials. *Adv. Gas Chromatogr. Agric. Biomed. Ind. Appl.* **2012**, 21.
- (50) Kusch, P. Identification of Synthetic Polymers and Copolymers by Analytical Pyrolysis Gas Chromatography/Mass Spectrometry. *J. Chem. Educ.* **2014**, *91*, 1725–1728.
- (51) Hendrickson, E. S.; Robertson, I. J. An evaluation of illicit stimulants and metabolites in wastewater effluent and the Wisconsin river along the Central Wisconsin river basin. *Acta Sci. Pol. Form. Circumiectus* **2015**, *14* (3), 65–74.
- (52) Alvarado, J. S.; Carnahan, J. W. Reductive Pyrolysis for the Determination of Aqueous Sulfur-Compounds With a Helium Microwave-Induced Plasma. *Anal. Chem.* **1993**, *65* (22), 3295–3298.
- (53) Fischer, M.; Scholz-Böttcher, B. M. Simultaneous Trace Identification and Quantification of Common Types of Microplastics in Environmental Samples by Pyrolysis-Gas Chromatography-Mass Spectrometry. *Environ. Sci. Technol.* **2017**, *51* (9), 5052–5060.
- (54) Abdulla, H. A. N.; Minor, E. C.; Dias, R. F.; Hatcher, P. G. Changes in the compound classes of dissolved organic matter along an estuarine transect: A study using FTIR and ¹³C NMR. *Geochim. Cosmochim. Acta* **2010**, *74* (13), 3815–3838.
- (55) Dris, R.; Gasperi, J.; Saad, M.; Mirande, C.; Tassin, B. Synthetic fibers in atmospheric fallout: A source of microplastics in the environment? *Mar. Pollut. Bull.* **2016**, *104* (1–2), 290–293.
- (56) Nelson, D.; Elmer, H.; Held, R.; Forsythe, D.; Casey, S.; Stirratt, H.; Bergeron, D.; Lichtkoppler, F.; Schomberg, J.; Dolor, M. NOAA Technical Memorandum GLERL-153 LAURENTIAN GREAT LAKES BASIN CLIMATE CHANGE ADAPTATION in consultation with. *Environ. Res.* 1–43.
- (57) News, M. P. R. Minnesota Senate bans soaps with plastic microbeads <https://www.mprnews.org/story/2015/05/05/microbeads>.
- (58) Eriksen, M.; Cummins, A.; Maximenko, N.; Thiel, M.; Lattin, G.; Wilson, S.; Hafner, J.; Zellers, A.; Rifman, S. Plastic Pollution in the South Pacific Subtropical Gyre. *Plast. Eng.* **69** (5), 38.
- (59) Moore, C. J.; Moore, S. L.; Leecaster, M. K.; Weisberg, S. B. A comparison of plastic and plankton in the North Pacific Central Gyre. *Mar. Pollut. Bull.* **2001**, *42* (12), 1297–1300.
- (60) Toraman, H. E.; Dijkmans, T.; Djokic, M. R.; Van Geem, K. M.; Marin, G. B. Detailed compositional characterization of plastic waste pyrolysis oil by comprehensive two-dimensional gas-chromatography coupled to multiple detectors. *J. Chromatogr. A* **2014**, *1359* (x), 237–246.
- (61) Shim, W. J.; Hong, S. H.; Eo, S. E. Identification methods in microplastic analysis: a review. *Anal. Methods* **2017**, *9* (9), 1384–1391.
- (62) Käßler, A.; Fischer, D.; Oberbeckmann, S.; Schernewski, G.; Labrenz, M.;

- Eichhorn, K. J.; Voit, B. Analysis of environmental microplastics by vibrational microspectroscopy: FTIR, Raman or both? *Anal. Bioanal. Chem.* **2016**, *408* (29), 8377–8391.
- (63) Li, H.; Minor, E. C. Biogeochemical characteristics of settling particulate organic matter in Lake Superior: A seasonal comparison. *Org. Geochem.* **2015**, *85*, 76–88.
- (64) Huang, J.-C. Miscibility of PVC with chlorinated PE and chlorinated PVC. *Int. J. Polym. Mater.* **2003**, *52* (8), 673–683.
- (65) Obbard, R. W.; Sadri, S.; Wong, Y. Q.; Khitun, A. A.; Baker, I.; Richard, C. Earth 's Future Global warming releases microplastic legacy frozen in Arctic Sea ice Earth 's Future. **2014**, 1–6.
- (66) Lubowski, R. N.; Vesterby, M.; Bucholtz, S.; Baez, A.; Roberts, M. J. *Major Uses of Land in the United States, 2007; 2006; Vol. 77.*
- (67) Patterson, C.; Tilton, G.; Inghram, M. Age of the Earth. *Am. Assoc. Adv. Sci.* **1955**, *121* (January, 21st, 1955), 69–75.
- (68) Kim, M.; Hyun, S. Estimation of the Environmental Load of High- and Low-Density Polyethylene From South Korea Using a Mass Balance Approach. *Arch. Environ. Contam. Toxicol.* **2015**, *69* (3), 367–373.

Tables:

<u>Polymer</u>	<u>Density (g•cm⁻³)</u>
Polyethylene (PE, low to high density)	0.89-0.98
Polypropylene (PP)	0.85-0.92
Polystyrene (PS)	1.04-1.08 (0.01-0.04 if expanded)
Polyvinyl Chloride (PVC)	1.38-1.41
Polyethylene Terephthalate (PET)	1.38-1.41

Table I: Reference polymers and their respective densities. Data from Driedger, et al., 2015.

<u>Sample Site</u>	<u>Sample Site Label</u>	<u>Coordinates:</u>
Inner Estuary/Harbor	Site A	46°44.15'N, 92°07.96'W
Near Wastewater Treatment Plant	Site B	46°45.43'N, 92°06.97' W
Dock, Harbor	Site C	46°45.86'N, 92°05.68' W
Near 21 st Ave	Site D	46°48.08'N, 92°03.89' W
Duluth Outskirts/Palmers	Site E	46°52.60'N, 91°54.08'W
Two Harbors	Site F	46°59.02' N, 91°39.42' W
Western Mooring	Site G	47°19.266'N, 89°50.465'W
Port Wing	Site H	46°48.01' N, 91°23.44'W
Wisconsin Forest	Site I	46°44.25'N, 91°41.03' W
Superior/Wisconsin Point	Site J	46°41.46' N, 91°57.52'W
Nemadji River	Site K	46°42.51' N, 92°01.77' W
Center Bay	Site L	46°47.04' N, 91°49.23' W

Table II Sample sites, labels, and coordinates.

<u>Morphological Category</u>	<u>Description</u>
Fibers/Fibrous Bundles	Length of the particle is at least 3 times greater than the width. Particle should be uniform throughout and cylindrical (ignoring fraying and biofouling). The upper size limit of <5.0 mm in all dimensions was exempted for fibers. Fibrous bundles treated as a single particle due to difficulty in untangling, unaccountable breaking of fibers when untangling, and assumed mobilization in the environment as a bundle.
Films	Length and width are significantly larger than depth of particle, where depth is likely to be paper thin. Films are typically malleable. The particle should appear to be a 2-dimensional particle.
Foams	Reminiscent of styrofoam. Has a sponge or bubble-like structure.
Fragments	Irregularly shaped, typically rigid particle. The particle should appear to be 3-dimensional
Spheres/Beads	Relatively spherical or circular. Likely to be a primary microplastic.
Other	Particle does not conform solely to 1 category and/or has features not described by the other morphological categories.

Table III: Morphological categories and their respective definitions.

<u>Sample Site</u>	<u>Total Number of Particles Isolated</u>	<u>Total Number of Fibers</u>	<u>Total Number of Films</u>	<u>Total Number of Fragments</u>	<u>Total Number of Foams</u>	<u>Total Number of Spheres/Beads</u>	<u>Total Number of Others</u>
Site A (Estuary/Harbor, 8/15/16)	19	10	0	7	0	0	2
Site B (Estuary/Harbor, 8/15/16)	45	21	2	20	0	0	2
*Site C (Estuary/Harbor, 8/15/16)	31	1	4	21	1	2	2
Site J (Shoreline, 8/15/16)	18	2	3	10	0	2	1
Site E (Shoreline, 8/17/16)	55	32	8	13	0	0	2
**Site H (Shoreline, 8/17/16)	87	17	45	23	0	2	0
Site I (Shoreline, 8/17/16)	48	9	12	22	1	0	4
Site F (Shoreline, 8/17/16)	28	10	4	14	0	0	0
Site E (Shoreline, 9/28/16)	13	13	0	0	0	0	0
Site G (Open Water, 9/30/16)	79	46	15	15	0	0	3
*Site L (Open Water, 9/30/16)	15	14	0	1	0	0	0
Site H (Shoreline, 9/30/16)	42	26	2	14	0	0	0
Site D (Shoreline, 3/19/17)	19	12	5	2	0	0	0
Site L (Open Water, 5/9/17)	50	5	16	27	0	0	2
Site K (Estuary/Harbor, 7/5/17)	35	11	5	11	1	4	3
Total	584	229	121	200	3	10	21
Mean	39	15	8.1	13	0.2	0.7	1.4

Table IV: Frequency of particles by morphology at all surface water sites. Fibers were the most commonly observed particles, followed by fragments, and then films. Beads/spheres, foams, and others observed in lesser quantities. *Denotes concentrations that may be biased due microscopic exams conducted before the introduction of a melt test. **Denotes concentration that may be biased high due to inconsistent melt test applied.

Sample Site	Number of Microplastic Particles Isolated	Number of Particles Used in Characterization	Tow Length (m)	Areal Concentration (particles•km⁻²)	Total Mass Collected (mg)	Mass/Area (mg•km⁻²)	Number Particles In Sampling Ambient Control	Corrected Number of Isolated Particles	Corrected Areal Concentration (particles•km⁻²)
Site A (Estuary/Harbor, 8/15/16)	19	-	517	43,000	< 0.1	N/A	0	16	36,000
Site B (Estuary/Harbor, 8/15/16)	45	6	450	120,000	0.3	789	2	40	110,000
*Site C (Estuary/Harbor, 8/15/16)	31	16	1489	24,000	0.9	692	1	27	21,000
Site J (Shoreline, 8/15/16)	18	5	1031	21,000	0.5	568	1	14	16,000
Site E (Shoreline, 8/17/16)	55	6	1498	43,000	0.4	308	3	49	38,000
**Site H (Shoreline, 8/17/16)	87	10	1438	83,000	2.6	2,167	2	82	78,000
Site I (Shoreline, 8/17/16)	48	5	1484	38,000	0.4	308	1	44	35,000
Site F (Shoreline, 8/17/16)	28	-	1553	21,000	< 0.1	N/A	1	24	18,000
Site E (Shoreline, 9/28/16)	13	5	1366	11,000	0.4	333	12	<5	<MDL
Site G (Open Water, 9/30/16)	79	8	1632	57,000	2.1	1,500	2	74	54,000
*Site L (Open Water, 9/30/16)	15	7	478	37,000	0.5	1,220	2	10	25,000
Site H (Shoreline, 9/30/16)	42	-	1235	40,000	< 0.1	N/A	10	29	28,000
Site D (Shoreline, 3/19/17)	19	5	1253	18,000	0.1	91	1	15	14,000
Site L (Open Water, 5/9/17)	50	-	1916	31,000	4.7	2,938	0	47	29,000
Site K (Estuary/Harbor, 7/5/17)	35	-	766	54,000	2.3	3,538	1	31	48,000
Total	584	73	18106	-	15.2	-	39	502	-
Mean	39.1	7.3	1208	43,000	1.3	1,200	2.6	36	39,000

Table V: Surface water sites with number microplastic particles collected, number of particles used in characterization, tow length, areal concentrations, and particles collected from sampling ambient control samples, corrected number of particles collected, and corrected areal concentrations. *Denotes concentrations that may be biased due microscopic exams conducted before the introduction of a melt test. **Denotes concentration that may be biased high due to inconsistent melt test applied.

<u>Sample Site</u>	<u>Cores Composited</u>	<u>Particles Isolated From Flocculent Sediments</u>	<u>Flocculent Sediment Concentration (particles•m⁻²)</u>	<u>Corrected Number of Particles From Flocculent Sediments</u>	<u>Corrected Flocculent Concentration (particles•m⁻²)</u>	<u>Particles From 0-2 cm Sediments</u>	<u>0-2 cm Sediment Areal Concentration (particles•m⁻²)</u>	<u>Corrected Number of Particles From 0-2 cm Sediments</u>	<u>Particles In Sampling Ambient Control</u>
Site E (Shoreline, 9/28/16)	1	8	1000	<5	<MDL	4	510	<5 (under MDL)	12
Site G (Open Water, 9/30/16)	2	21	1,300	16	1,000	3	190	<5 (under MDL)	2
Site K (Shoreline, 7/5/17)	3	1	40	<5	<MDL	0	0	<5 (under MDL)	1
Total	8	30	-	16	-	7	-	-	15
Mean	2.7	10	617	5.3	333	2.3	617	-	5

Table VI: Sediment sites with number microplastic particles collected, number of particles used in characterization, area of sediment encompassed/number of cores used, areal concentrations, and particles collected from sampling and sample processing ambient control samples.

<u>QC Polymer and Morphology</u>	<u>Original Mass (mg)</u>	<u>Mass Recovery (%)</u>	<u>Original Count (Number of Particles)</u>	<u>Count Recovery (%)</u>
Good Fellow MDPE Powder (~350 μm)	Rep 1: 10 Rep 2: 20	Rep 1: 90% (9 mg) Rep 2: 95% (19 mg) Mean: 93%	Rep 1: 646 Rep 2: 1,265	90.1% (582 particles) 95.81% (1,212 particles) Mean: 93.0%
Good Fellow PS Powder (~250 μm)	Rep 1: 13 Rep 2: 20	Rep 1: 92% (12 mg) Rep 2: 95% (19 mg) Mean: 94%	Rep 1: 1,095 Rep 2: 1,577	77.0% (843 particles) 79.96% (1,261 particles) Mean: 78.5%
Good Fellow PET Powder (~300 μm)	Rep 1: 19 Rep 2: 21	Rep 1: 79% (15mg) Rep 2: 52% (11 mg) Mean: 66%	Rep 1: 1,064 Rep 2: 1,176	83.9% (893 particles) 77.6% (913 particles) Mean: 80.8%
Good Fellow PVC Powder (~250 μm)	Rep 1: 17 Rep 2: 16	Rep 1: 10% (2 mg) Rep 2: 6% (1 mg) Mean: 8%	Rep 1: 3,859 Rep 2: 3,632	16.1% (622 particles) 7.00% (253 particles) Mean: 11.6%
Sigma Aldrich PP Ground Amorphous Particles (size range varies)	Rep 1: 16 Rep 2: 19	Rep 1: 63% (10 mg) Rep 2: 71% (14 mg) Mean: 67%	Rep 1: 358 Rep 2: 3,355	82.1% (294 particles) 71.0% (252 particles) Mean: 76.6%

Table VII: Recoveries by mass and by count for each standard polymer used in method testing; Rep 1 and Rep 2 refer to replicate separation tests. Mass recoveries primarily were dictated by density, where lower density polymers PE and PS exhibited greater recoveries and heavier polymers PET and PVC exhibited moderate and low recoveries. While PP is a lower density polymer, moderate mass recoveries were observed; this was attributed to the standard being manually ground and loss of particles smaller than the 180 μm nylon filter. Counts largely reflected trends observed in mass recoveries, but with greater recoveries for PP and PET and less recoveries for PS.

Sample Site	Number of Particles From Supernatant	Number of Particles From Pellet	Total Particles Extracted from Sample	Recovery of Particles from Supernatant
Site A (Estuary/Harbor, 8/15/16)	12	7	19	63%
Site B (Estuary/Harbor, 8/15/16)	41	4	45	91%
Site J (Shoreline, 8/15/16)	15	3	18	83%
Site E (Shoreline, 8/17/16)	24	31	55	44%
**Site H (Shoreline, 8/17/16)	83	4	87	95%
Site I (Shoreline, 8/17/16)	41	7	48	85%
Site F (Shoreline, 8/17/16)	26	3	28	89%
Site E (Shoreline, 9/28/16)	9	4	13	69%
Site G (Open Water, 9/30/16)	67	12	79	85%
Site H (Shoreline, 9/30/16)	26	16	42	62%
Site D (Shoreline., 3/19/17)	15	4	19	75%
Site L (Open Water, 5/9/17)	47	3	50	94%
Site K (Estuary/Harbor, 7/5/17)	23	12	35	65%
Total	429	110	538	-
Mean	33	8.5	41	77%

Table VIII: Density separation efficiency upon the number of microplastic particles isolated from supernatants and pellets of surface water samples. Sites C (Dock harbor, 8/15/17) and L (center bay, 9/30/17) were not included here due to prevalent cotton misidentification, and therefore, efficiency could not be confidently established for these samples. A mean 77% recovery implied that the use of NaCl for density separation and isolation of microplastic particles from surface waters is fairly effective, but should only be used for work where highly accurate and precise data is sought after.

Figures:

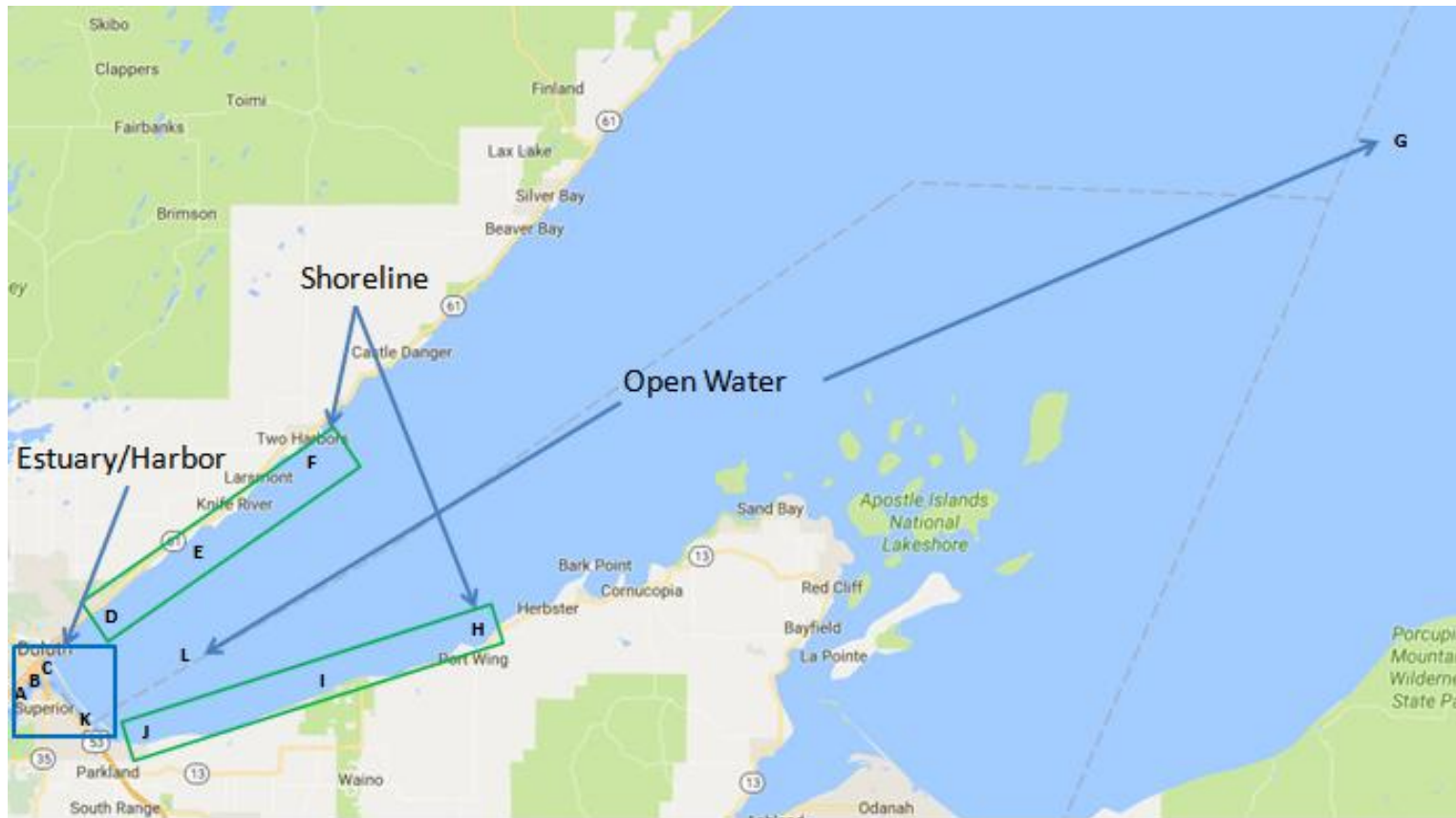


Figure I: Sample site map with defined regions. Image obtained via Google Maps© 2016 data.

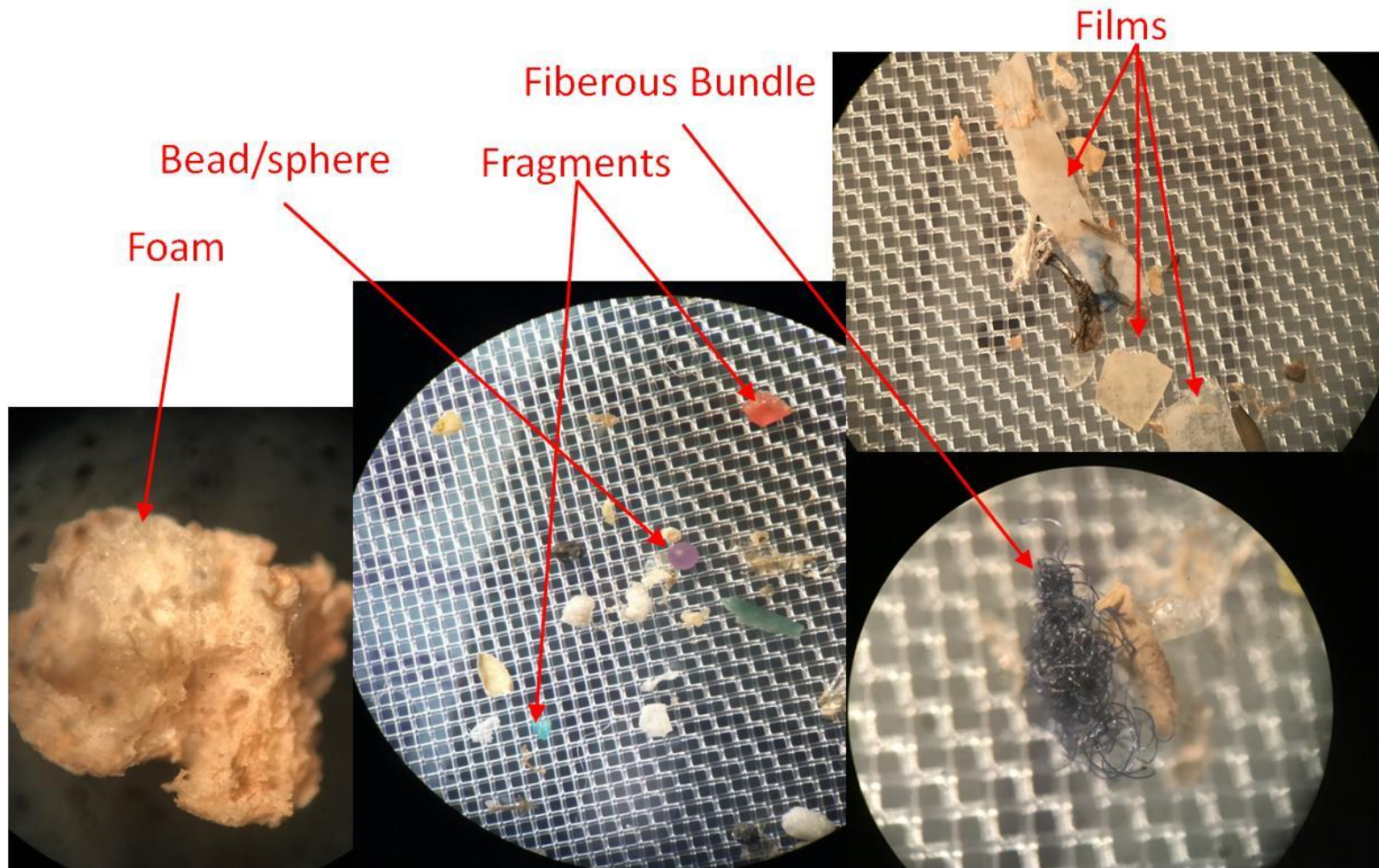


Figure II: Examples of morphological categories observed during microscopic examinations.

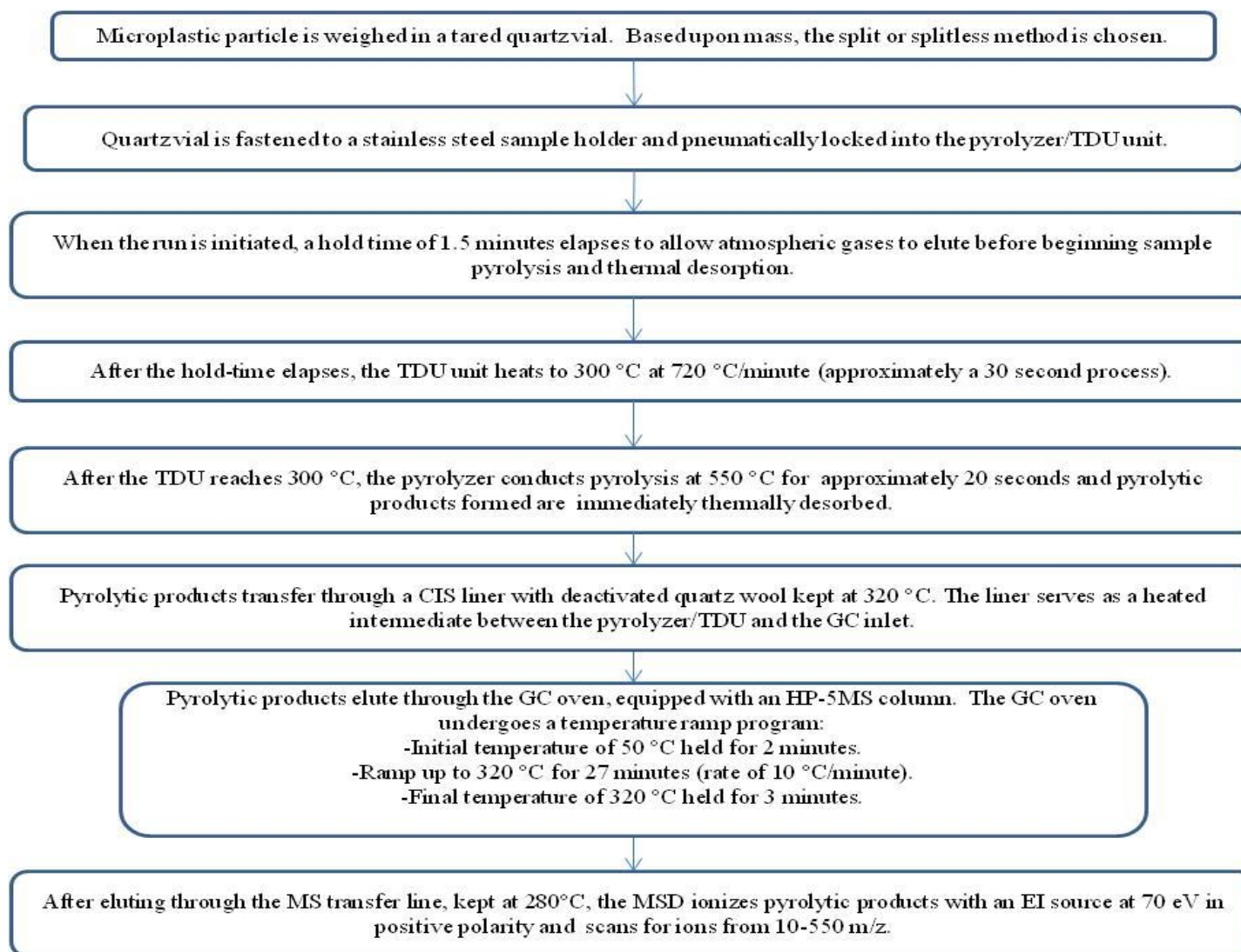


Figure III: Pyr-GC/MS method flow-chart

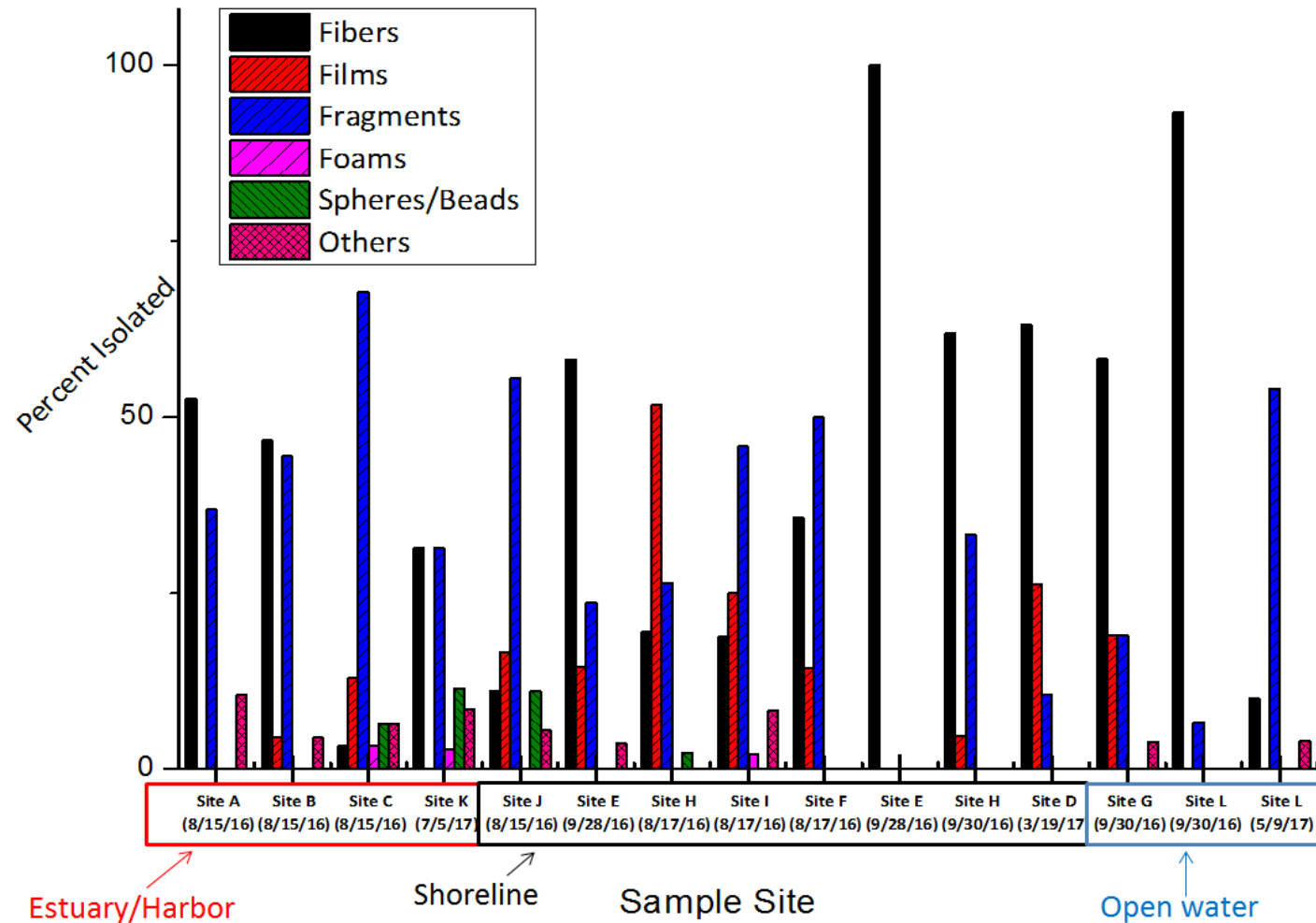


Figure IV: Particle morphology by percent of total particles collected for each surface water site. Regions established in Figure 1 are labeled accordingly. Dominant morphology varied between fibers, fragments, and films depending on the sample site. The frequency of fibers throughout sample sites suggested that atmospheric deposition and greywater/wastewater effluents are significant sources of microplastic particle in Lake Superior. Films and fragments, typically secondary microplastic particles, were likely transported via land run-off, effluents, and riverine inputs.

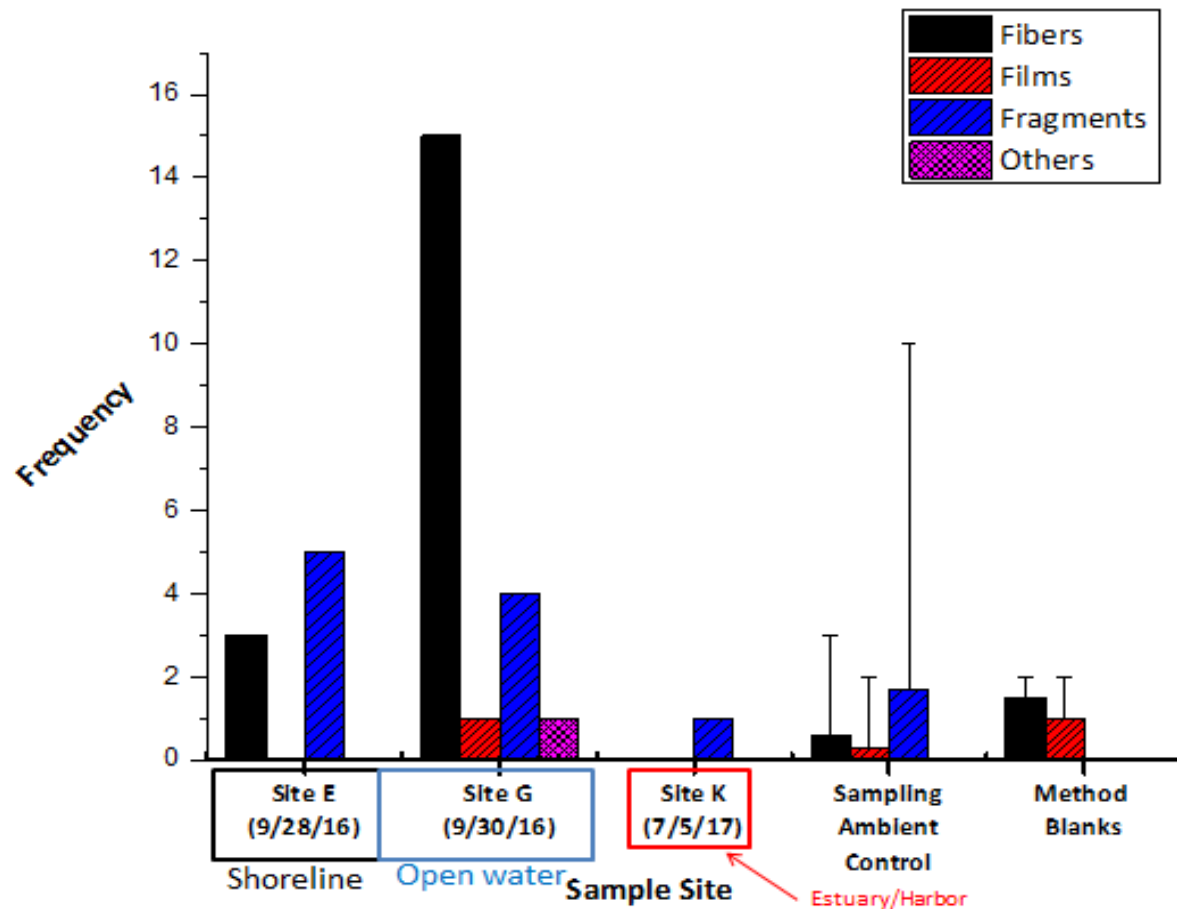


Figure V: Number of particles observed by morphology for flocculent sediment samples and average particle frequency for sampling ambient control samples and for method blanks. Error bars on each column for the ambient control samples and method blanks represent the maximum number of particles observed for the respective morphological category. Due to the extent of particles ambiently contaminating controls and method blanks, only 1 flocculent sediment concentration, Western Mooring, could be reported with confidence after corrections were applied ($1,000 \text{ particles} \cdot \text{m}^{-2}$).

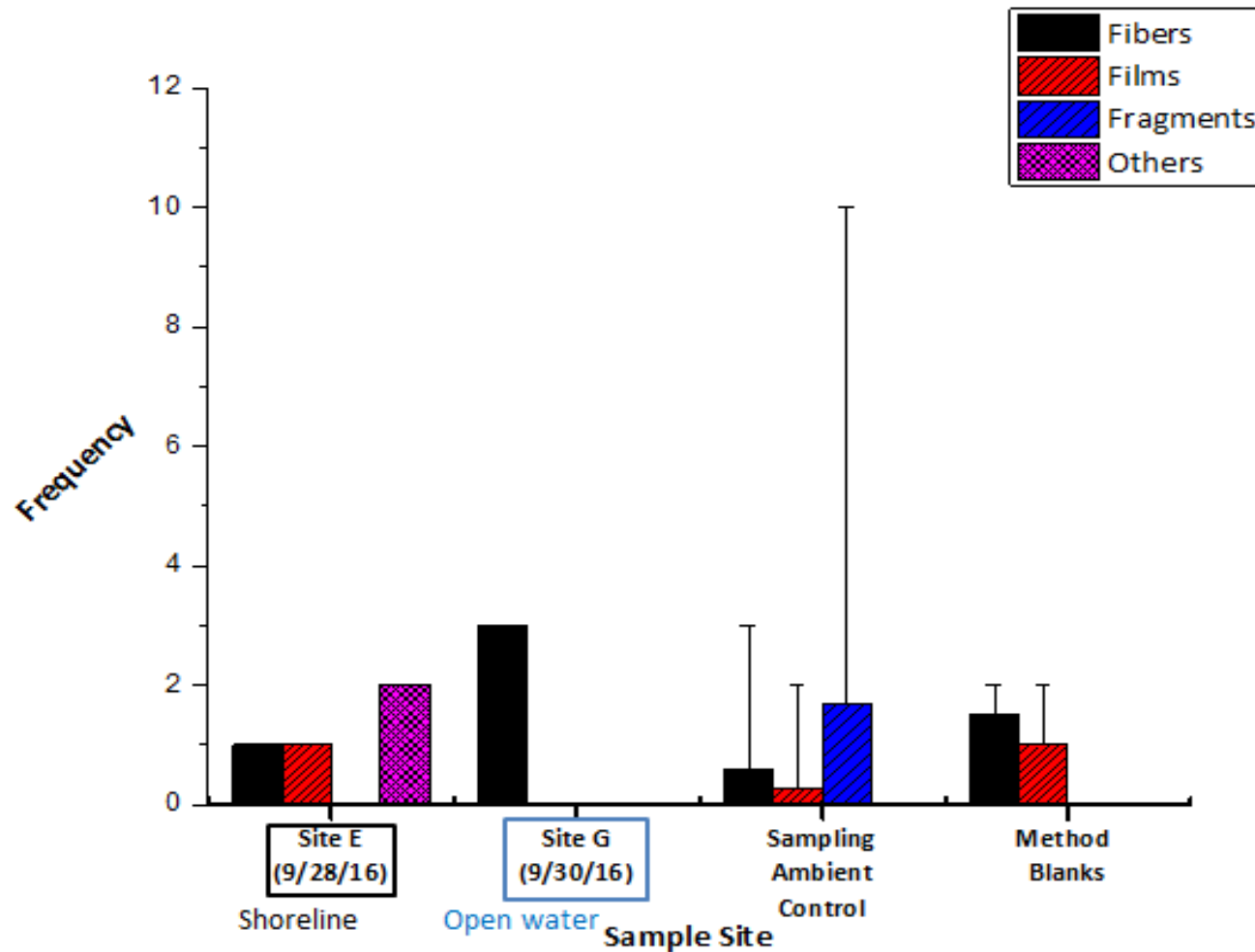


Figure VI: Number of particles observed by morphology for 0-2 cm consolidated sediment samples and average particle frequency for sampling ambient control samples and for sample processing ambient control samples. Error bars on each column for the ambient control samples and method blanks represent the maximum number of particles observed for the respective morphological category. Due to the extent of contamination in sampling ambient control samples and method blanks, none of the 0-2 cm consolidated sediment concentrations could be reported with confidence after corrections.

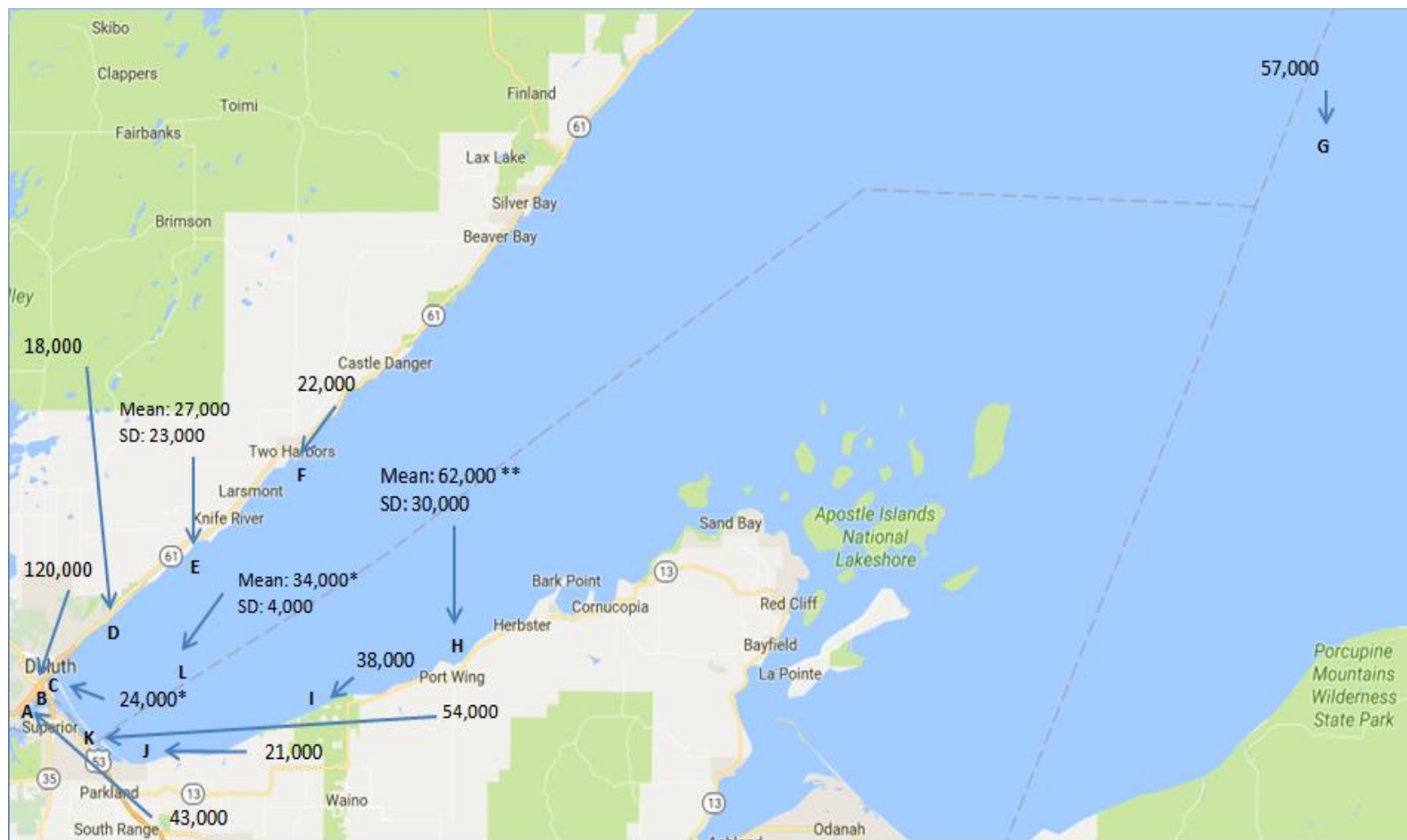


Figure VII: Map of surface water sample sites with uncorrected areal concentrations (particles•km⁻²). *Denotes concentrations that may be biased due microscopic exams conducted before the introduction of a melt test. **Denotes concentration that may be biased high due to inconsistent melt test applied.

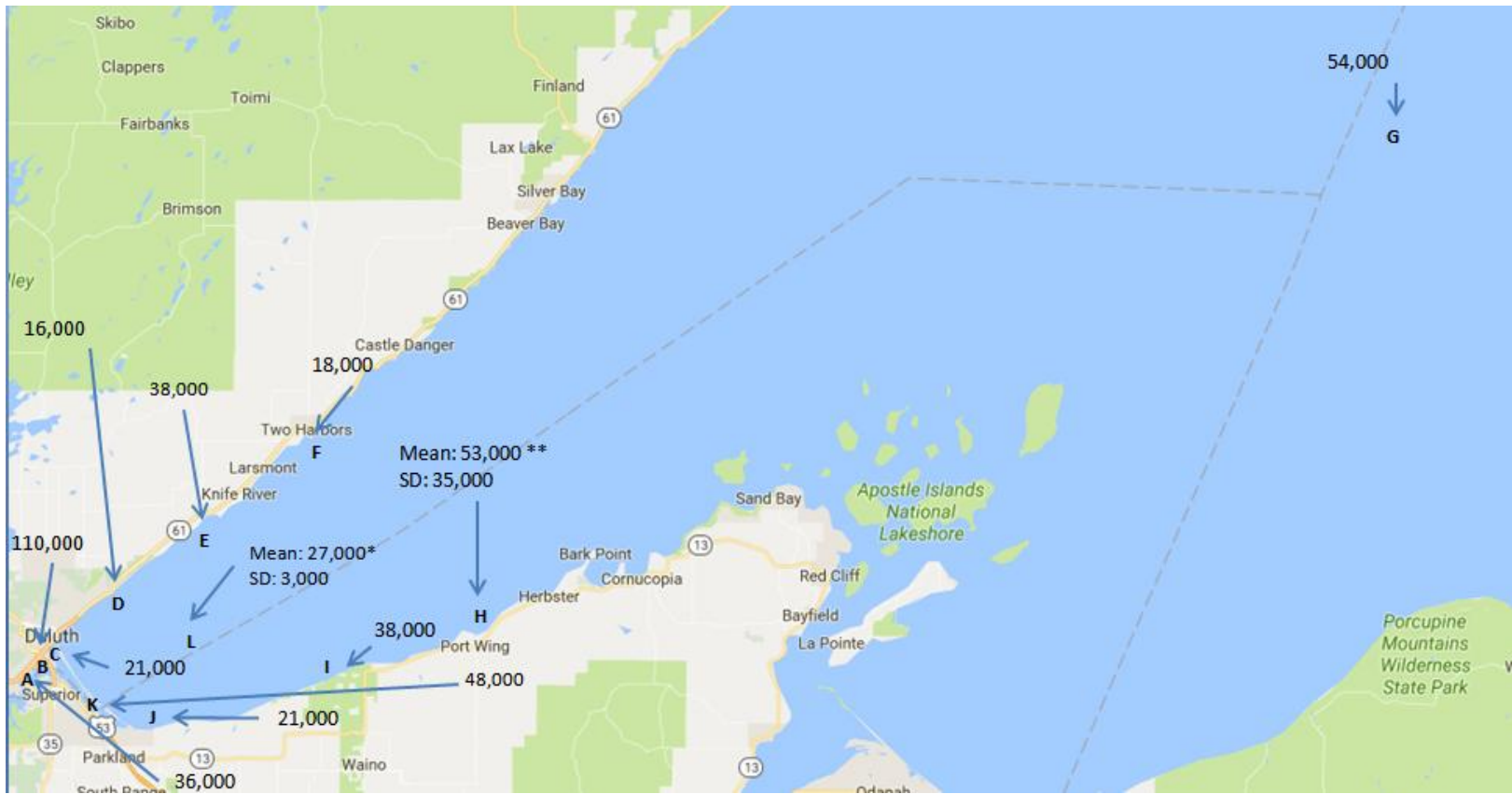


Figure VIII: Map of surface water sample sites with corrected areal concentrations (particles•km⁻²). *Denotes concentrations that may be biased due microscopic exams conducted before the introduction of a melt test. **Denotes concentration that may be biased high due to inconsistent melt test applied.

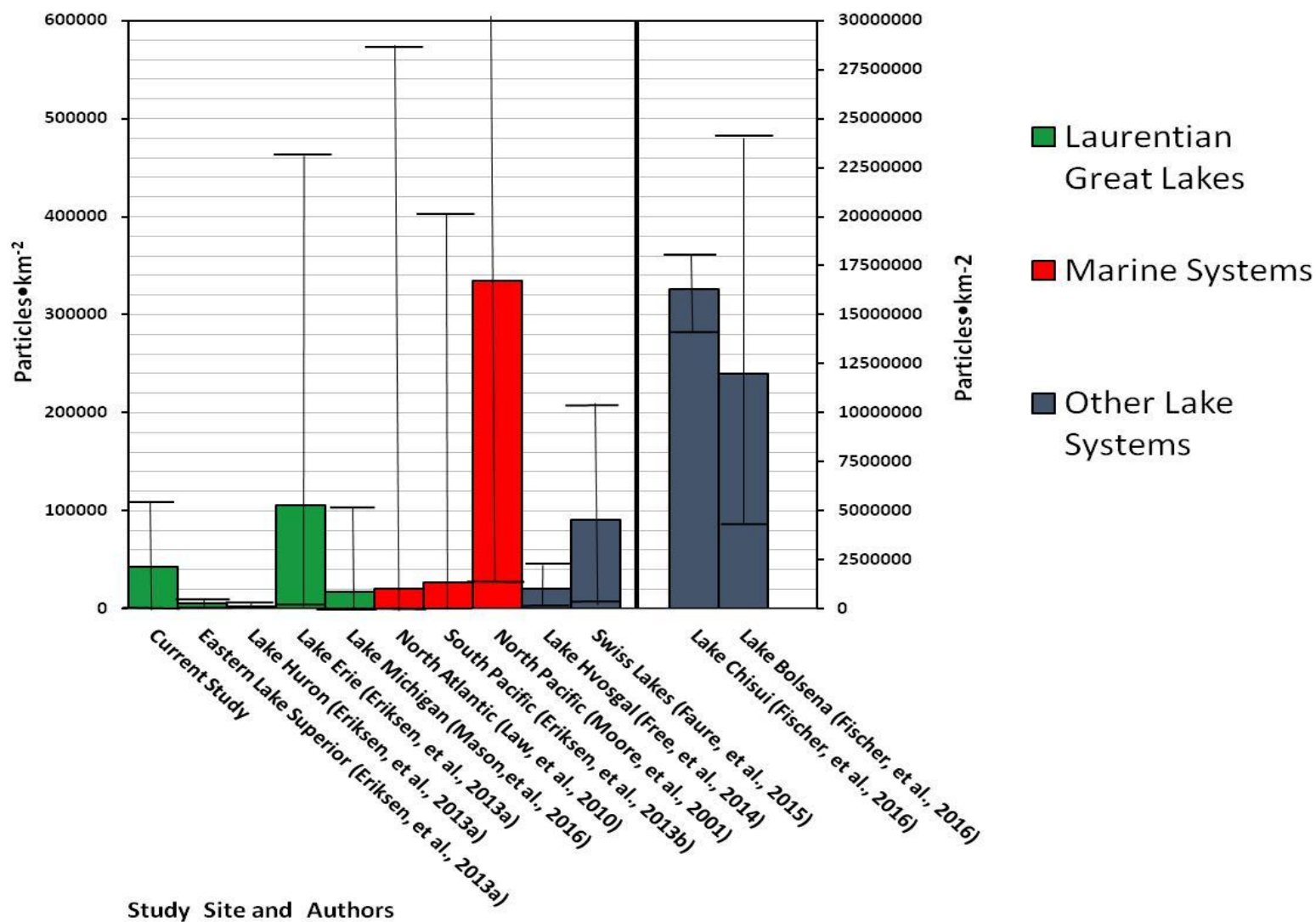


Figure IX: Comparison between the current study, microplastic studies regarding the Laurentian Great Lakes, marine systems, and other inland lake systems. The large bars represent average areal concentrations, while error bars represent minimum and maximum areal concentrations (all in particles·km⁻²).

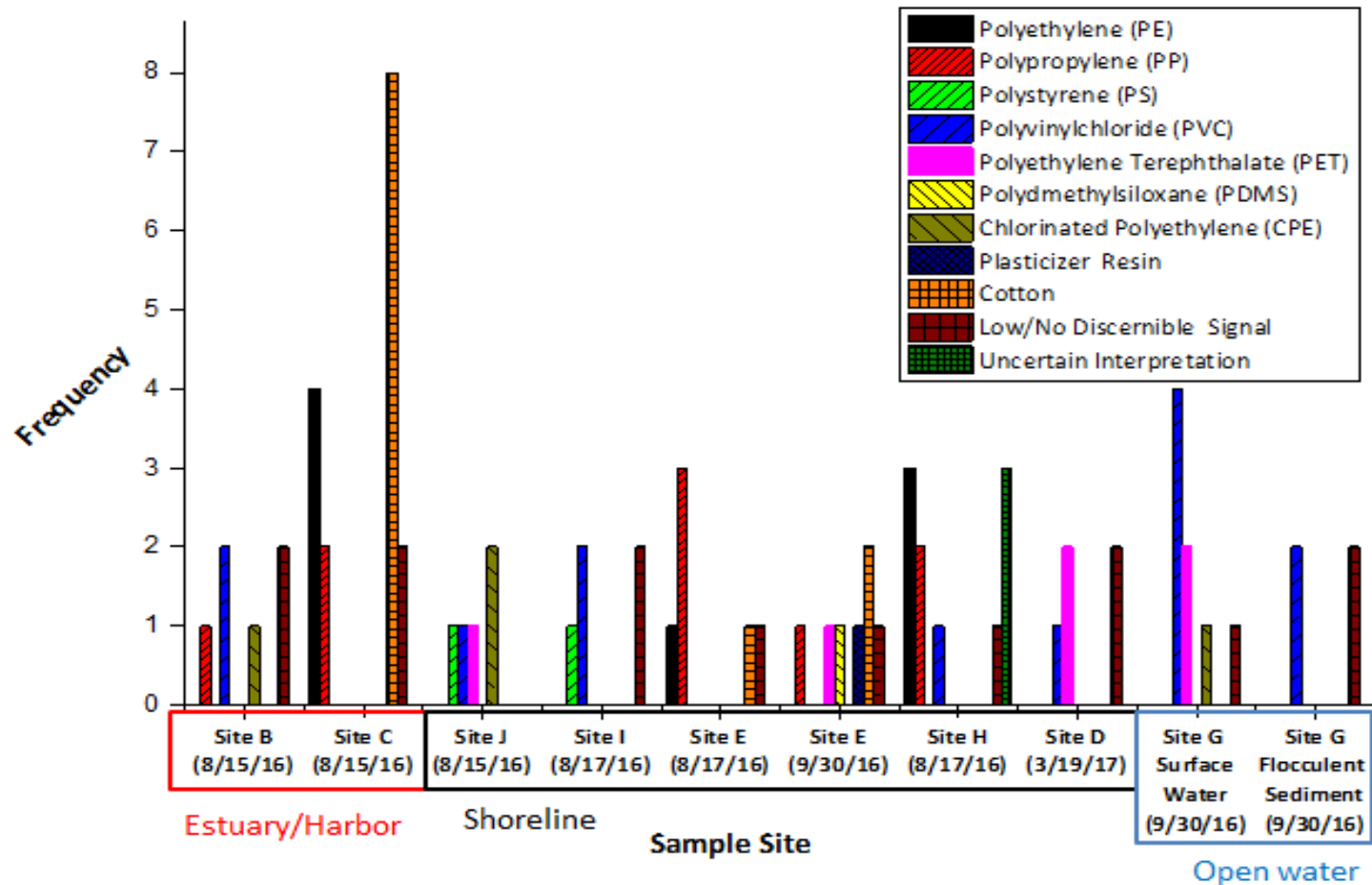


Figure X: Frequency of particles identified as various polymers at each analyzed surface water site as determined by Pyr-GC/MS. In descending order of most frequently observed plastic polymers: PVC (13), PP (9), PE (8), PET (7), CPE (4), PS (2), PDMS (1), and didecyl phthalate resin (1). Cotton fibers were commonly misidentified in samples prior to the introduction of the melt test (11). Particles with no or low signals (14) were frequently observed; these particles were typically fibers or fragments. In 3 instances, pyrograms could not be interpreted with certainty.

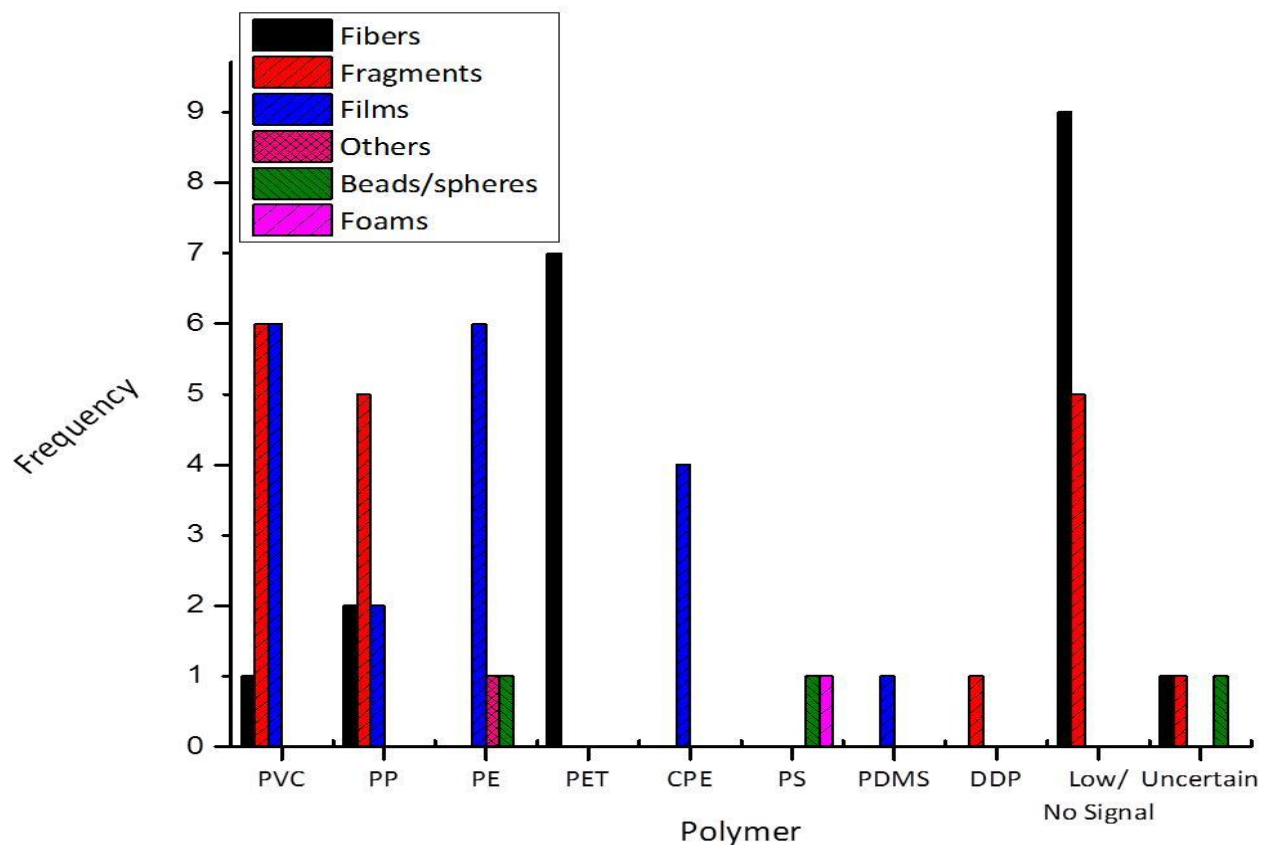


Figure XI: Frequency of particles identified as various polymers by morphological categories. Low or no discernible signals were common, particularly when analyzing fibrous particles. Fibrous particles, when yielded discernible signals, tended to be PET, with lesser quantities of PP, PVC, and an uncertain interpretation in one instance. Fragments and films were composed of a variety of different polymers. Fragments were most commonly composed of PVC and PP, while films were typically PVC and PE.

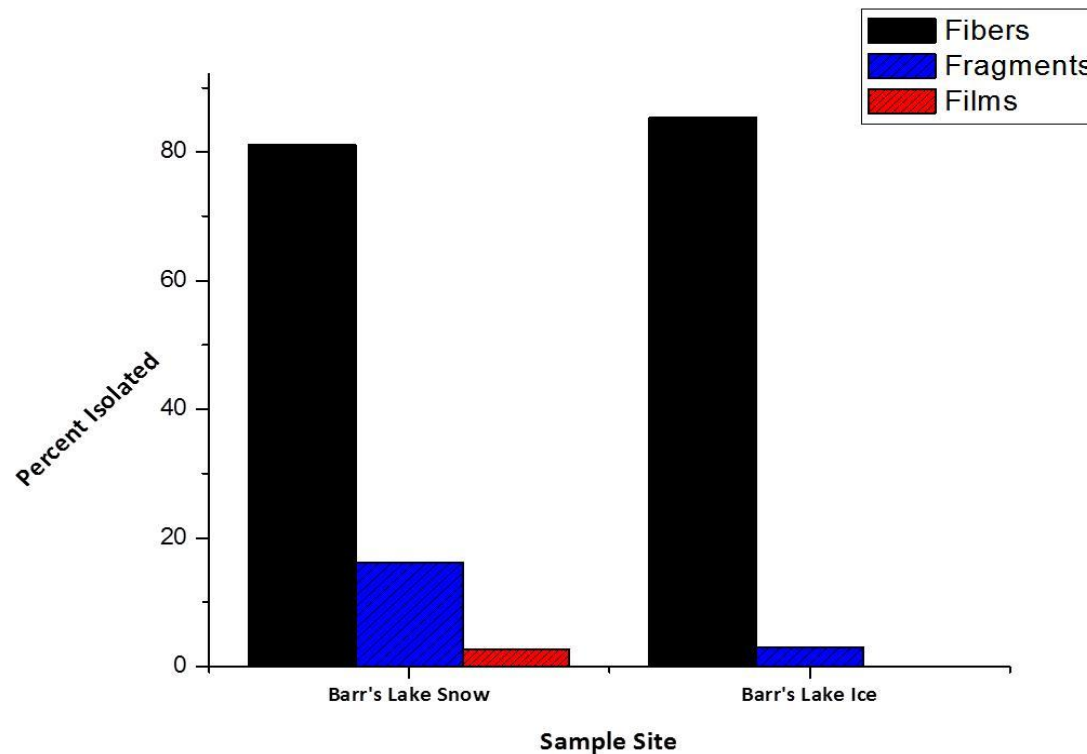


Figure XII: Particle morphology by percent of total particles collected for snow and ice sample from Barr's Lake. Fibers were the most common particles isolated from all samples where microplastic particles were present (snow: 30, ice: 29). For the snow sample, 15 of the fibers included here were suspected to have originated from sampler gloves. Fragments (6 and 5, respectively) were observed in lesser quantities, as well as a film particle for the snow sample. Similarly to Lake Superior, the prevalence of fibers suggested that atmospheric deposition and greywater/wastewater were more significant sources of microplastics to Barr's Lake.

Appendix:

Sampling Ambient Control Sample	Number of Microplastic Particles Isolated	Total Number of Fibers	Total Number of Films	Total Number of Fragments
Site A (Estuary/Harbor, 8/15/16)	0	0	0	0
Site B (Estuary/Harbor, 8/15/16)	2	1	1	0
Site C (Estuary/Harbor, 8/15/16)	1	0	1	0
Site J (Shoreline, 8/15/16)	1	1	0	0
Site E (Shoreline, 8/17/16)	3	0	0	3
Site H (Shoreline, 8/17/16)	2	0	0	2
Site I (Shoreline, 8/17/16)	1	0	0	1
Site F (Shoreline, 8/17/16)	1	0	0	1
Site E (Shoreline, 9/28/16)	12	2	2	8
Site G (Open Water, 9/30/16)	2	2	0	0
Site L (Open Water, 9/30/16)	2	3	0	0
Site H (Shoreline, 9/30/16)	10	0	0	10
Site D (Shoreline, 3/19/17)	1	0	0	1
Site L (Open Water, 5/9/17)	0	0	0	0
Site K (Estuary/Harbor, 7/5/17)	1	1	0	0
Total	39	9	4	26
Mean	2.6	0.6	0.27	1.7

Table I: Particles isolated from sampling ambient control samples. Total number of microplastic particles isolated ranged from 0-12. Fragments were most commonly observed (26), followed by fibers (9), and films (4). Fragments were particularly prevalent in ambient controls of Duluth Outskirts (9/28/16) and Port Wing (9/30/16). The average number isolated from sampling ambient control samples (2.6) was used in conjunction with the average number isolated from method blanks (2.5) for creating an MDL of 5 particles.

<u>Surface Water Lab Processing Ambient Sample</u>	<u>Number of Microplastic Particles Isolated</u>	<u>Total Number of Fibers</u>	<u>Total Number of Films</u>	<u>Total Number of Fragments</u>	<u>Total Number of Others</u>
Site A (Estuary/Harbor, 8/15/16)	6	2	1	3	0
Site B (Estuary/Harbor, 8/15/16)	10	5	0	4	1
Site C (Estuary/Harbor, 8/15/16)	3	2	0	1	0
Site J (Shoreline, 8/15/16)	7	2	1	4	0
Site E (Shoreline, 8/17/16)	9	7	1	1	0
Site H (Shoreline, 8/17/16)	0	0	0	0	0
Site I (Shoreline, 8/17/16)	7	5	0	2	0
Site F (Shoreline, 8/17/16)	18	3	0	15	0
Site E (Shoreline, 9/28/16)	4	4	0	0	0
Site G (Open Water, 9/30/16)	7	4	0	3	0
Site L (Open Water, 9/30/16)	0	0	0	0	0
Site H (Shoreline, 9/30/16)	20	4	0	12	4
Site D (Shoreline, 3/19/17)	1	0	0	1	0
Site L (Open Water, 5/9/17)	4	3	0	1	0
Site K (Estuary/Harbor, 7/5/17)	4	2	0	2	0
Total	100	43	3	49	5
Mean	6.7	2.9	0.2	3.3	0.3

Table II: Particles isolated from surface water sample processing ambient control samples. Total number of microplastic particles isolated ranged from 0-20. Fragments were most commonly observed (49), followed by fibers (43), others (5), and films (3). Fragments were particularly prevalent in ambient controls of Two Harbors and Port Wing (9/30/16).

<u>Flocculent Sediment Lab Processing Ambient Sample</u>	<u>Total Number of Microplastic Particles</u>	<u>Total Number of Fibers</u>	<u>Total Number of Fragments</u>
Site E (Shoreline, 9/28/16)	3	2	1
Site G (Open Water, 9/30/16)	6	2	4
Site K (Estuary/Harbor, 7/5/17)	0	0	0
Total	9	4	5
Mean	3	1.3	1.7

Table III: Particles isolated from flocculent sediment sample processing ambient controls. Total number of microplastic particles isolated ranged from 0-6. Fragments (5) and fibers (4) were the only morphological categories observed.

<u>0-2 cm Sediment Processing Ambient Sample</u>	<u>Total Number of Microplastic Particles</u>	<u>Total Number of Fibers</u>	<u>Total Number of Films</u>	<u>Total Number of Fragments</u>
Site E (Shoreline, 9/28/16)	5	2	0	3
Site G (Open Water, 9/30/16)	3	1	1	1
Site K (Estuary/Harbor, 7/5/17)	1	1	0	0
Total	9	4	1	4
Mean	3	1.3	0.3	1.3

Table IV: Particles isolated from flocculent sediment sample processing ambient controls. Total number of microplastic particles isolated ranged from 1-5. Fragments (4) and fibers (4) were most commonly observed, with an instance of a film isolated from an ambient control sample.

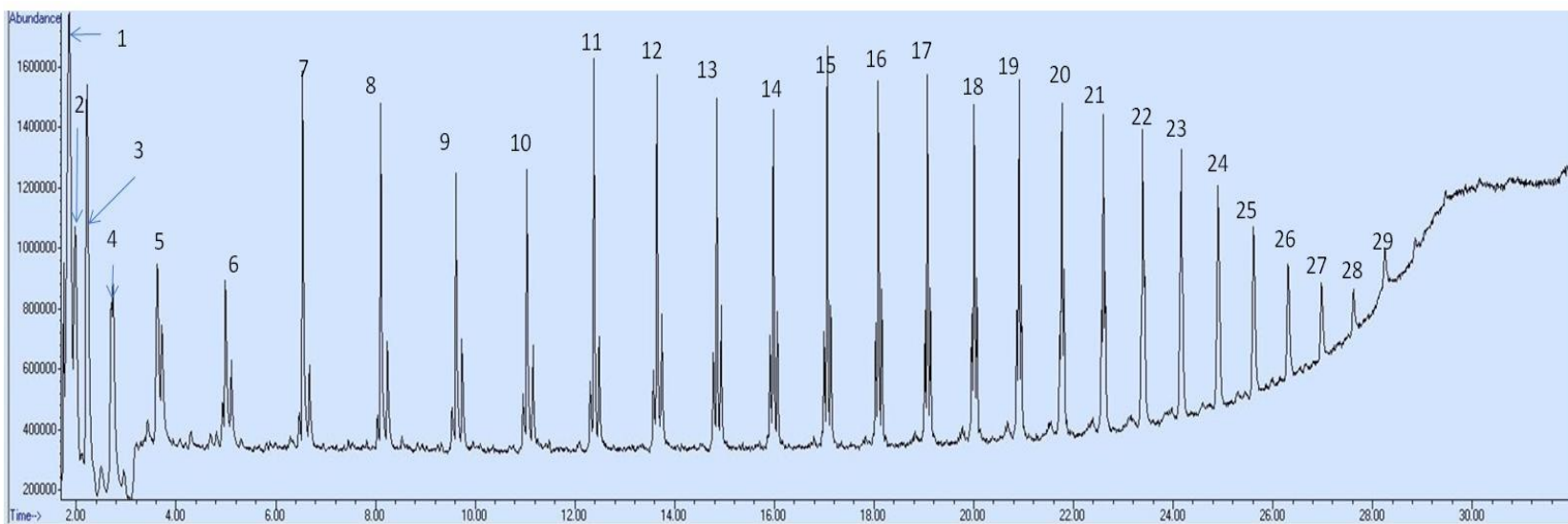


Figure I: Pyrogram of PE identified particle with pyrolytic products numerically labeled. Pyrolysis of PE yielded triplet peaks, where the first peak corresponded with terminal alkydienes, followed by a terminal alkene, and an alkane of the same carbon chain length. Groups of peaks increased 1 carbon in chain length with each successive peak over time. Resolution faded between peaks in triplet over time, favoring formation of the alkene. Labels correspond with table below.

Peak #	Retention Time (± 0.5 minutes)	Pyrolytic Product	Parent m/z
1	1.8	1-propene/propane/1-butene	42/44/56
2	2.0	1-pentene	70
3	2.2	1-hexene	84
4	2.7	1-heptene	98
5-21	3.6-22.6	Terminal diene, alkene, and alkane for carbon chain lengths C8-C24	110-334, 112-336, 114-338
22-29	23.4-28.2	C25-C32 terminal alkene	350-448

Table V: Pyrolytic products of PE with retention times and parent m/z's.

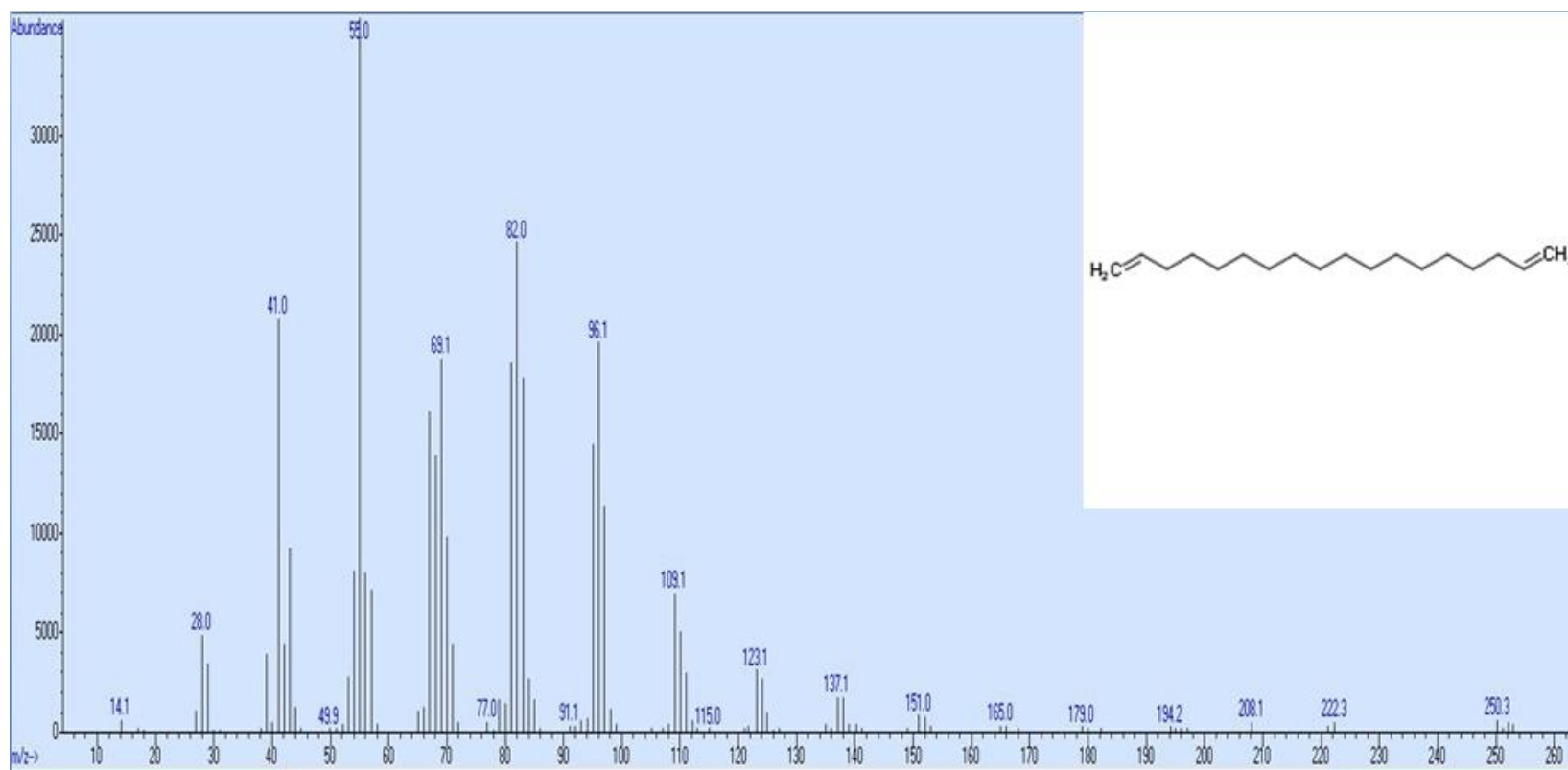


Figure II: Mass spectra of PE pyrolytic product 1,17-octadecadiene. Alkyldienes were the first peaks in triplets of PE pyrograms. Parent m/z of 250. Image of structure from www.chemspider.com

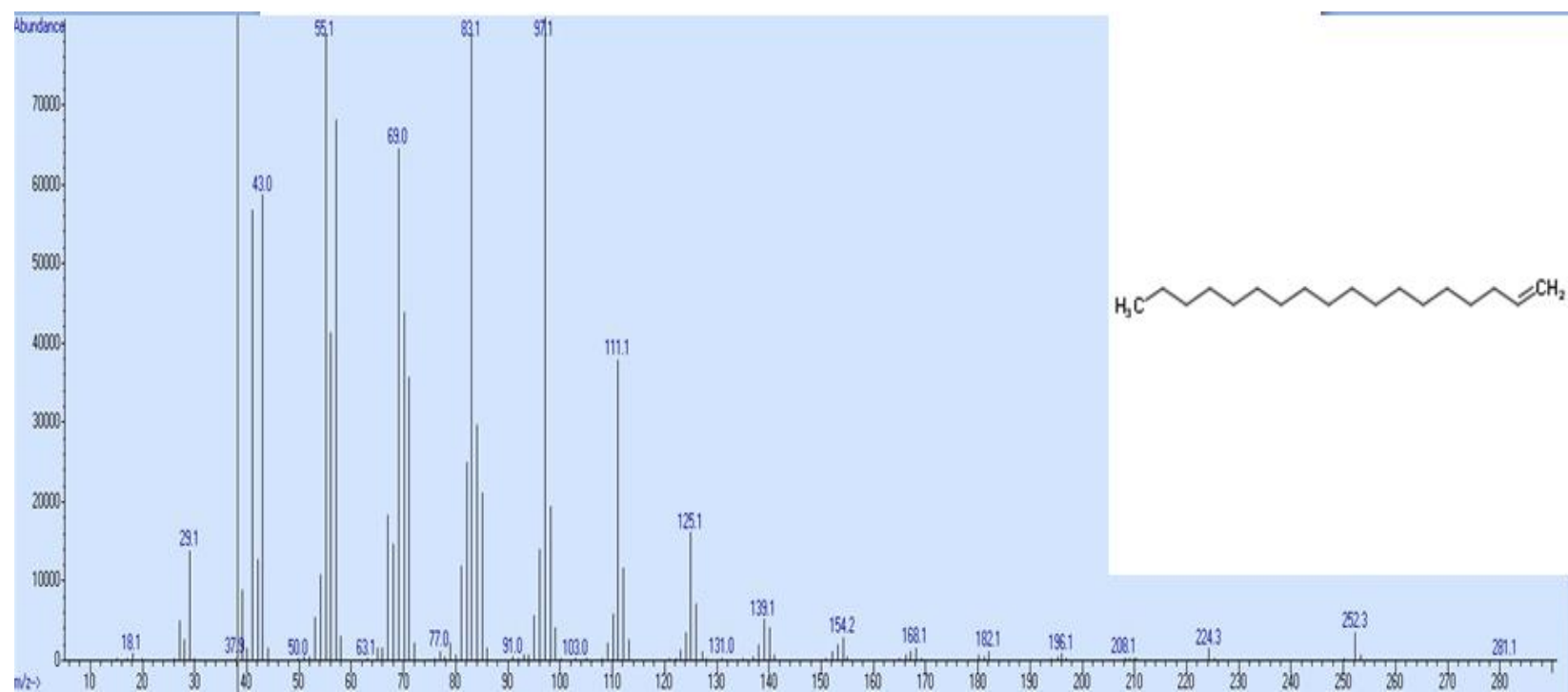


Figure III: Mass spectra of PE pyrolytic product 1-octadecene. Alkenes were the middle peaks in triplets of PE pyrograms. Parent m/z of 252. Image of structure from www.chemspider.com

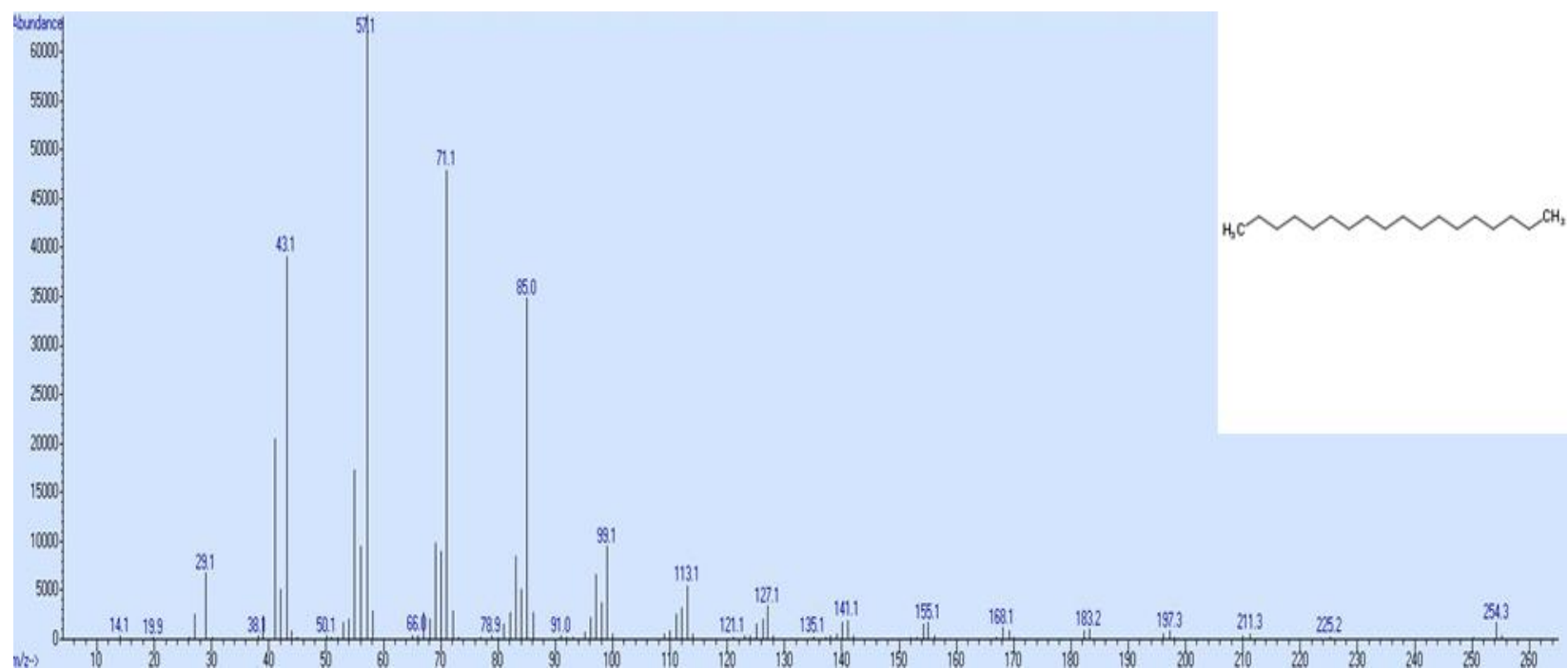


Figure IV: Mass spectra of PE pyrolytic product octadecane. Alkanes were the last peaks in triplets of PE pyrograms. Parent m/z of 254. Image of structure from www.chemspider.com

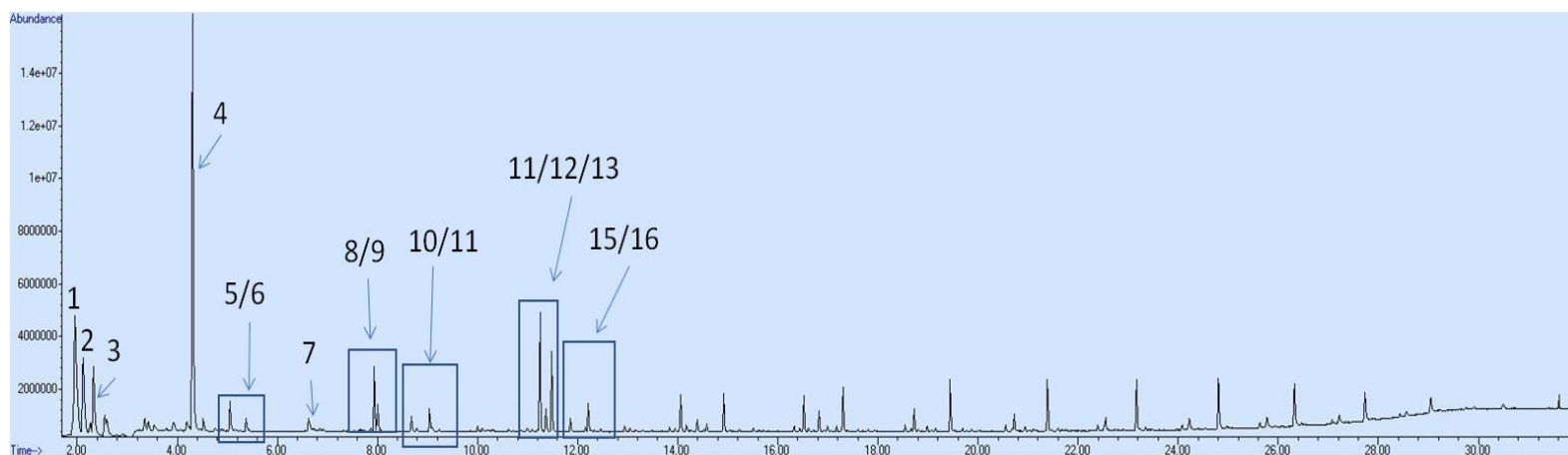


Figure V: Pyrogram of PP identified particle with pyrolytic products numerically labeled. The dominant pyrolytic product of PP was 2,4-dimethylheptene. Subsequent groups of peak 2 or 3 roughly formed a pattern, where the first peak alternated in having either 1 carbon longer in chain length or methylation of the second to last carbon. The other peaks were stereoisomers of the first peak. Labels correspond with table below.

Peak #	Retention Time (± 0.5 minutes)	Pyrolytic Product	Parent m/z
1	2.0	Propene	42
2	2.1	Pentane	72
3	2.3	2-methyl-1-pentene	84
4	4.3	2,4-Dimethyl-heptene	126
5/6	5.0/5.3	2, 4, 6-trimethyl-1-heptene; 2, 4, 6-trimethyl-1, 6-heptadiene	140/138
7	6.6	4, 6-dimethyl-2-nonene (meso)	154
8, 9	7.9	2, 4, 6-trimethyl-1-nonene (1st, meso; 2nd, racemic)	168
10/11	8.7/9.0	2, 4, 6, 8-tetramethyl-1-nonene (racemic form); 2, 4, 6, 8-tetramethyl-1, 8-nonadiene (racemic form)	182/180
12/13/14	11.2/11.4/11.5	C15: 2, 4, 6, 8-tetramethyl-1-undecene (isotactic); 2, 4, 6, 8-tetramethyl-1-undecene (heterotactic); 2, 4, 6, 8-tetramethyl-1-undecene (syndiotactic).	210
15/16	11.9/12.2	2, 4, 6, 8, 10-pentamethyl-1-undecene (isotactic); 2, 4, 6, 8, 10-pentamethyl-1, 10-undecadiene (isotactic).	224/222

Table VI: Pyrolytic products of PP with retention times and parent m/z's.

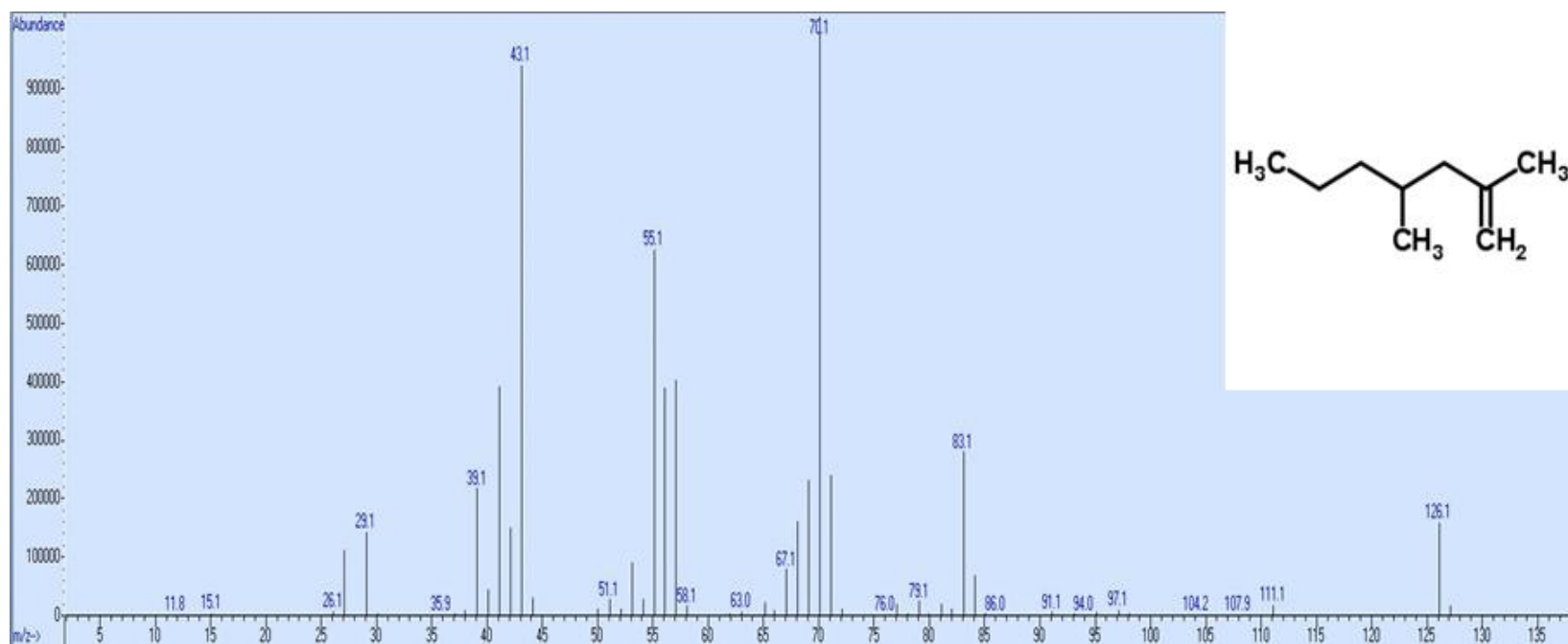


Figure VI: Mass spectra of PP pyrolytic product 2,4-dimethylheptene, the dominant pyrolytic product of PP. Parent m/z of 126. Image of structure from www.chemspider.com

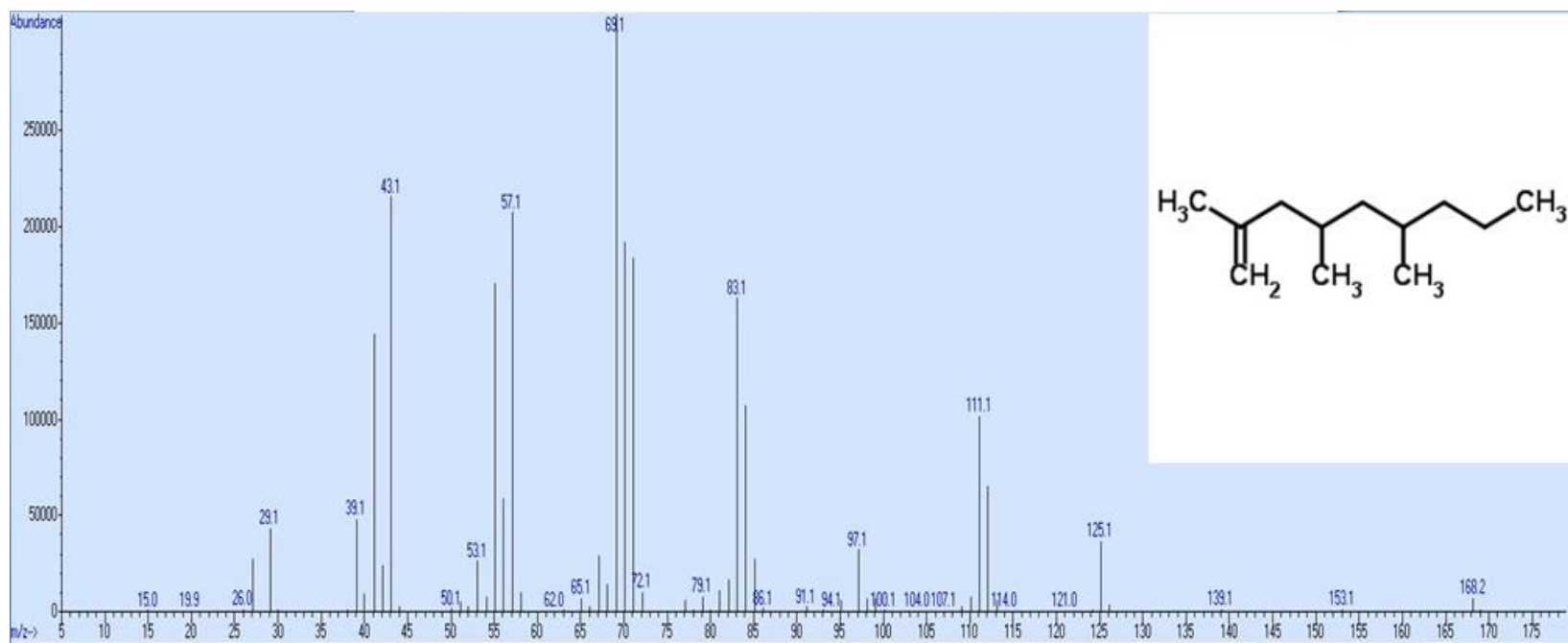


Figure VII: Mass spectra of PP pyrolytic product 2,4,6-trimethylnonene. Parent m/z of 168. Image of structure from www.chemspider.com.

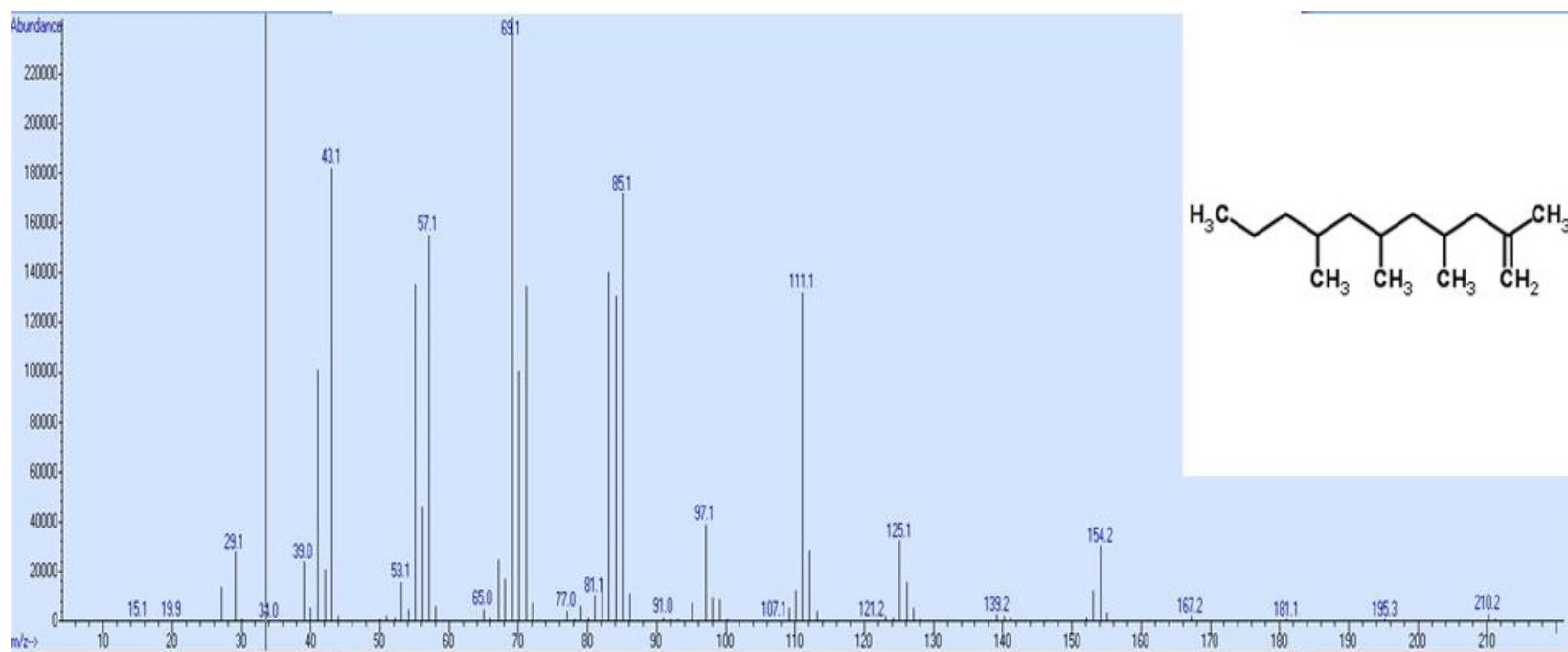


Figure VIII: Mass spectra of PP pyrolytic product 2,4,6,8-tetramethylundecene. Parent m/z of 210. Image of structure from www.chemspider.com.

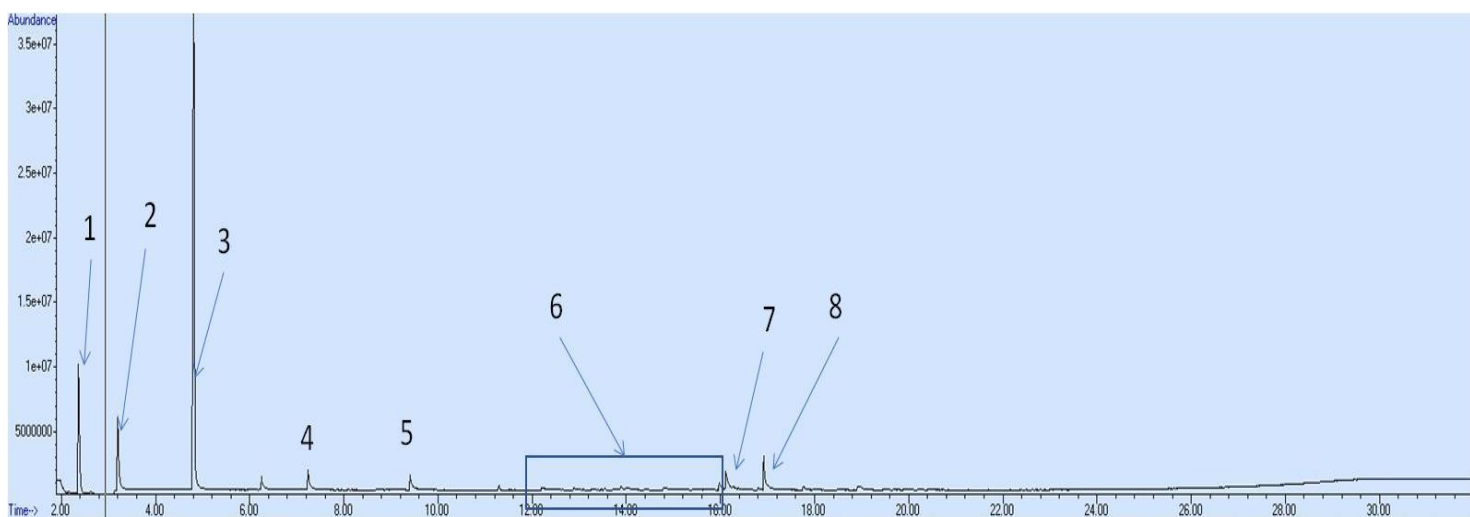


Figure IX: Pyrogram of PS identified particle with pyrolytic products numerically labeled. The dominant pyrolytic product was styrene, the monomer. Other pyrolytic products include various VOCs and PAHs. Labels correspond with table below.

Peak #	Retention Time (±0.5 minutes)	Pyrolytic Product	Parent m/z
1	2.4	Benzene	78
2	3.2	Toluene	92
3	4.8	Styrene	104
4	7.2	Indene	116
5	9.4	Naphthalene	128
6	-	Various (biphenyl, fluorene, bibenzyl)	Varies
7	16.9	Anthracene	178

Table VII: Pyrolytic products of PS with retention times and parent m/z's.

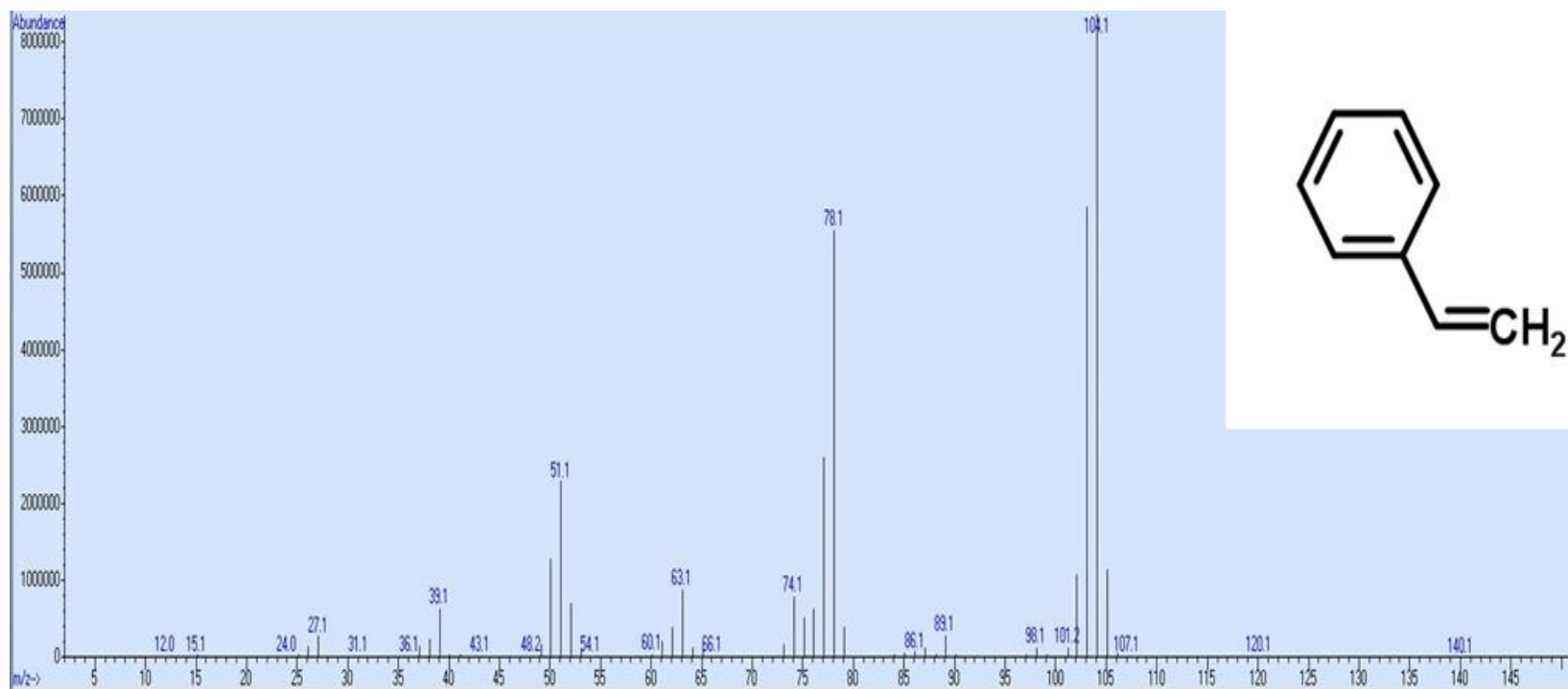


Figure X: Mass spectra of PS pyrolytic product styrene. Styrene was the dominant pyrolytic product of PS. Parent m/z of 104. Image of structure from www.chemspider.com.

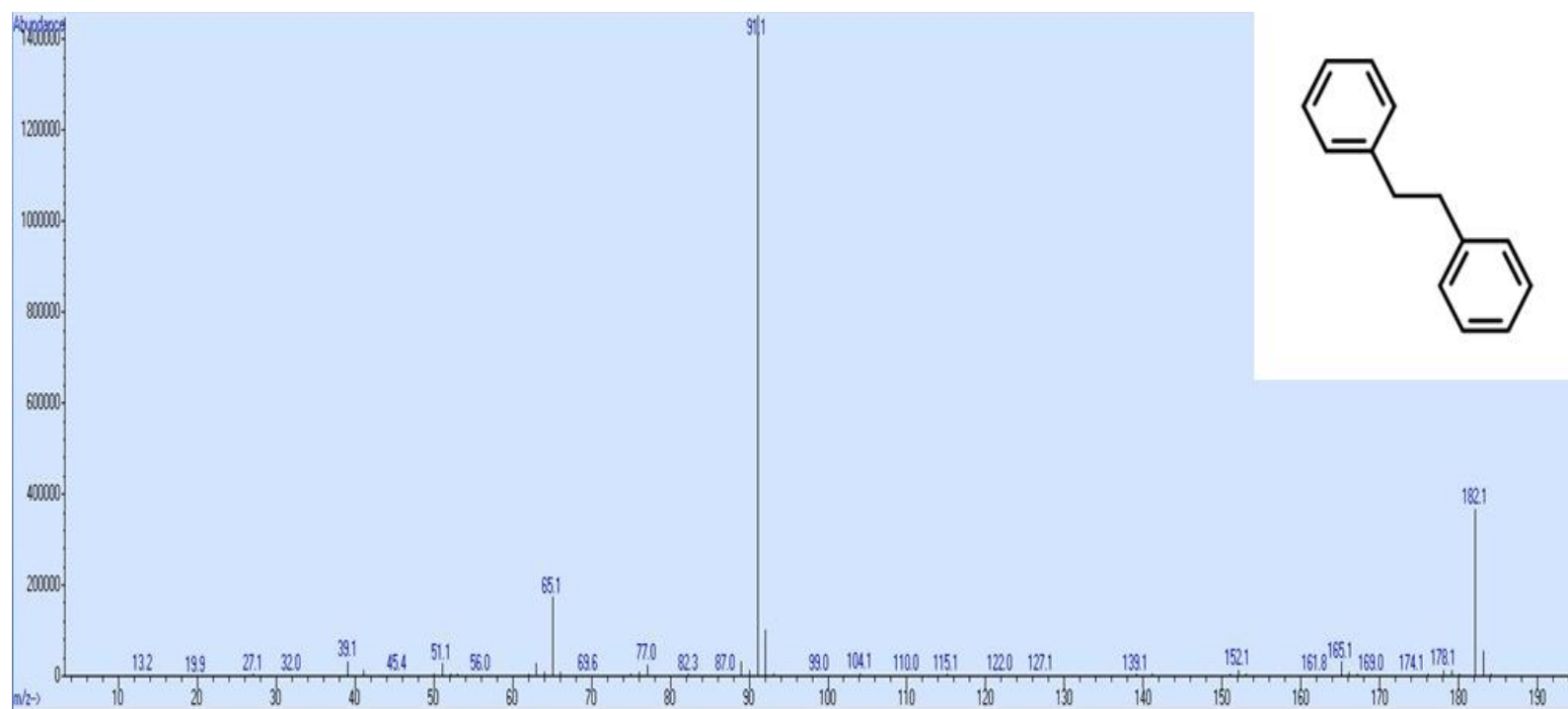


Figure XI: Mass spectra of PS pyrolytic product bibenzyl. Bibenzyl was a minor pyrolytic product of PS. Parent m/z of 182. Image of structure from www.chemspider.com.

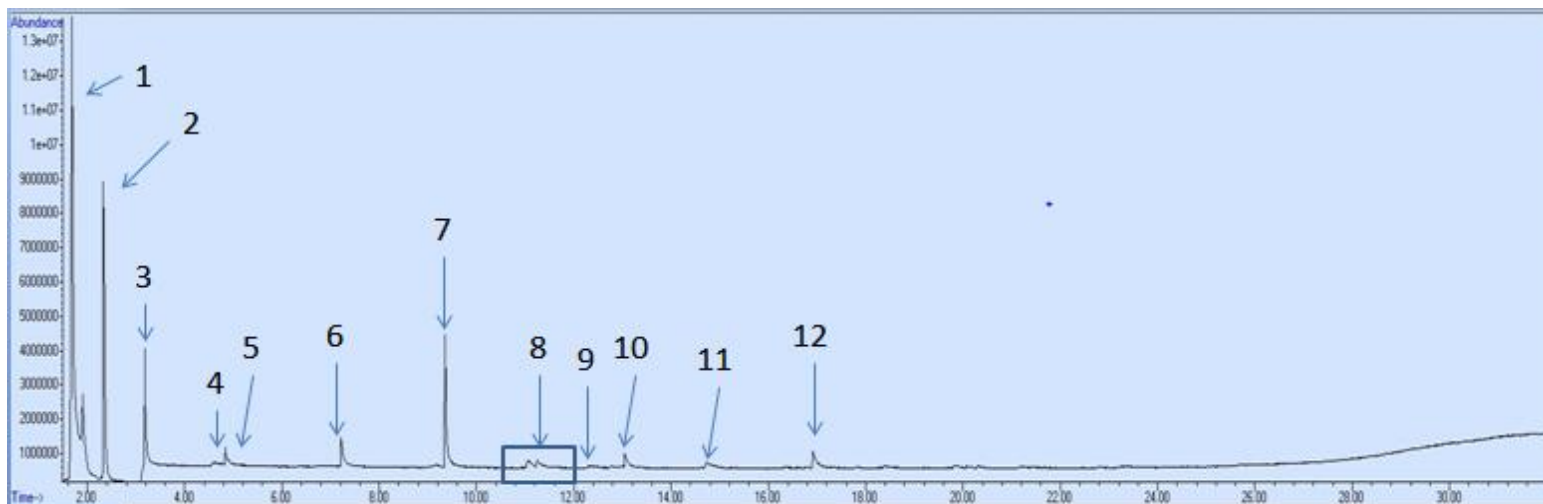


Figure XII: Pyrogram of PVC identified particle with pyrolytic products numerically labeled. Benzene was the dominant pyrolytic in splitless mode and naphthalene was in split mode. Other pyrolytic products include various VOCs and PAHs. Labels correspond with table below.

Peak #	Retention Time (± 0.5 minutes)	Pyrolytic Product	Parent m/z
1	1.8	Hydrogen Chloride/Sulfur Dioxide	36/64
2	2.4	Benzene	78
3	3.2	Toluene	92
4	4.6	Xylenes	106
5	4.8	Styrene	104
6	7.2	Indene	116
7	9.4	Naphthalene	128
8	11.0, 11.2	Methylated Naphthalenes	142
9	12.1	Biphenyl	154
10	13.1	Acenaphylene	152
11	14.7	Fluorene	166
12	16.9	Anthracene	178

Table VIII: Pyrolytic products of PVC with retention times and parent m/z's.

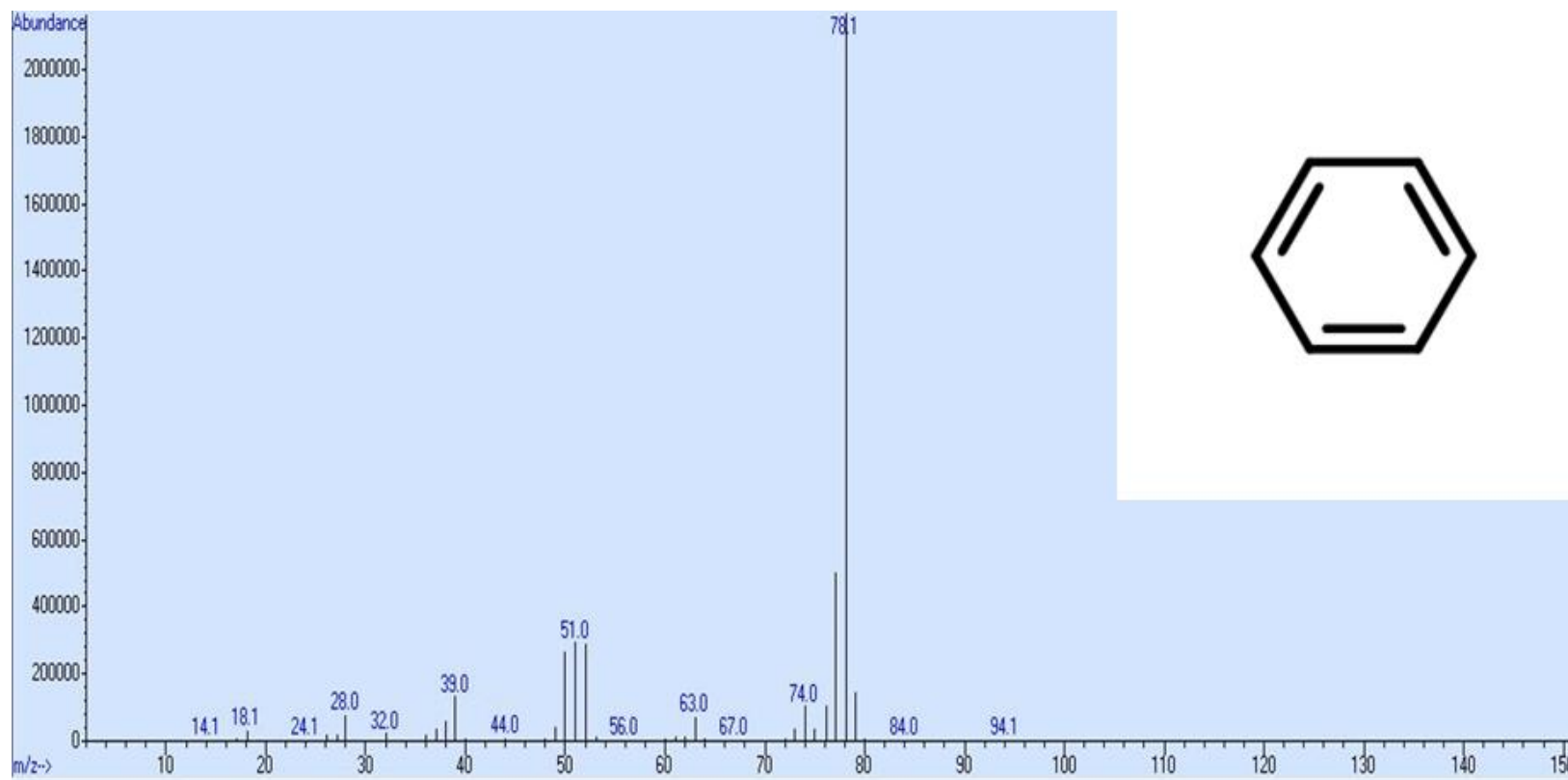


Figure XIII: Mass spectra of PVC pyrolytic product benzene. Benzene was the dominant pyrolytic product of PVC in splitless mode. Parent m/z of 78. Image of structure from www.chemspider.com.

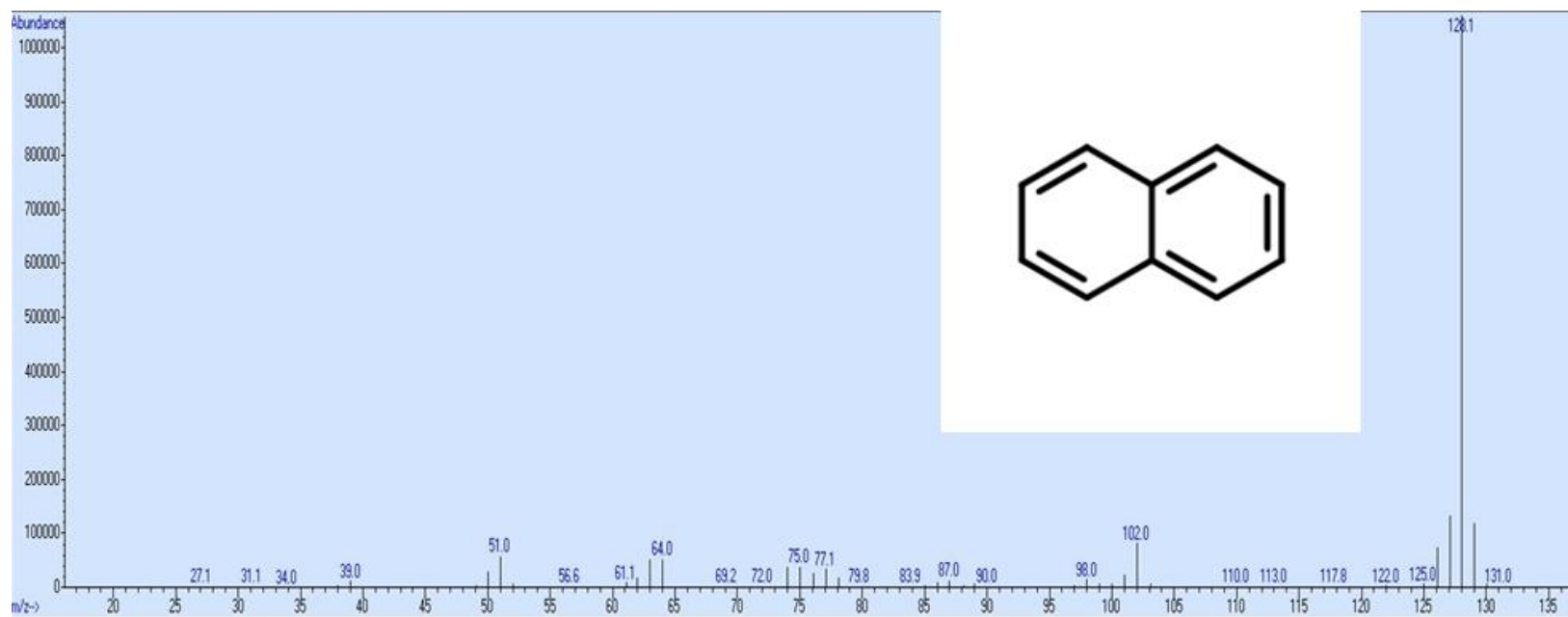


Figure XIV: Mass spectra of PVC pyrolytic product naphthalene. Naphthalene was the dominant pyrolytic product of PVC in split mode. Parent m/z of 128. Image of structure from www.chemspider.com.

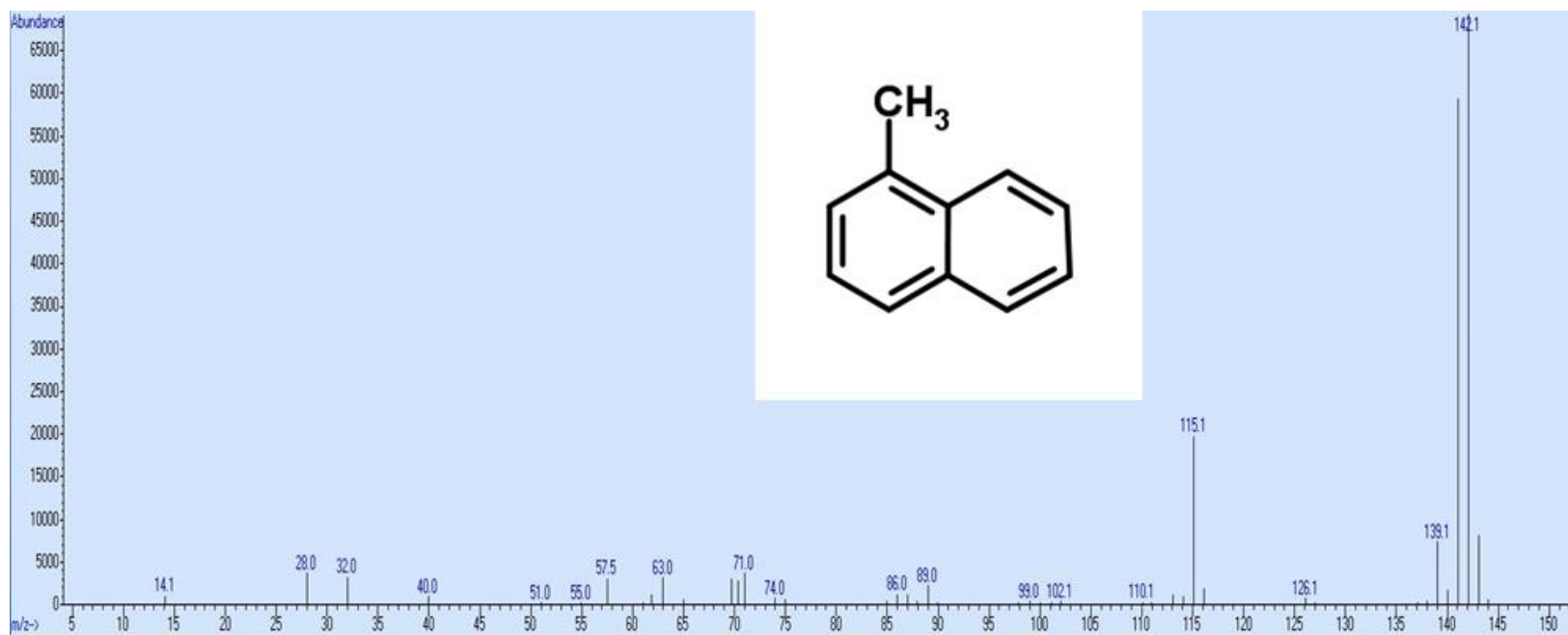


Figure XV: Mass spectra of PVC pyrolytic product methyl naphthalene. Methyl naphthalenes were minor pyrolytic products of PVC. Parent m/z of 142. Image of structure from www.chemspider.com.

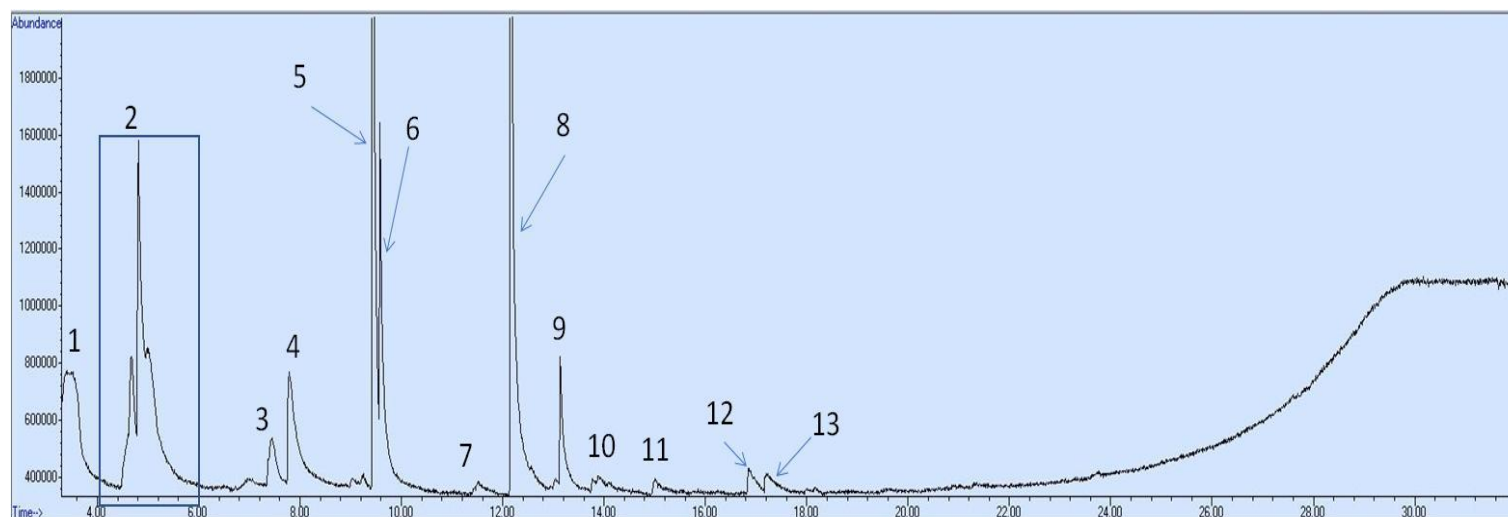


Figure XVI: Pyrogram of PET identified particle with pyrolytic products numerically labeled. Biphenyl was the dominant pyrolytic product. Other pyrolytic products include various VOCs and PAHs. Labels correspond with table below.

Peak #	Retention Time (± 0.5 minutes)	Pyrolytic Product	Parent m/z
1	3.2	Toluene	92
2	4.6/4.8	Xylenes; Styrene	106/104
3	7.2	Indene	116
4	7.9	Acetophenone	120
5	9.4	Naphthalene	128
6	9.5	Benzothiophene	134
7	11.6	1-methylnaphthalene	142
8	12.1	Biphenyl	154
9	13.1	Acenaphylene	152
10	13.9	4-methylbiphenyl	168
11	14.7	Fluorene	166
12	16.7	Dibenzothiophene	184
13	16.9	Anthracene	178

Table IX: Pyrolytic products of PET with retention times and parent m/z's.

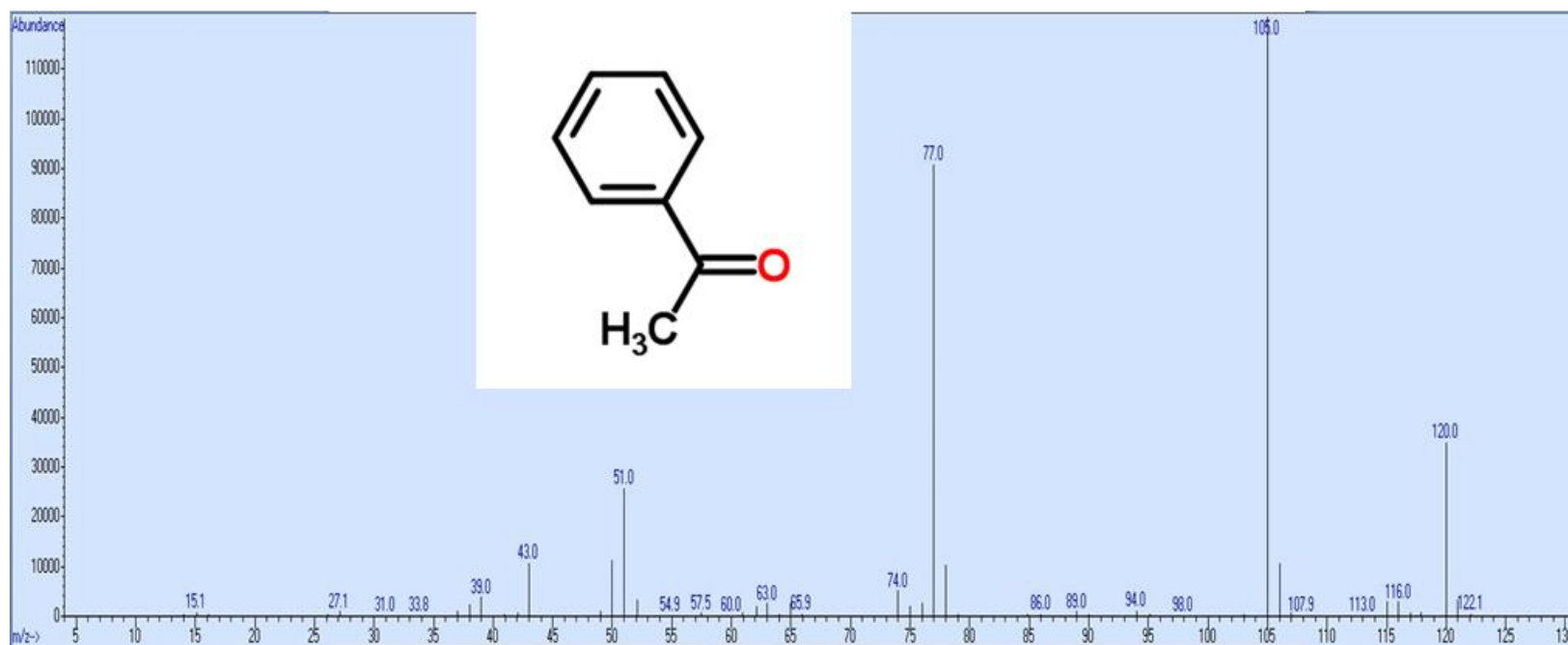


Figure XVII: Mass spectra of PET pyrolytic product acetophenone. Acetophenone was a minor pyrolytic product of PET. Parent m/z of 120. Image of structure from www.chemspider.com.

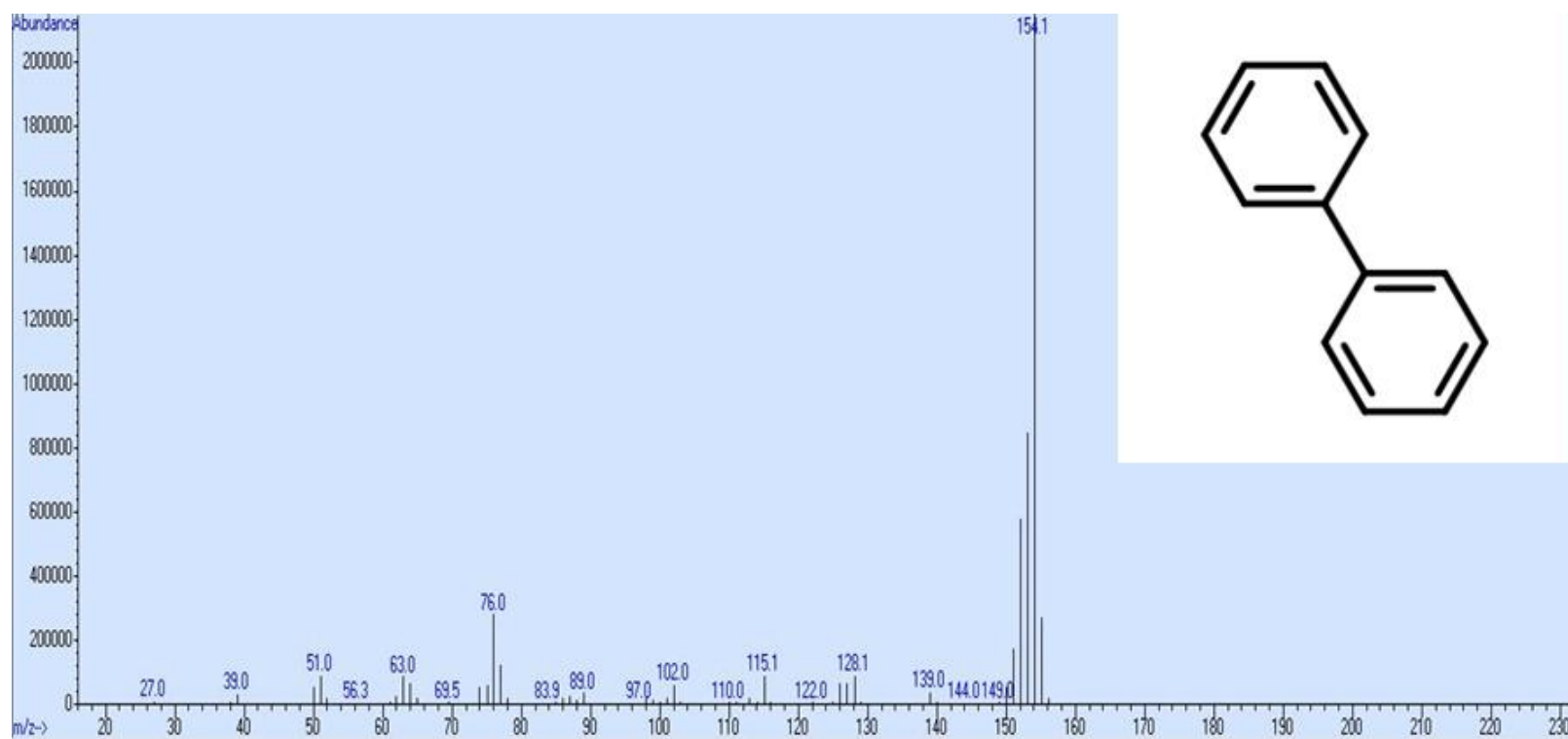


Figure XVIII: Mass spectra of PET pyrolytic product biphenyl. Biphenyl was the dominant pyrolytic product of PET. Parent m/z of 154. Image of structure from www.chemspider.com.

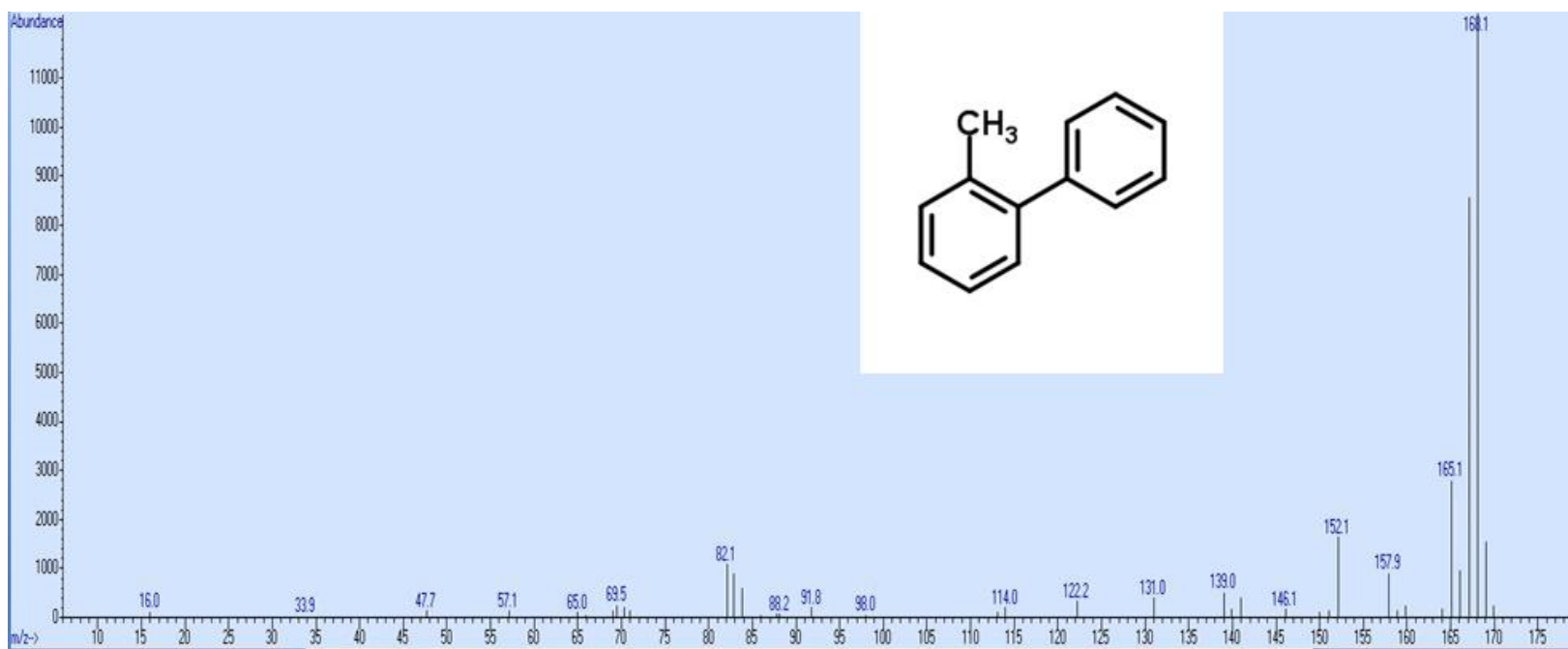


Figure XIX: Mass spectra of PET pyrolytic product methylbiphenyl. Methylbiphenyl was a minor pyrolytic product of PET. Parent m/z of 168. Image of structure from www.chemspider.com.

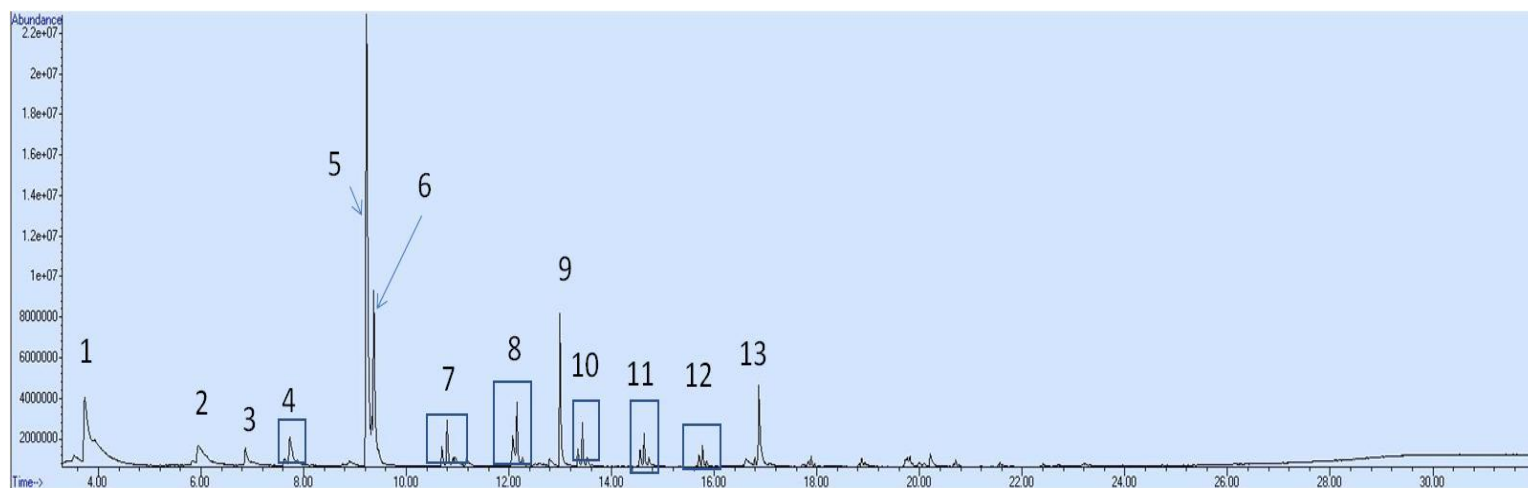


Figure XX: Pyrogram of CPE identified particle with pyrolytic products numerically labeled. A number of pyrolytic products were similar to those of PS, PVC, and PET (VOCs and PAHs) as well as aliphatic hydrocarbons similar to PE. Labels correspond with table below.

Peak #	Retention Time (± 0.5 minutes)	Pyrolytic Product	Parent m/z
1	4.0	Styrene	104
2	6.0	1-decene	140
3	6.9	Indene	116
4	7.7	C11 terminal diene, alkene, and alkane..	152, 154, 156
5	9.2	Naphthalene	128
6	9.4	Benzothiophene	134
7	10.8	C13 terminal diene, alkene, and alkane..	180, 182, 184
8	12.2	C14 terminal diene, alkene, and alkane..	194, 196, 198
9	13.1	Acenaphylene	152
10-12	13,.4, 14.6, 15.8	C15-C17 terminal diene, alkene, and alkane..	208-236, 210-238, 212-240
13	16.9	Acenaphylene	152

Table X: Pyrolytic products of CPE with retention times and parent m/z's.

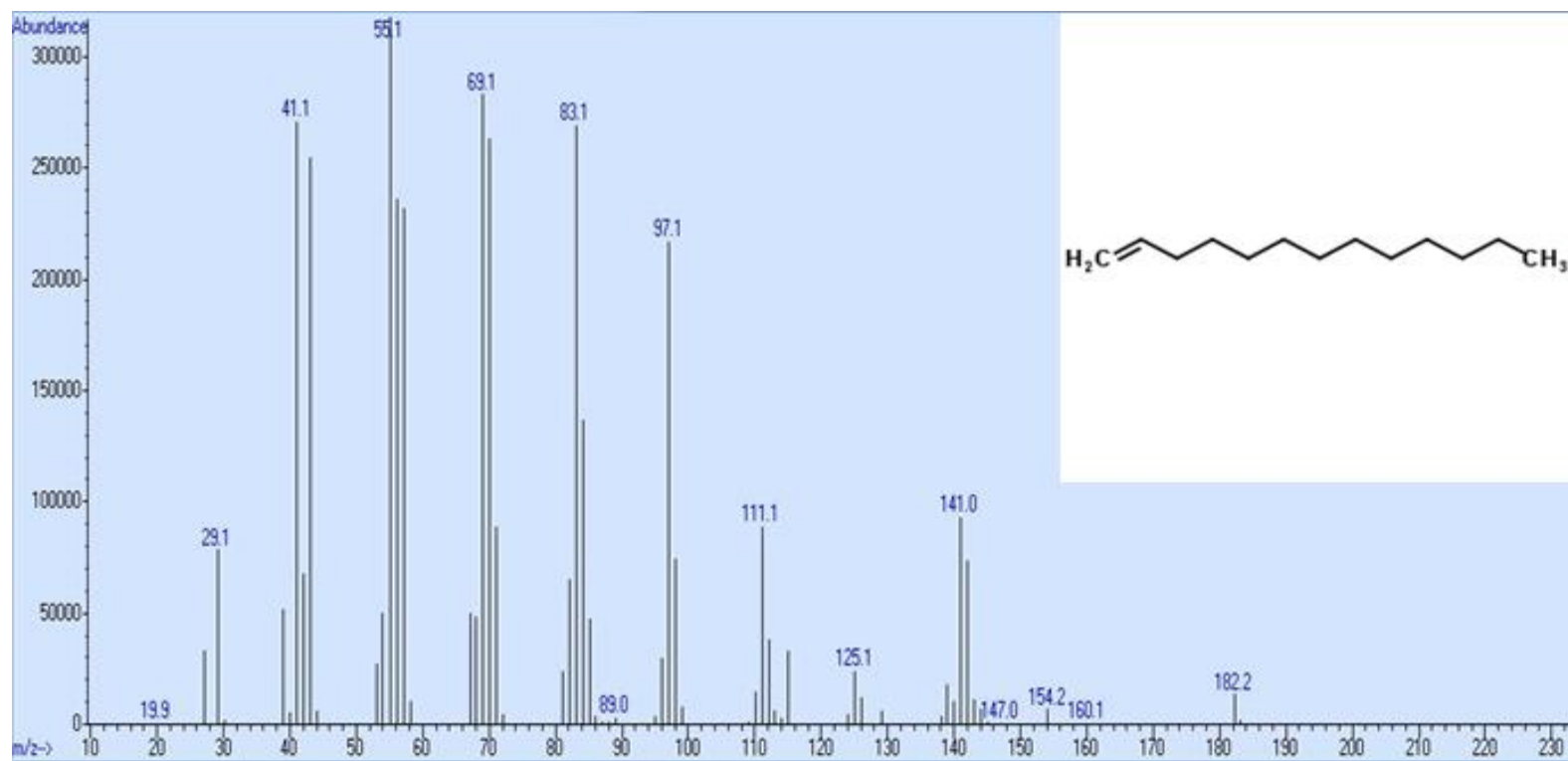


Figure XXI: Mass spectra of CPE pyrolytic product 1-tridecene. 1-tridecene is an example of an aliphatic pyrolytic product of CPE. Parent m/z of 168. Image of structure from www.chemspider.com.

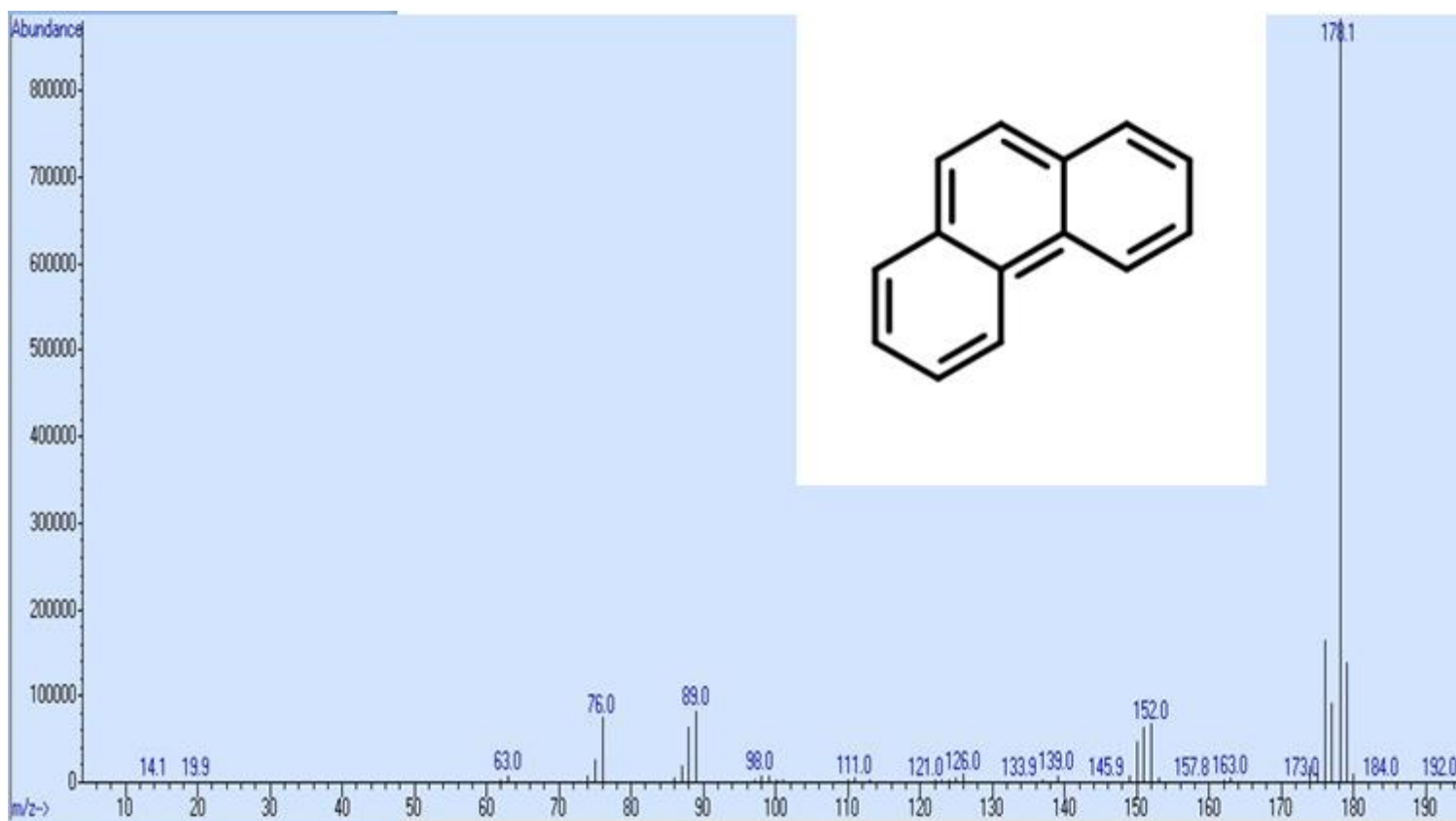


Figure XXII: Mass spectra of CPE pyrolytic product phenanthrene. Phenanthrene is an example of a PAH pyrolytic product of CPE (also seen in PVC, PS, and PET). Parent m/z of 168. Image of structure from www.chemspider.com.

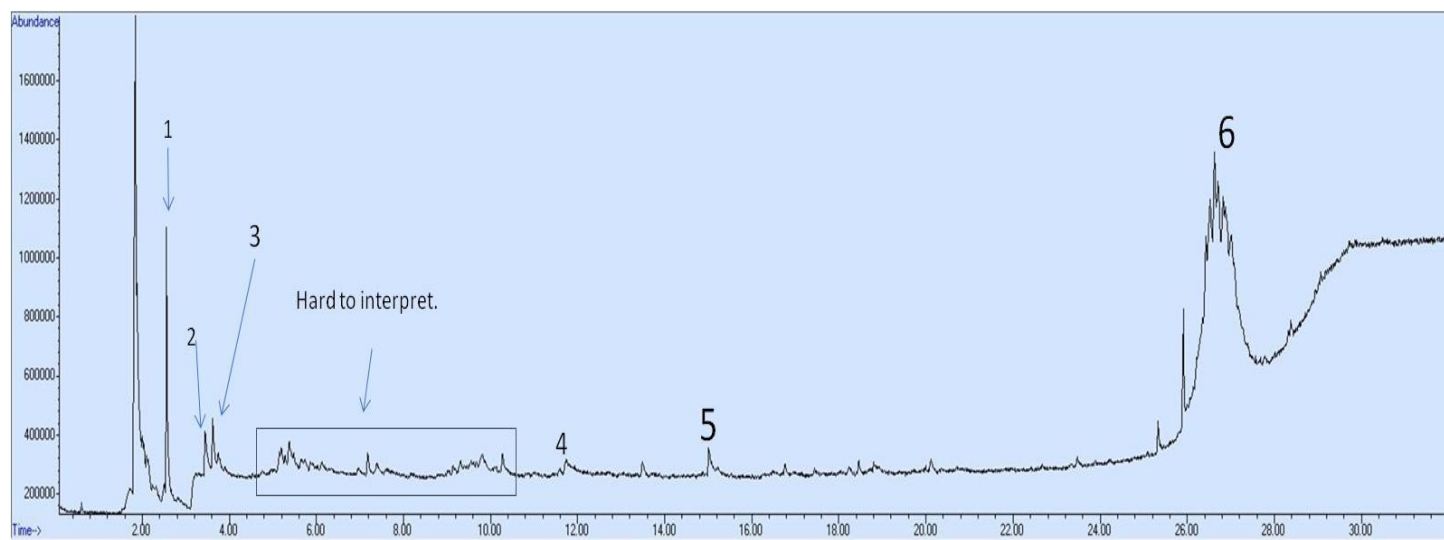


Figure XXIII: Pyrogram of didecyl phthalate resin identified particle with pyrolytic products numerically labeled. Labels correspond with table below.

<u>Peak #</u>	<u>Retention Time (± 0.5 minutes)</u>	<u>Pyrolytic Product</u>	<u>Parent m/z</u>
1	2.6	Benzene	78
2	3.4	Toluene	92
3	3.6	3-methylene-heptane	112
4	11.8	Phthalic Anhydride	148
5	15.0	Diethyl Phthalate	177
6	26.7	Didecyl Phthalate	446

Table XI: Pyrolytic products of didecyl phthalate resin with retention times and parent m/z's.

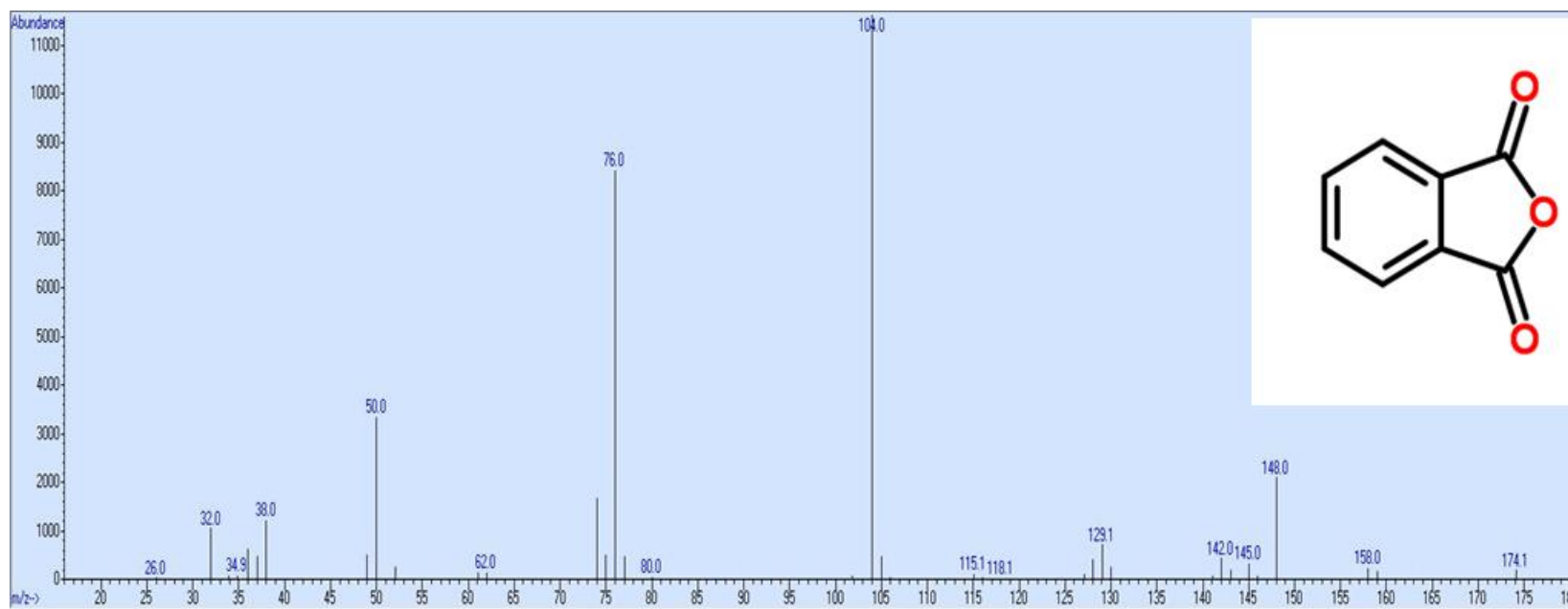


Figure XXIV: Mass spectra of didecyl phthalate resin pyrolytic product phthalic anhydride. Parent m/z of 148. Image of structure from www.chemspider.com.

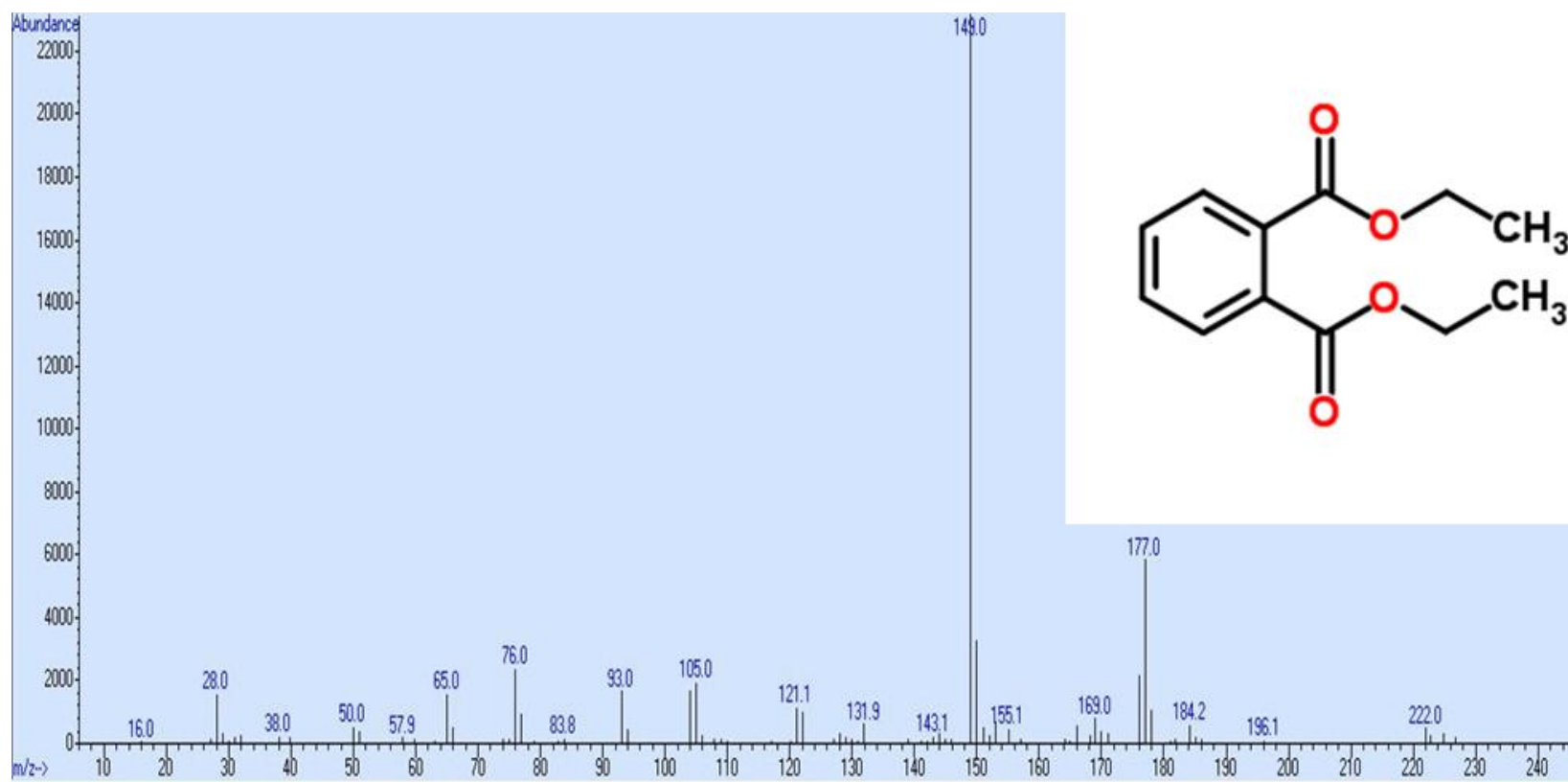


Figure XXV: Mass spectra of didecyl phthalate resin pyrolytic product diethyl phthalate. Parent m/z of 222. Image of structure from www.chemspider.com.

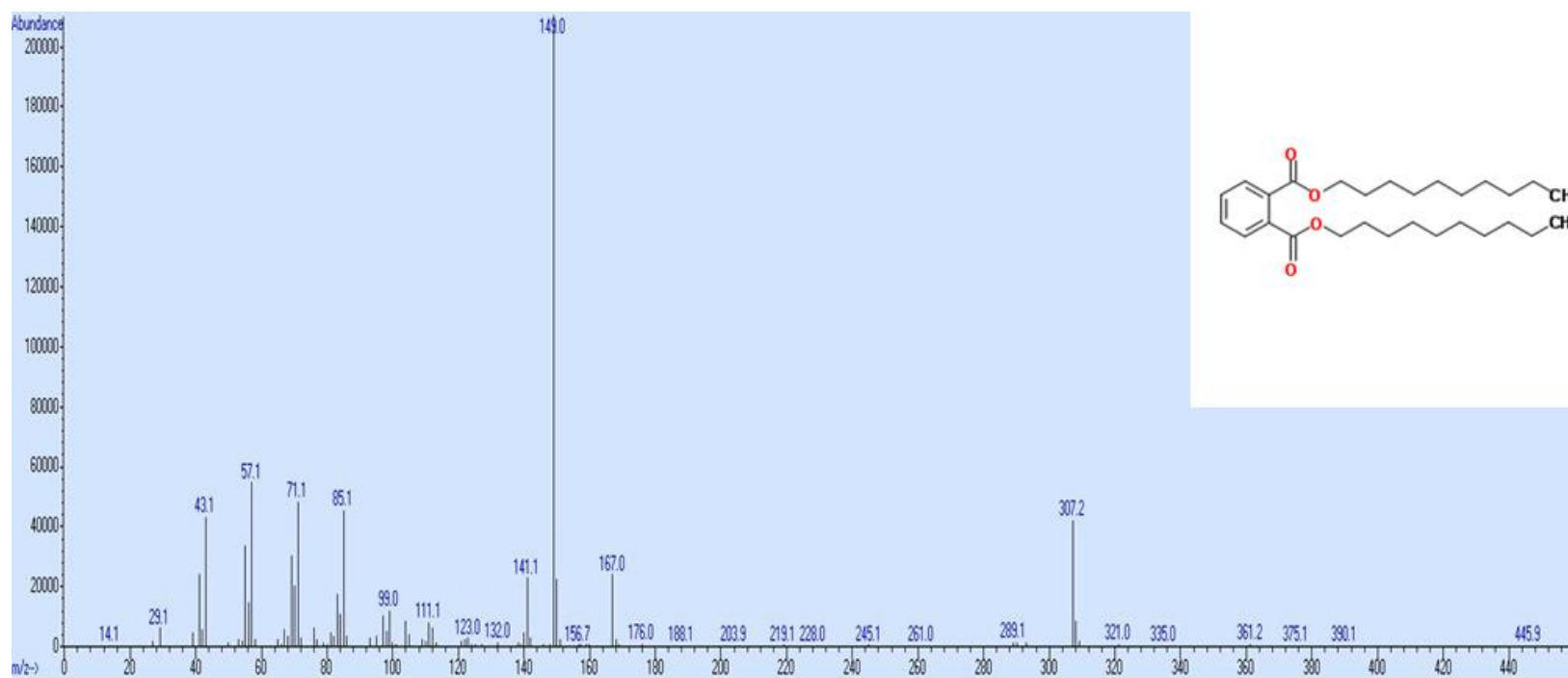


Figure XXVI: Mass spectra of didecyl phthalate resin pyrolytic product didecyl phthalate. Parent m/z of 446. Image of structure from www.chemspider.com.

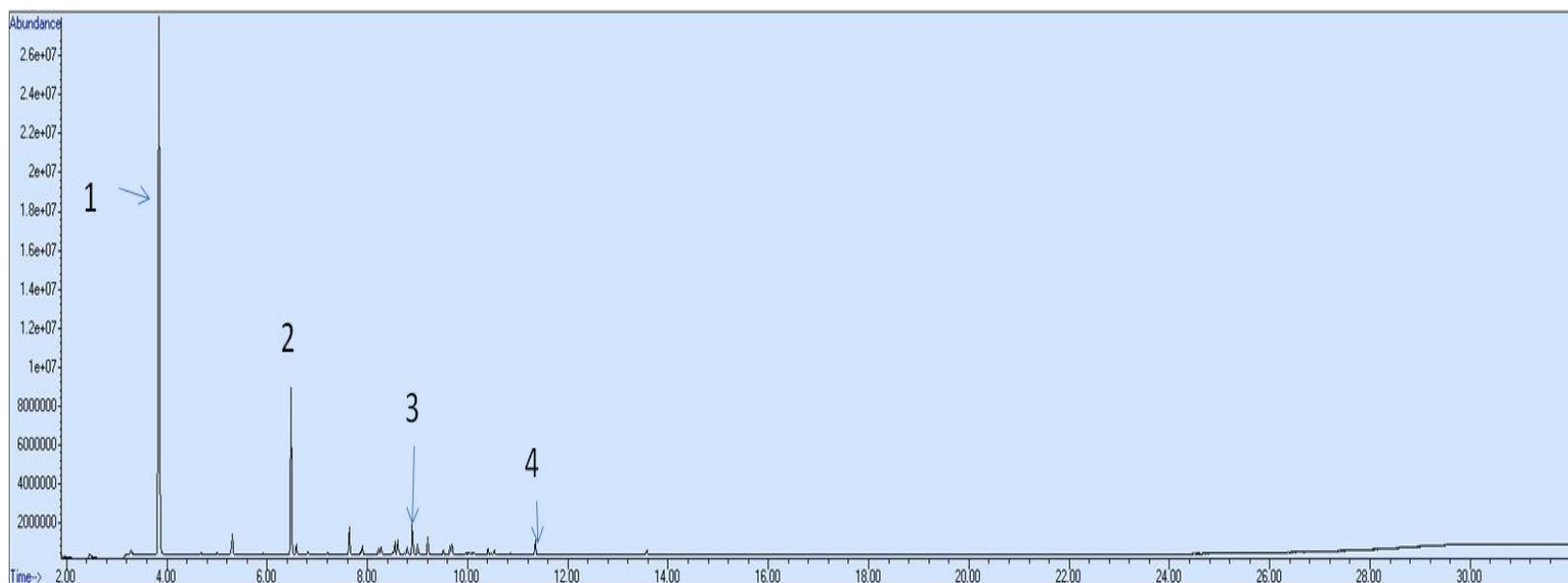


Figure XXVII: Pyrogram of PDMS identified particle with pyrolytic products numerically labeled. Labels correspond with table below.

Peak #	Retention Time (± 0.5 minutes)	Pyrolytic Product	Parent m/z
1	3.8	Hexamethylcyclotrisiloxane	222
2	6.5	Octamethylcyclotetrasiloxane	296
3	8.9	Decamethylcyclopentasiloxane	370
4	11.4	Dodecamethylcyclohexasiloxane	444

Table XII: Pyrolytic products of PDMS with retention times and parent m/z's

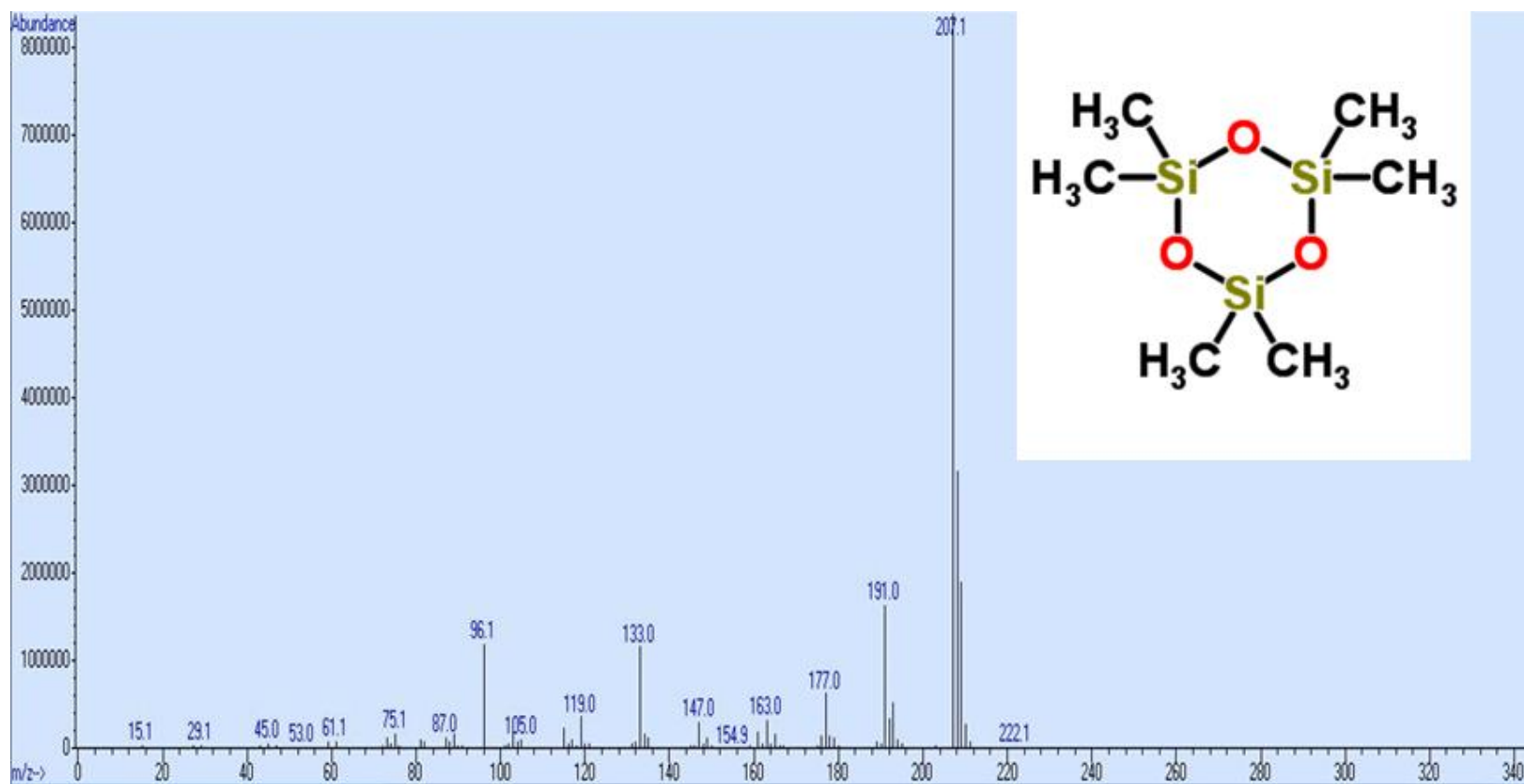


Figure XXVIII: Mass spectra of PDMS pyrolytic product hexamethylcyclotrisiloxane. Parent m/z of 222. Image of structure from www.chemspider.com.

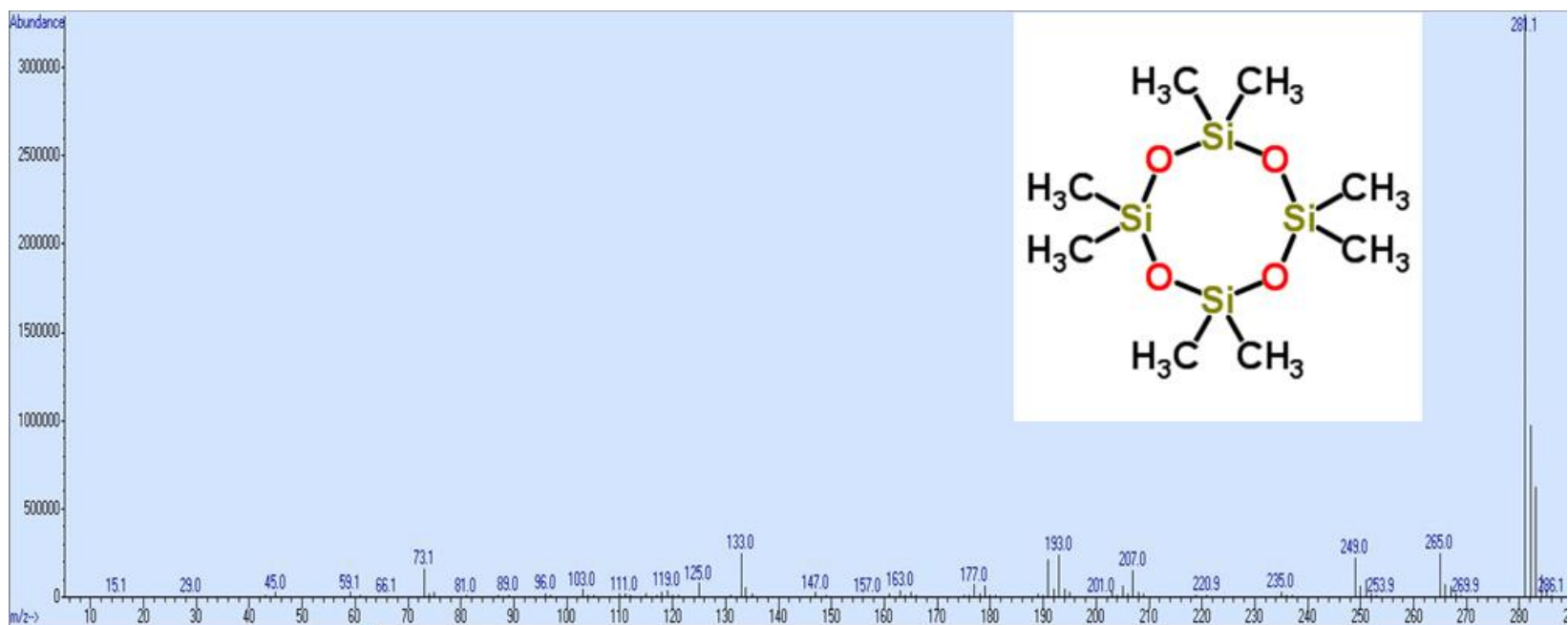


Figure XXIX: Mass spectra of PDMS pyrolytic product octamethylcyclotetrasiloxane. Parent m/z of 296. Image of structure from www.chemspider.com.

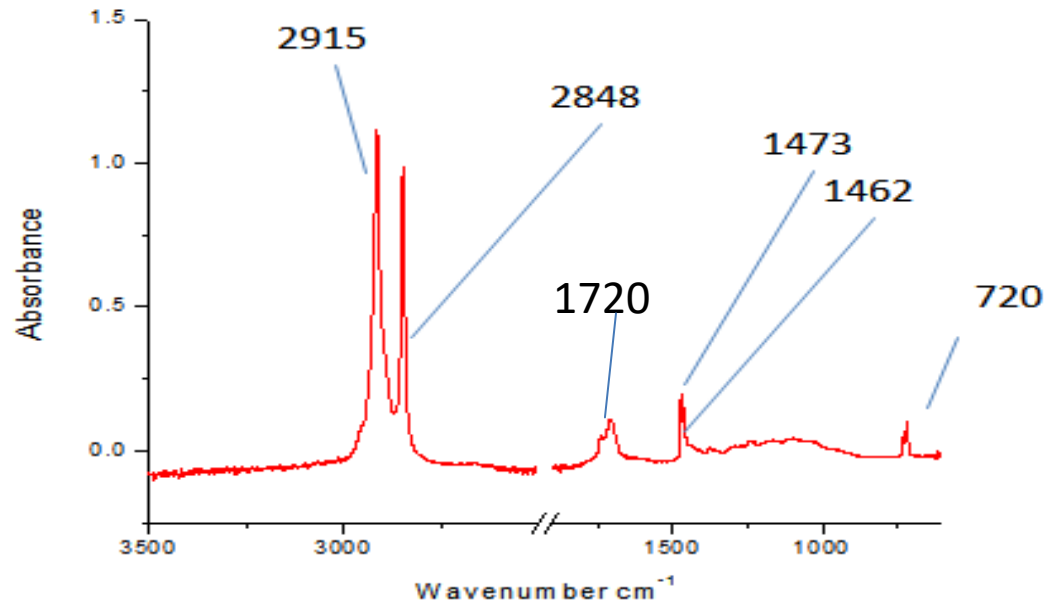


Figure XXX: Infrared spectrum of a PE identified particle. Wavenumbers labeled above are interpreted on the table below.

<u>Wavenumber (cm⁻¹)</u>	<u>Function Group and Vibration</u>
2,915; 2,848	C-H Stretching
1,720	C=O Stretching (photo-oxidation in the environment)
1,473; 1,462	CH₂ Rocking
720	Fingerprint Region Peak

Table XIII: Band wavenumber and vibration interpretations in PE spectrum above.

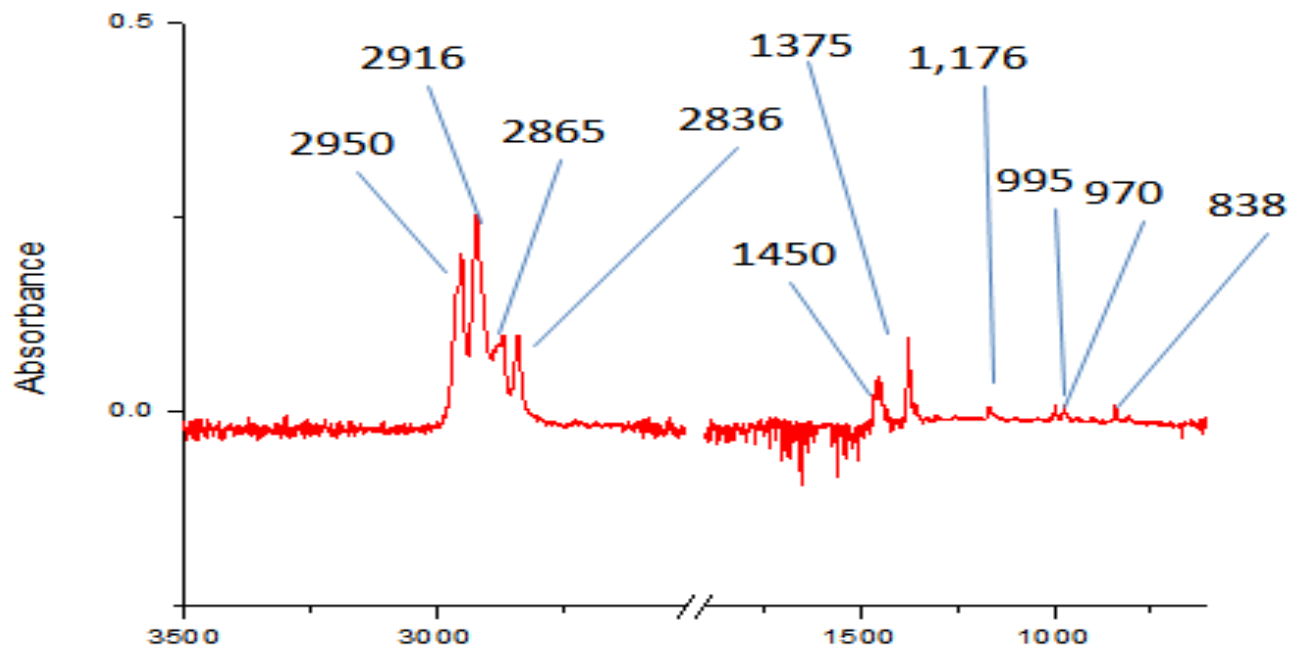


Figure XXXI: Infrared spectrum of a PP identified particle. Wavenumbers labeled above are interpreted on the table below.

<u>Wavenumber (cm⁻¹)</u>	<u>Function Group and Vibration</u>
2,950; 2,915; 2865; 2,836	Aliphatic C-H Stretching
1,473; 1,462	CH ₂ Rocking
1,176; 995; 970; 838	Fingerprint Region Peaks

Table XIV: Band wavenumber and vibration interpretations in PP spectrum above.

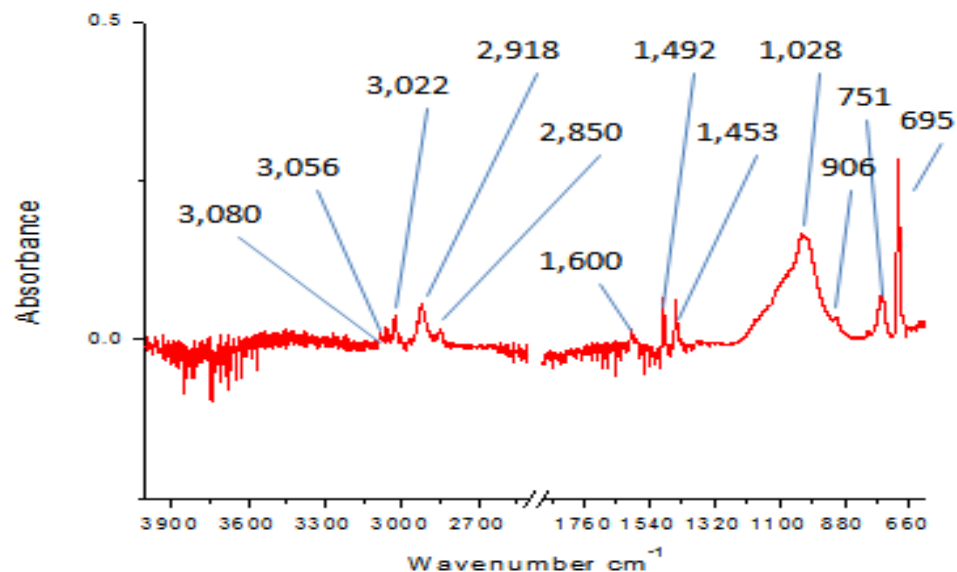


Figure XXXII: Infrared spectrum of a PS identified particle. Wavenumbers labeled above are interpreted on the table below.

<u>Wavenumber (cm⁻¹)</u>	<u>Function Group and Vibration</u>
3,080; 3,056; 3,022	Aromatic C-H Stretching
2,918; 2,850	Aliphatic C-H Stretching
1,600; 1,492; 1,453	Aromatic C-C Stretching
1,028; 906; 751; 695	Fingerprint Region Peaks

Table XV: Band wavenumber and vibration interpretations in PS spectrum above.

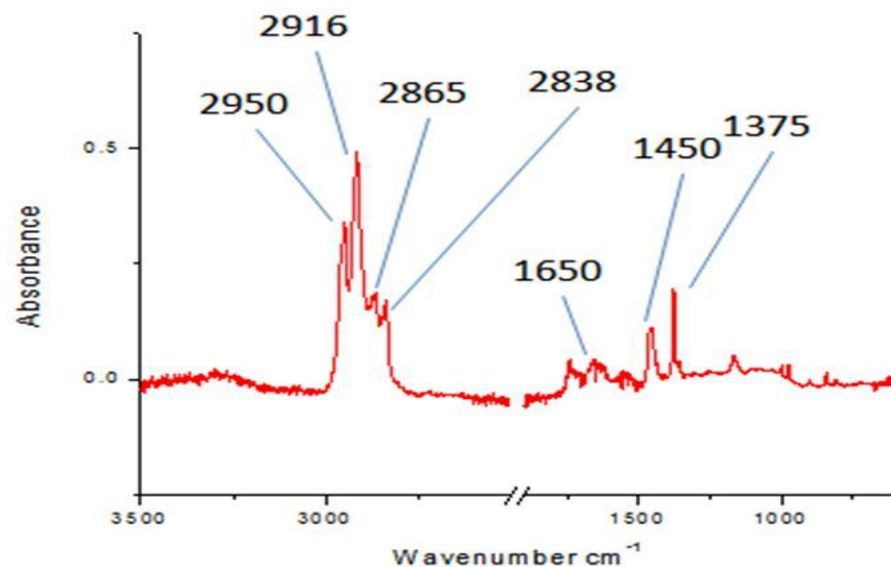


Figure XXXIII: Infrared spectrum of a PVC identified particle. Wavenumbers labeled above are interpreted on the table below.

<u>Wavenumber (cm⁻¹)</u>	<u>Function Group and Vibration</u>
2,950; 2,916; 2,865; 2,838	Aliphatic C-H Stretching
1,650	?
1,450; 1,375	CH ₂ Rocking
1,176; 995; 970; 838	Fingerprint Region Peaks

Table XVI: Band wavenumber and vibration interpretations in PVC spectrum above.

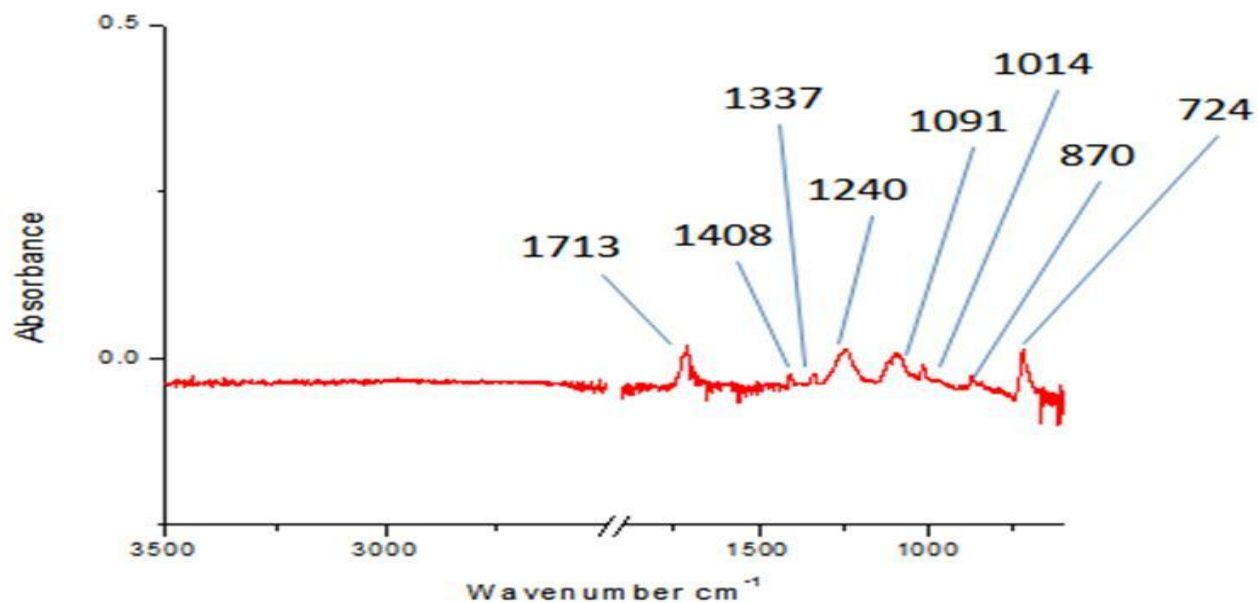


Figure XXXIV: Infrared spectrum of a PET identified particle. Wavenumbers labeled above are interpreted on the table below.

<u>Wavenumber (cm⁻¹)</u>	<u>Function Group and Vibration</u>
1,713	C=O Stretching
1,408; 1,337	CH ₂ Rocking
1,240; 1,091; 1,014; 870; 724	Fingerprint Region Peaks

Table XVII: Band wavenumber and vibration interpretations in PET spectrum above.

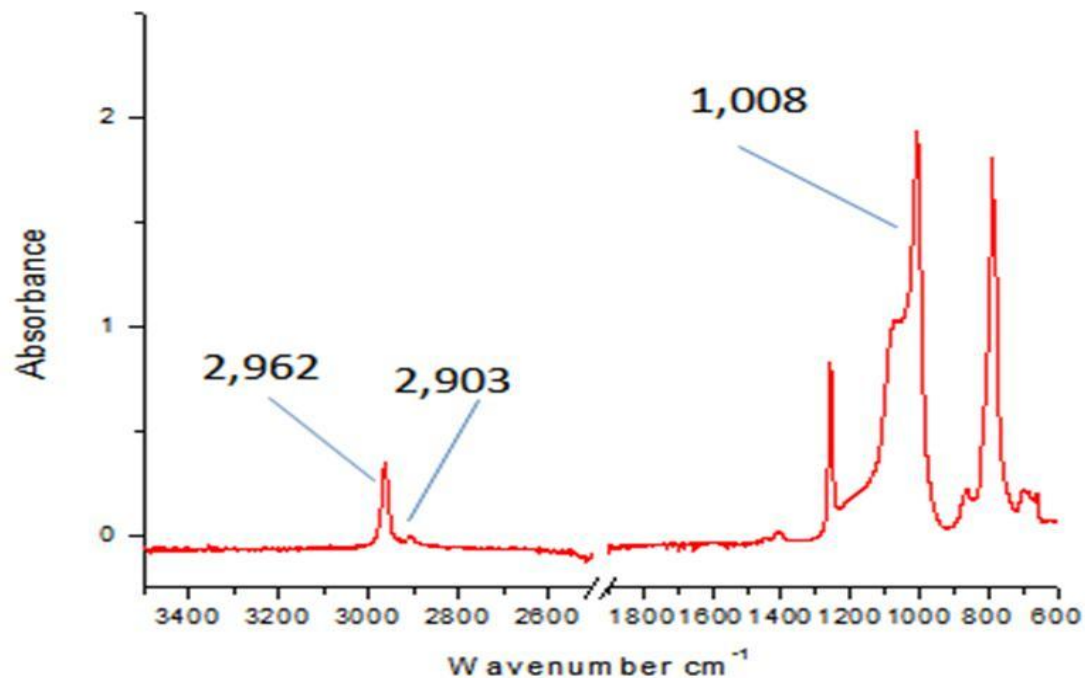


Figure XXXV: Infrared spectrum of a PDMS identified particle. Wavenumbers labeled above are interpreted on the table below.

<u>Wavenumber (cm⁻¹)</u>	<u>Function Group and Vibration</u>
2,962; 2,903	Aliphatic C-H Stretching
1,008	Si-O Stretching

Table XVIII: Band wavenumber and vibration interpretations in PDMS spectrum above.